Characterization of hydrogeological conditions and interactions between surface water, irrigation water, and groundwater in the Senegal River delta

Auteur : Weatherl, Robin
Promoteur(s) : Brouyere, Serge
Faculté : Faculté des Sciences appliquées
Diplôme : Master en ingénieur civil des mines et géologue, à finalité approfondie
Année académique : 2015-2016
URI/URL : http://hdl.handle.net/2268.2/1620

Université de Liège

Groundwater Characterization, Salinity Dynamics, and Interactions between Surface Water, Irrigation Water, and Groundwater in the Senegal River Delta

University of Liège, Faculty of Applied Sciences

Memoire conducted for the obtention of a Master's degree in Geological Engineering, by
Robin WEATHERL

2015-2016 Academic Year

Jury

Professor Serge Brouyère, Promoter
Professor Frédéric Nguyen
Dr. Philippe Orban Johan Denouane
Professor Alain Dassargues

Contents

Acknowledgements

There are a number of people who have added great value to my graduate formation, my time in Liège, in Dakar, in Saint Louis, and in the Senegal River delta.

I would like to express my deepest gratitude to my advisor, Professor Serge Brouyère at the University of Liège (ULg), for his mindful approach as an educator, and for creating such meaningful opportunities for myself and many other young scientists and engineers. I have benefited immensely from Pr. Brouyère's knowledge in the domain of hydrogeology and hydrochemistry. I would like to thank Dr. Philippe Orban as well for his constant willingness to help, his valuable scientific perceptions, and his sharing of knowledge in all that is hydrogeochemistry. Many thanks to Professor Frédéric Nguyen for his valuable counsel in the geophysical ventures for this project. Finally, I would like to thank Professor Alain Dassargues, who has attentively supervised the undertakings of the Hydrogeology and Environmental Geology department, under which this project has been carried out.

A profound thank you to the entire team of professors at the University of Cheikh Anta Diop (UCAD) and the University of Thiès who have helped with this project. First and foremost to Dr. Abdoul Aziz Gning, upon whose work this project has been constructed. Aside from sharing data and technical advice, Dr. Gning's practical aid offered to me once in Senegal was invaluable. Picking me up from the airport in Dakar at 1:00 AM, setting me up with hotels in Dakar and in Saint Louis, setting me up with a fabulous host family in Dakar, setting our team up with a kind technician in Saint Louis, and helping out with field work, all seemingly without a second thought. These gestures made for an incredible first experience in Senegal and in Africa, and a smoother transition into *Le Temps Senegalais*. The availability and kindness of Dr. Gning is not forgotten.

Thank you to Professor Raymond Malou, our project coordinator at UCAD. Our interactions, and your organization of our internships with UCAD are much appreciated. Thanks also to Dr. Mapathe Ndiaye for lending counsel and material in our geophysical surveys in the delta, for his continued availability in helping with geophysical data analysis.

A sincere thank you to my student intern partners from UCAD in the Senegal River delta, Cheikhna Dramé and Elhadji Moussa Sarr. Their kindness, their company, their astuteness in the field, and their protection in the markets (and when crossing streets) of Dakar and Saint Louis greatly increased the productivity and fluidity of our team. *Vous êtes des vrais hommes de terrain.*

Sincere thanks to Jules Keita, technician-at-hand in the Senegal River delta, as well as to the entire Keita family for welcoming us into their home. Mr. Keita's practical knowledge of the hydrology and geography of the delta served our project greatly. Accompanying us on every single field excursion, twice a week for over a month, showed great care and interest for future generations, and for the future of his homeland. Thanks also to the beautiful Mrs. Keita, and the fabulous Keita daughters, who showed great heart in ensuring that we had a warm meal waiting for us after every single field outing, and incidentally fed us every single day for the duration of our stay in Saint Louis. I thank them for the good times we shared around a kettle of tea, or a pot of Kinkiléba!

Special thanks to the nameless driver, providing transport from Saint Louis into the delta on a bi-weekly basis, and without whom we would not have been able to carry out our work. Knowledge of those terrains which were at times rough and roadless, and the ease at which he managed them ensured safe delivery and relative comfort to all of us.

My deepest appreciation to fellow student hydrogeologist Thérèse Tine and the entire Tine family for hosting me in their home in Dakar, for feeding me, giving me a bed to sleep in, and offering me my very own Senegalese dress! Thanks to Thérèse for accompanying me in the *Car Rapide* to the university, to the markets, and to the airport for my departure.

Many thanks to all of the doctoral and post-doctoral researchers in the department at ULg who have offered their help and advice, including Gaël Dumont in geophysics, and Pierre Briers in hydrochemistry.

I would also like to thank my fellow Master 2 classmates in our cozy department at ULg: Carlo Ortolani, Pierre Penant, Olivier Vopat, and Arthur Longrée, all of whom have taught me how to work more effectively in a team during our innumerable group projects. Thanks also to the Master 1 students, many of with whom I have also worked and progressed, including Robin Thibaut, Annie Royen, and Alexis Guerin. Special thanks also to our Erasmus visitor, a fellow female engineer, Sara Rozzoni: gone but never forgotten!

I offer my greatest thanks to my family. I am richer because of the love that exists between all of us. To my engineer father, Mike Weatherl, who has supported me emotionally, scientifically, and financially throughout all of my academic endeavors. Thanks to my stepmother, Renay for the love and patience that you show to all of your children, and for bringing me Tex-Mex salsa every time you come to visit! I thank my mother, Ann Erbert-Matteson, for inviting such openness and honesty in our relationship. To my brothers and sister: Mike Jr., Ben, Glenn, Tyler, and Allie, all of whom I hold so dear... we can't help but remain close, no matter what life throws at us. Love you all to the moon and back.

Last, but certainly not least, I thank my beau, Yoann Guillot. He has been constantly by my side in Liège, supporting my aspirations, encouraging me when I am discouraged, congratulating me when I succeed. I am fortunate to have found somebody so calm and so patient to balance my own restlessness.

There is no price to lay on the impression that these undertakings in Belgium and in Senegal have had on my scientific development. A sincere thank you to all who have been a part of them.

Introduction

Groundwater salinization by continental marine intrusion is one of the most widespread sources of aquifer contamination in the world. Coastal regions everywhere know this all too well, as coastlines are the most vulnerable to such mechanisms by their very nature of proximity to the ocean and often direct communication between the ocean and the groundwater. And while groundwater salinziation is a naturally occuring process, the intensity of it's occurence and impact can be compounded by modern human development, population growth, and other anthropic pressures.

The Senegal River delta is a coastal delta located in a semi-arid sahelian zone of West Africa. Due to low pluviometry in the delta, this river is an exceptionally important water resource for the region. The importance of surface water from the Senegal River is elevated more by the fact that much of the groundwater accessible by shallow wells is saline.

Salinization in the Senegal River delta originates from marine water invasion, both past and present, into the continent. Marine invasion and even full transgressions have been known to what is now the delta throughout geological history. Evidence of cyclical marine transgressions and regressions go back to the Jurassic, and multiple transgressions have occured in the Quaternary period alone.[1] In modern times, invasions of varying intensity occur on a seasonal basis, following from a tropical climate regime. Invasion has intensified in recent years because of a drought that has been established throughout the country, beginning in the 1970s and arguably still ongoing. In any case, resources have not fully recoverd from the subsequent water shortages. Fresh water availability has diminished and marine water invasion has augmented.

The saline aquifer that is the subject of the present work lies within a shallow, unconfined aquifer system, including a Quaternary aquifer and an alluvial aquifer, with irregular spatial contact and communication between the two.[1] This system is found to have an exceptionally shallow water table (< 1 meter). Recent marine transgressions are the main source of formation for the Quaternary aquifer, as well as the source of salt deposits in the soil which are nowdays readily dissolved into the water. The alluvial aquifer was formed mostly by river dynamics, with sediment transport and meander paths leaving a prominent mark on the alluvial aquifer form. To be sure, recent transgressions have also left salt precipitates in the alluvial sediments.

As these shallow, unconfined aquifers are still in direct communication with the Atlantic Ocean, they serve as a conduit for solutes moving from the sea into the continental subsurface, sometimes up to 100 km or more.[10]. As the water table for these aquifers is so shallow, groundwater is able to travel to the surface by capillary effect, and an important quantity of groundwater is subsequently lost by high evapotranspiration values. Evaporation leaves salt evaporites in the shallow subsurface and at the surface, leading to heavy soil degradation. The remaining brackish and saline groundwaters have a tendancy to increase in concentration towards brines.

Speaking of anthropic pressure in a hydrologically compromised region: agriculture is practiced extensively in the delta, and has been for centuries. Seasonal rainfed agriculture was the traditional practice for thousands of years, on the other hand, irrigated agriculture has now become the established method, slowly replacing traditional practice until becoming the dominant approach in the 20th and 21st century. Currently, the delta and valley of the Senegal River is a region with some of the most irrigated lands in all of West Africa.[10]

Major crops include rice (by far the most cultivated), tomatoes, and onions.

Irrigation practices are a burden to the soil and groundwater - added on top of the already-existing burden of salinization - and have not only accelerated damage to soil, but have secured infertile soils for the foreseeable future in some areas, and has likely diminished the impact of water freshening mechanisms due to presence of heavily concentrated dissolved solids. But irrigation practices have also played a major hand in the move towards food self-sufficiency in Senegal, and is needed for continual and long term food security in the country. As the population is only forecasted to increase, there is a need for increased crop yield. Unfortunately, the utility of irrigated agriculture is diminished by salinization, as there is widespread soil degradation and thus lower crop yield. For the time being, Senegal is a net-importer for food.[10]

Efforts have been made to lower the impact of marine invasion on groundwater salinization, including construction two multi-purpose dams; the Manantali dam in western Mali, near the headwaters of the Senegal river, and the Diama dam in the low delta, on the border with Mauritania. Both were constructed in the 1980s. The Diama dam function is both to normalize river levels throughout the year, effectively erasing the natural seasonal variations in river head, and to prevent saltwater intrusion upstream. While saline water is still present in the shallow delta, saltwater intrusion has been significantly diminished because of this dam. This alteration of the natural hydraulic function of the low delta has not gone without consequence - natural ecosystems and habitat have been destroyed because of the diminished salinity of salt marshes and other saline environments.[31] However, this aspect is outside the scope of the current study.

The direct interest of this work is on the hydrogeological aspect of salinization of shallow aquifers in the the Senegal River delta. The objective is to be able to characterize salinization dynamics and the related surfacewater-groundwater interactions. Identifying mechanisms of groundwater freshening, and to understand the role of surface river water to this end, will be investigated in depth. Irrigated agriculture is not a primary object of study, although it's presence and impact on groundwater is closely linked and evaluated.

A primary goal is to be able to determine the extent of salinization and the direction of propagation for salinated waters, and eventually the penetration and direction of flow of fresh river water in the aquifer. Localizing regions of surfacewater-groundwater interactions may increase the understanding their spatial dispersion. Determining relevant causes and effects of surface water-groundwater interactions may lead to more effective management in the future.

Previous studies[16][20][30] have built a hypothesis that the salinized quaternary aquifer does have some communication with the surface river water, and that through this mechanism, there is a freshwater recharge from the river into the groundwater. Not to mention, general literature on saline groundwater recognizes that fresh water from lakes and rivers can, and often does, penetrate into groundwater. This hypothesis is the major point of investigation for the current report. As an accessory, the continuity of a thin aquitard within the shallow sediments was also explored. It is known that this aquitard exists, creating two separate saturated zones. It has been assumed up to this point that this aquitard is not continuous, and therefore there is concrete communication between 'separate' saturated layers within the shallow aquifer.

The current work is not the first of it's kind. While data availability is not as abundant as in other areas, there is still a sizeable amount of data from previous studies revolving around

the issue of salinization in the delta. Projects have involved the University of Cheikh Anta Diop, the University of Liège, the National Society of Organization and Exploitation of the Senegal River Delta Lands and the Senegal River Valley and of the Faleme River (french acronym S.A.E.D.), and the Senegal River Basin Development Authority (french acronym O.M.V.S.), among others. Geological reconnaissance projects, hydrological and hydrogeological projects, agriculture science projects, and anti-sel projects have been carried out.

To approach the problematic, a combination of literature review, experimentation, and data analysis was used. Specifically, the steps of study were as follows:

1. Literature review and organization for the purpose of characterizing the Senegal River delta's physical setting;
2. Field work to gather observational, geological, geochemical and geophysical data, including the installation of a piezometer monitoring network;
3. Analysis of collected data, as well as analysis and integration of historical data, in order to lay out realistic hydraulic patterns between surface water and groundwater in the delta.

This final report is organized according to these steps. Relevant contexts are discussed, followed by a description of experimental approach that includes information on the sites chosen and piezometer installation, as well as theory on geochemistry and geophysics and their application in groundwater salinization studies. Finally, hydrogeophysical and hydrogeochemical results are presented and compared. A final discussion includes suggestions for future work to be done.

Part I

Context - Senegal River Delta

1 Geography

The Senegal River is born out of the merging of several large tributaries, including the Bafing in Guinea and the Bakoy in Mali, with the merger point found in Bafoulabé, Mali. The Senegal River comprises three global compartments: the upper basin, the valley, and the delta, in all extending over approximately 1500 kilometers (literature reports of the Senegal River length vary between 1100 km and 1800 km)[10],[30], and comprising a basin of approximately 30 000 km^2 (reports for the basin size are also variable). Much of the western path of the River, including the delta, forms a natural border between the northern region of Senegal and the southern region of Mauritania. Further upstream, the river forms a border between the eastern region of Senegal and the western frontier of Mali. A localization and layout of the basin and River may be seen in figure 1.

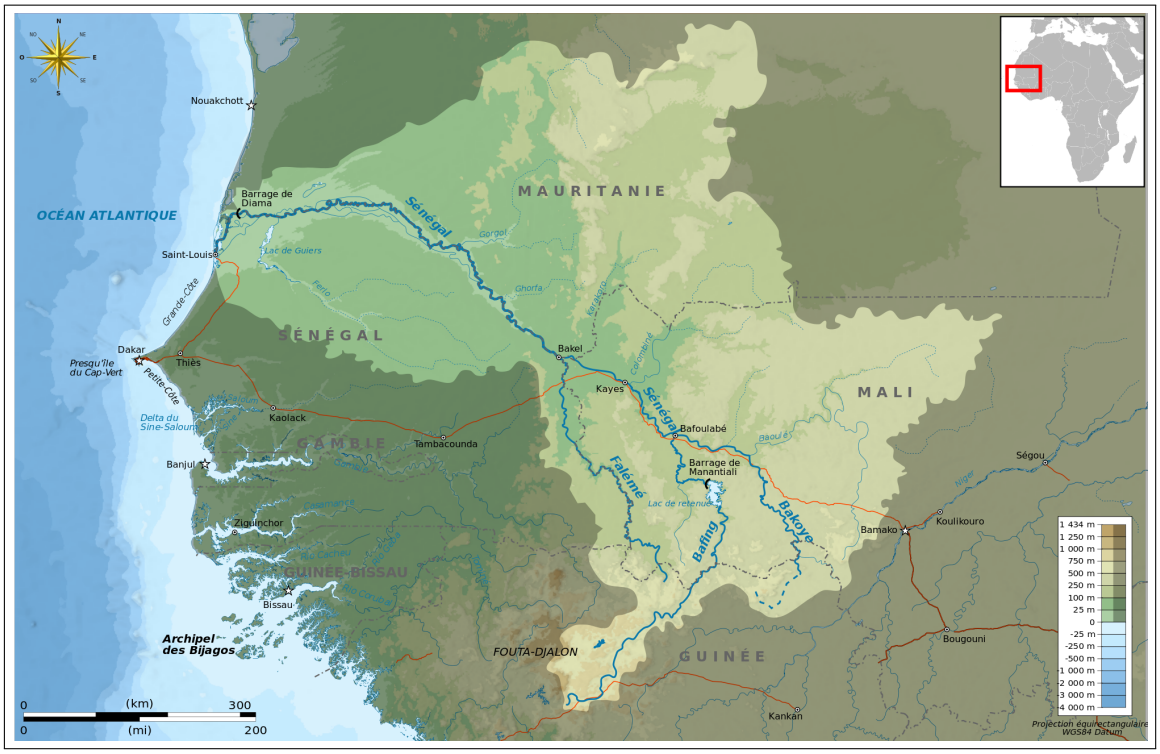

Figure 1: *Localisation of the Senegal River and it's drainage basin. Note elevation information included. Source: WikiMedia Commons user 'Bourrichon', with data from USGS.*

The delta is found at the north-west corner of Senegal and is defined in Senegalese territory between the cities of Richard Toll and Saint Louis, and between the Guiers Lake - with the Ferlo to the east - and the Atlantic Ocean (see figure 2). Geographically, the delta may be defined between 15^{o}35' and 16^{o}35' N latitude, and 15^{o}40' and 16^{o}35' W longitude.[19] The delta includes approximately 150 kilometers of River (measured via Google Earth), a delta basin of 3400 km^2 [13], and more than 100 km total length of distributaries. The river opens up directly into the Atlantic ocean at the tip of the 'Langue de Barbarie' sandspit,

just south of the city of Saint Louis. A less expansive deltaic landscape is also present on the right bank of the river in Mauritania.

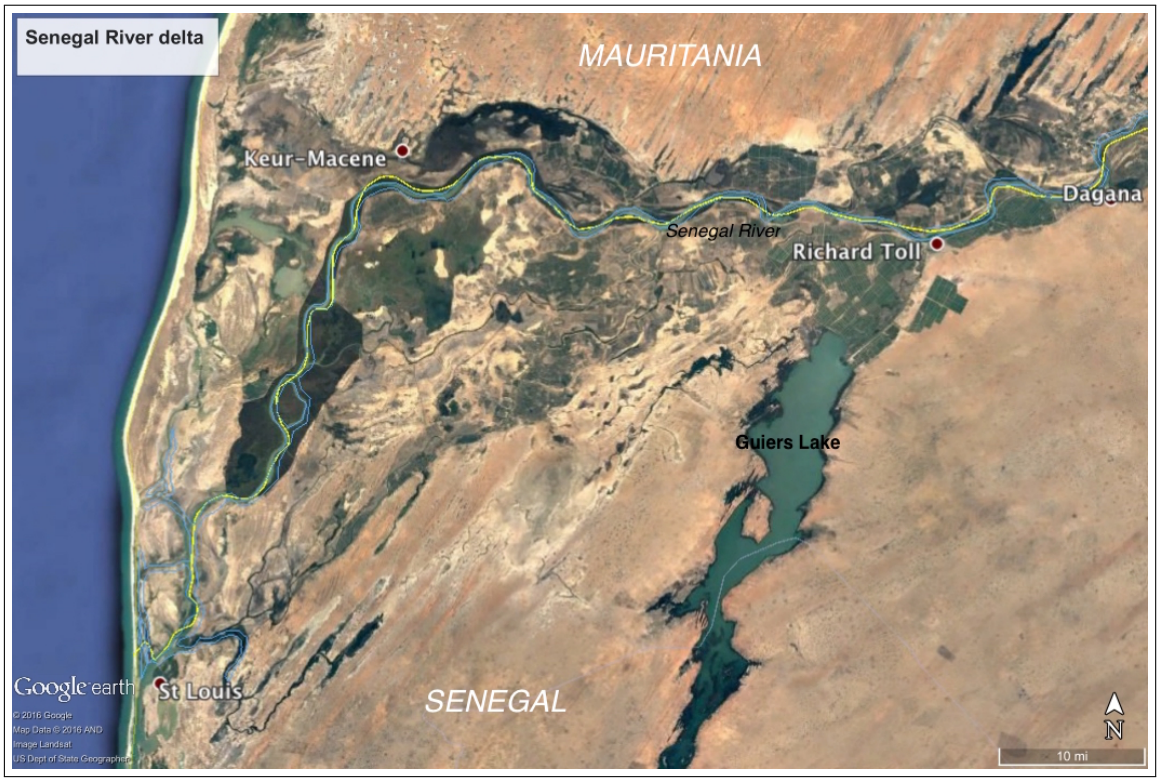

Figure 2: *Layout of the Senegal River delta in the NW corner of Senegal, opening up directly to the Atlantic Ocean to the west. Image via Google Earth.*

2 Climate

The delta region is located in sub-saharan West Africa, in a coastal-to-sahel climate zone. Not far north is the Sahara desert. To the south, savannah and woodlands are found, which eventually evolve into to dense tropical forests.

The entirety of the River, it's major tributaries, and the river basins all lie within the tropics. The climate is dominated by highly contrasted seasonal variations in rainfall, namely, a dry season and a rainy season. Precipitation occurs almost exclusively in the rainy season, with highest rains between the months of September and October at the level of the delta. These seasons are born of dynamic movements and interactions of various trade winds and of monsoon winds, detailed below.

Due to it's proximity to the Atlantic Ocean, the low delta is subject to a coastal climate, with high *alizé maritime* trade winds coming from the N-NW and dominating especially in the early months of the year. These mildly humid winds are cool, keeping the atmospheric temperature lower than temperatures found further inland at the same latitude, throughout the year. In contrast, *alizé continental* trade winds, which are relatively dry, come in from the continental NE at the same time and dominate the climate of the inland/high delta. A third current of trade winds, the continental *harmattan* moves in over the delta from the E. The *harmattan* is warm and very dry, fixing high temperatures and low rainfall in the NE delta. [20]

Mousson or monsoon winds move in to the delta from the S-SW. These massive winds aid in the formation of an intertropical front as they come into contact with the *alizé continental* and *harmattan* of the N-NE. The monsoon is warm and very humid, passing over the delta between the months of July and October, and generating the rainy season. During the monsoon period, the *alizé maritime* continue to hit the low delta, slowing the advance of the rainy season in this zone and marking a clear coastal-to-sahel transition zone.[20],[16]

Climactic conditions of the upper River basin are worth discussing, as some of these conditions carry an impact into the delta. In the climactic conditions of the upper river basin to the SE of the delta, the *alizé continental* is less influential, and the magnitude and extension of the dry season is diminished, giving way to a more prolonged rainy season - the upper basin enjoys more precipitation, more regularly. Historical data maintains that the number of days which are considered on average to be biologically dry in the delta is in excess of 200 days per year. In contrast, the upper basin is situated in a zone of less than 100 days per year which are biologically dry.[20] 'Biologically dry' signifies that there is not enough water to sustain the needs of the life that is present (or that could reasonably be present) in a given region.

Inland temperature variations between seasons in the delta are low; average temperatures reach 30°C in the rainy season, and do not fall below 20°C in the dry season. Near the city of Saint Louis, temperatures can fall to 15°C during the dry season due to coastal winds. Maximal temperatures near the coast in the rainy season are suppressed, and generally do not reach 30°C.[10]

The delta constitutes lowlands, while the upper basin has significant relief in it's landscape, such that topography becomes an important climactic factor. Elevation is on the order of 0.5 cm/km in the western and low delta, and 1 cm/km to the eastern limits of the delt near the town of Richard Toll[2], and so is not considered to have any significant climactic

or hydraulic effect.

2.1 Rainfall

The physical atmosphere as well as subsufrace conditions evolve rather drastically from the Senegal River delta to it's headwaters in the upper basin. While the delta is located in the arid zone of the Sahel, the upper basin is located in the humid south Sudanian zone, with higher pluviometric levels - approximately five times greater than those found in the delta. Annual pluviometric levels in the delta generally do not exceed 300 mm, while levels in the upper basin can reach 1500 or 2000 mm per year.[10],[20] Related plant density increases north to south from savannah to forests, following pluviometric tendancies. Precipitation in the upper basin stimulates recharge in river and groundwater levels along the entire river.

Data from a weather station in Saint Louis has been organized and provided from the (Gning, 2015) doctoral work, and covers 116 years of information, from 1892 - 2008. Among the information provided are monthly rain levels (in millimeters) from which the cumulative annual rainfall and an annual Standard Pluviometric Index can be calculated. Comparing monthly and annual trends allows us to identify the average trends and norms of rainfall levels for a given time period, and to quantify the level of 'wetness' each year by making use of average values. Wetness levels will identify exceptionally humid years and exceptionally dry years, as well as drought periods spanning two years or more. The data used is specific to the city of Saint Louis, where rainfall is expected to be higher than in the upper delta. Regardless that rainfall levels across the delta may evolve (diminish) from the coast to the ferlo, the pattern of exceptionally wet years and dry years is considered equivalent.

An evolution in humidity and rainfall levels in the delta has been observed in the last century. Around 1968, a relative deficit in yearly precipitation was established in the region, and has persisted up to the present day. Climactic data reflects this pluviometric shift in a concrete manner.

Average monthly rainfall of two different time series is represented in figure 3. First, the pluviometric difference between the rainy season and the dry season is evident, with nearly all precipitation falling between June and October, and two-thirds of which falls during the months of August and September. The two sections used (1892 - 1970 and 1971 - 2008) separate the two aforementioned distinctive humidity regimes in the delta. There is a clear drop in pluviometry between the first timeframe and the second.

The Standard Pluviometric Index (SPI), developed by (McKee et al. 1995) is a popular method used to quantify precipitation excess and deficit over multiple time scales. A simple physical relation is given as:

$$SPI = \frac{P_i - P_m}{\sigma} \tag{1}$$

with

- P_i the cumulative rainfall level for a year i
- P_m the average rainfall level over the series, a.k.a. timescale
- σ the standard deviation of the series

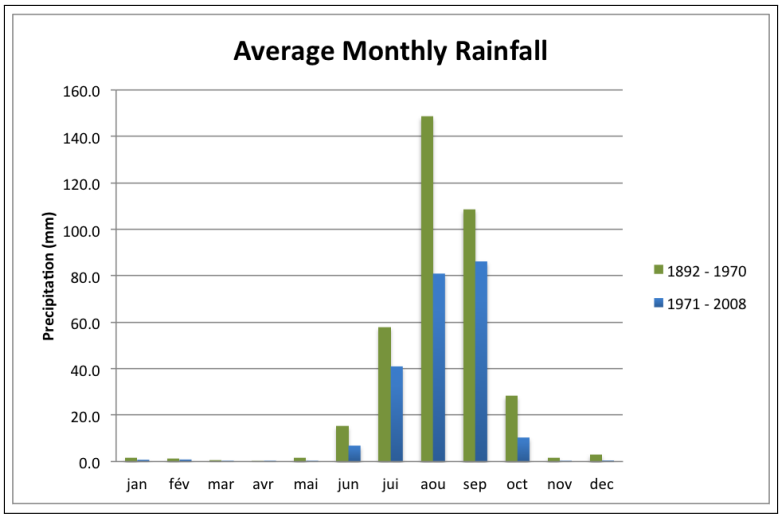

Figure 3: *Average monthly rainfall (in mm), demonstrates the level of contrast between the dry season and the rainy season. Rainfall levels have notably dropped since the 1970's. Data from Saint Louis weather station 1892 - 2008.*

An SPI > 1 signifies a humid year, SPI < 1 signifies a dry year, and SPI < 0 signifies drought conditions.

The SPI thus permits the user to define relative humidity in a given environment, and to reveal patterns in precipitation over 50 years, 100 years, 500 years, or on whatever time scale is the most suitable. With the historic data that is available, patterns in humidity can be charted over the entire 20th century.

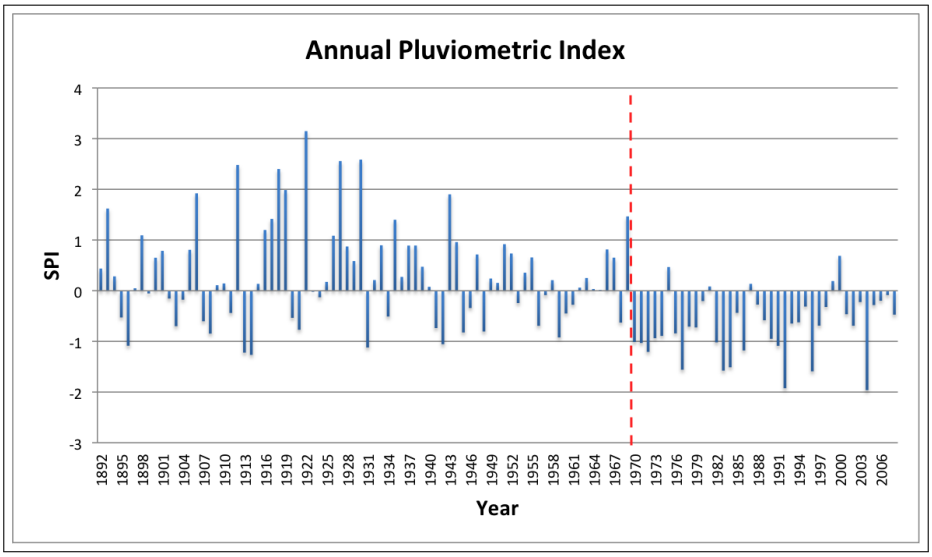

Figure 4: *Standard Pluviometric Index (SPI) calculated for rainfall data from Saint Louis, between 1892 - 2008.*

Figure 4 represents the SPI calculated over the period of 1892 - 2008 with data from the Saint Louis weather station. The dashed red line marks the period around 1968 when the relatively humid climate of the first half of the 20th century began to experience highly deficient rainfall and devastating drought conditions. It is thus clear that the rainfall

regime has undergone an important shift during the last century. From this graphic, the SPI does not one time reach a value of 1 after 1968. The SPI could also be calculated separately in two series: 1892-1968 and 1969-2008, to offer better detail on these separate regimes. The SPI index calculated in these timeframes is displayed in the Appendix.

2.2 Humidity and Evapotranspiration

The humidity that might have been enjoyed by precipitation levels in the delta is significantly diminished by high evaporation, or more accurately, taking into account plant biology, evapotranspiration rates. The rate of sun exposure in the delta region is very high, and vegetation cover is low. These arid and sunny conditions drive high evapotranspiration rates, which exceed yearly rainfall by a rather large margin.[7] Only a very small percentage of rainwater which falls in the delta is able to percolate directly into the aquifer, meaning that recharge by direct percolation is very weak. Nonetheless, previous studies by (Diaw, 2009) and (Gning, 2015) have noted that a small rise is observed in delta groundwater levels with a delayed response after rain events. Still, much of the rainwater will evaporate at the surface. And further, some existing groundwater will evaporate as well. It is the upper basin, with it's humidity and high rains, which acts as a primary fresh water recharge for the River and shallow deltaic aquifer. Ocean water also may act to recharge the shallow aquifer.

(Mean, 2011) used several methods to calculate potential evalotranspiration (ETP) rates in the delta. ETP is commonly defined as the amount of evaporation + plant transpiration that would occur if a sufficient amount of water were available. The methods used were the Thornthwaite Method, the Walker Method, and the Turc Method.

These methods take the following parameters into account, in various combinations, for their calculations: temperature, sun exposure, albedo, relative humidity, and latitude. Averages of these values were calculated with data gathered from the weather stations of Richard Toll (RT) and Saint Louis (STL), between the years of 1996 and 2003. Details may be referenced in the original work of (Mean, 2011). A summary of results is given in table 1.

Method	Annual ETP - STL	Annual ETP - RT
Thornthwaite	1041	1090
Walker	1341	1540
Turc	1538	1790

Table 1: *Annual average ETP calculated between 1996-2003 via weather station data from Saint Louis and from Richard Toll.*^{mean}

(Mean, 2011) comments that the Thornthwaite method almost certainly underestimates the ETP values of the delta, as temperature is the only parameter accounted for in the calculation. The Turc Method is likely the most accurate of the three methods presented in table 1. In contrast, (Diaw, 2008) calculated ETP values of nearly 2300 for the period between 1986 - 2004. In all cases, it may be surmised that the annual ETP values in the Senegal River delta are four to eight times greater than annual precipitation.

3 Land Use in the Delta

Despite an environment with low precipitation rates and high evaporation rates, land use in the Senegal River delta is dominated by irrigated agriculture, made possible by the dense network of fresh river water. And, despite this arid climate, the delta is still one of the most humid regions in northern Senegal and is thus a suitable target for activity demanding large quantities of water. Large areas of the delta have been dedicated to agriculture (both cultivation and livestock) for thousands of years.

The modern Senegalese government is highly invested in promoting self-sufficiency of alimentation for the country, which is a merited investment. Senegal is still a net importer of food, so there is work yet to be done in reaching this goal.[10] The practice of irrigation has been born of these efforts to increase agricultural activity. In addition to irrigation, large-scale activity has been aided greatly by installation of the Diama anti-sel dam and the Manatali dam in the 1980s. Other water management methods include the creation and use of surface water holding ponds, most notably the Guirs Lake.

Figure 5: *Diama dam, February 2016.*

According to the S.A.E.D., in 2012 over 85000 hectares of land were set up for irrigation in the delta out of a potential of 150000 hectares. Over the course of the 19th and 20th century, in addition to extensive installation of irrigated perimeters, great strides have been made in irrigation technology throughout the delta. What began as the digging out of embankments for partial control of seasonal flooding has evolved into extensive canal systems, water pumps, small dykes, and surface drainage canals. The S.A.E.D., a public organization, had almost complete control over irrigated agriculture in the 20th century, and are primarily responsible for ameliorations in water management during this time. In the 21st cenury, agriculture has moved more and more into the private sector.[10]

Multiple types of crops are grown on these lands, including rice, onions, tomatos, and sugar. The method of irrigation can change from one crop to another; where rice fields require flooding for extended time periods (days), tomato and onion fields are flooded and drained in the same day. The timeframe of topsoil saturation is variable, and the amount of water used differs considerably from one crop to another.

Both private/village-level irrigated perimeters, as well as large agro-industry perimeters exist. Small, private perimeters are generally simpler than industrial perimeters. While the existence of such perimeters allows for direct control over activity by villagers or small private holders, these perimeters commonly have poor drainage systems or even no drainage system at all, which can be devastating for soils, in the short term as well as in the long term. Large agro-industrial perimeters are generally more complex, and include a large pumping station, primary canals which disperse water directly from the rivers (usually with the aid of a single pump), secondary canals which disperse water from the primary canal, and eventually tertiary canals which disperse water within a given parcel. Drainage systems exist, although they are mostly surficial and thus highly subject to evaporation and precipitation of dissolved solutes. Perimeters are generally divided into parcels, sometimes with multiple crop types in close vicinity (see figure 6).

Figure 6: *Difference in irrigation methods between rice fields (on the right) and onion fields (on the left).*

There is no doubt, agriculture in the delta can be a devastation for soils which are already salinized and stripped of nutrients. Large zones exist which previously served as irrigated parcels and have since been abandoned due to this extensive soil degradation. To provide relief to soil, parcel rotation is a method commonly used, but even so, there is still a net loss of usable lands.[**?**]

To note, land activity additional to irrigation includes includes villages and the direct needs of these populations. Livestock grazing is also in occurence, which is easily considered to be part of agricultural activity.

4 Geology and Geomorphology

The Senegal river valley and delta are located in the Senegalo-Mauritanian sedimentary basin, which is the westernmost basin of the west african craton. The basin, including the delta, is considered to be a zone in subsidence. The basin is bordered by the Atlantic Ocean

to the west, the Paleozoic Mauritanide Mountains to the east-southeast, the Reguibat ridge to the north, and the Bové basin to the south-west.[20][1]

As previously mentioned, the principal geologic features of the delta result from a series of marine transgressions and regressions during the Cenozoic and Mesozoic eras. Presence of multiple layers of fine-grained deep-ocean facies, separated by larger-grained near-shore facies confirm these occurences. Over the entire basin, these meso-cenozoic deposits thin out from the east to the west. In addition, the deltaic region has undergone at least three transgression periods in the Quaternary alone. This Quaternary transgression-regression pattern has resulted in the formation of multiple shallow aquifers that are separated vertically by marine-sediment aquitards, and separated laterally by Quaternary and alluvial geomorphological units. The shallow aquifers tend to be saline as a result of seawater intrusion.

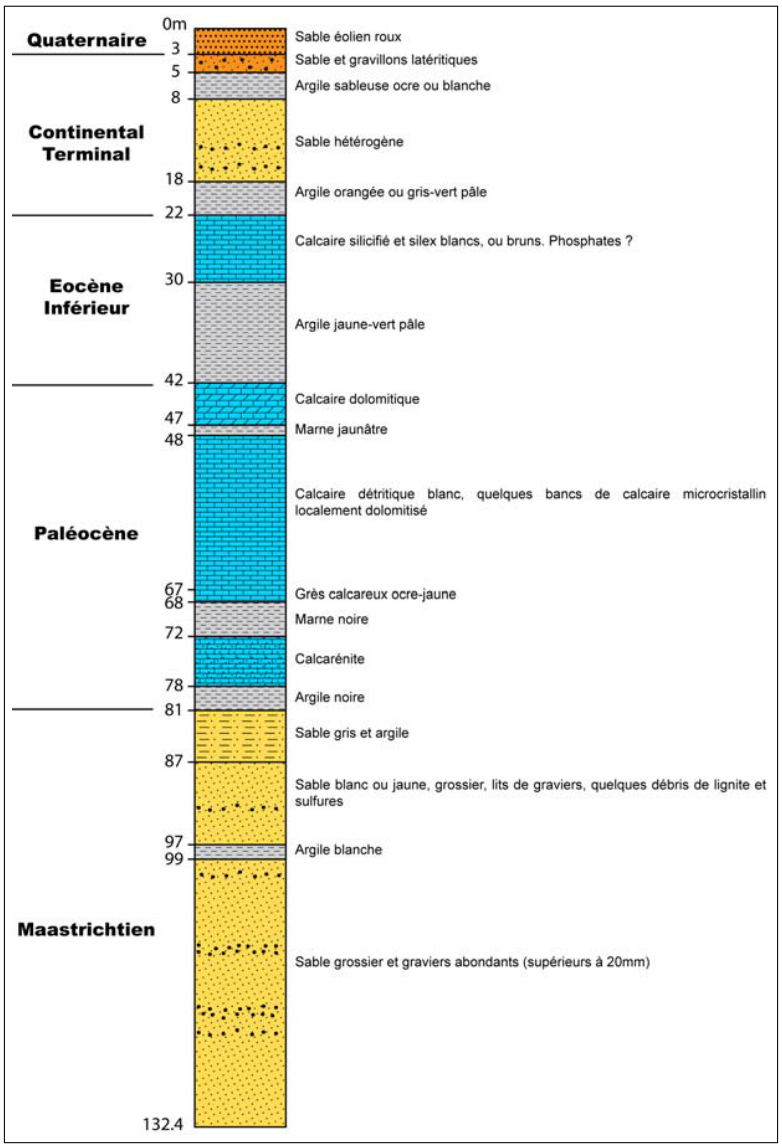

Figure 7: *Geological log from the dome of the Guirs Lake, at the eastern extremity of the Senegal River delta; from (Roger, 2009).*

A geological log, originally introduced in a map of the River basin at 1/200000 by (Roger,

2009), is given in figure 7. This log was taken from the Guirs Lake in the northeast delta. It can be deduced from this log that the 'bedrock', defined below Quaternary and Saloum (Continental Terminal) sediment is of a limestone composition with intercalations of clay and marnish layers. At depth, the large-grained sandstones and gravels of the Maastrictian is intersected. Saturated zones are present in the Quaternary, the Eocene, and in the Maastrichtian.

It is worth noting that along the delta, the 'left bank' and the 'right bank' of the valley differ considerably at the Eocene ages. In essence, the River is flowing near a border between a continental-sedimentary domain and a marine-sedimentary domain. The left bank - on the Senegalese side - is largely marine. The right bank in Mauritania contains a small zone of marine sediments, but is otherwise principally composed of littoral and continental sediments.[10]

The geology of the Senegalo-Mauritanian basin has been coverd by previous authors (Geological Maps, 1969; Audibert, 1970; Michel, 1973; Roger, 2009; Gning, 2015; Mean, 2011; among others). In this report, the geological focus will rest with Quaternary and alluvial sediments. These layers are the most significant for the geomorphology, hydrogeology, and salinization dynamics in the valley and delta.

4.1 Quaternary Period

The Quaternary Period is defined from 2.59 million years BP (before-present) to the present, and is formally divided into the Pleistocene and Holocene epochs. This period is defined all over the world by cyclical glacial and interglacial terms and the climactic and environmental evolutions that came with these cycles. Quaternary deposits of the Senegal River delta leave testimony of fluctuating sea levels and subsequent changes in humidity as a result of these cycles. This period has given direct form to the modern morphology of the delta and valley.

A geological map of near-surface sediment in the delta is given in figure 8. As can be seen, Quaternary and alluvial sediments in the delta are somewhat diverse, as a result of the unique interactions between a fluvial deltaic environment with that of a coastal and oceanic one in a semi-arid environment. The evolution of river meander paths and of marine invasion in the delta has created such morphological units as settling basins, alluvial sand bars, alluvial terrasses, alluvial dunes, lagunar sands, wind dunes, and iron formations. These units differ in their origins, composition, granulometry, topography, orientation, and salinity. Sand dunes are largely of eolian origins during exceptionally dry periods, while settling basins are of fluvial origin. Settling basins are of relatively low elevation, and tend to have lower permeability over their surface areas due to the presence of silt and clay layers. Consequentially, these basins are most often sought after for cultivated parcels due to their low elevation and ability to hold water at the surface for field flooding. On the other hand, fluvial and oceanic terrasses, as well as sand bars, are of a relatively 'high' elevation and often contain some of the most saline waters in the delta - concentrated brines - due to the fact that invasive marine waters are easily isolated from regular groundwater rinsing. The same salinity issue may be observed in sand dunes and ergs.

The two monitoring sites constructed for this study are outlined in black-dashed ovals in figure 8. At both sites, note the presence of sediments labeled "FlZ4", which are fluvial-lacustrine (lakeside) clays and silts making up the aforementioned settling basins. At

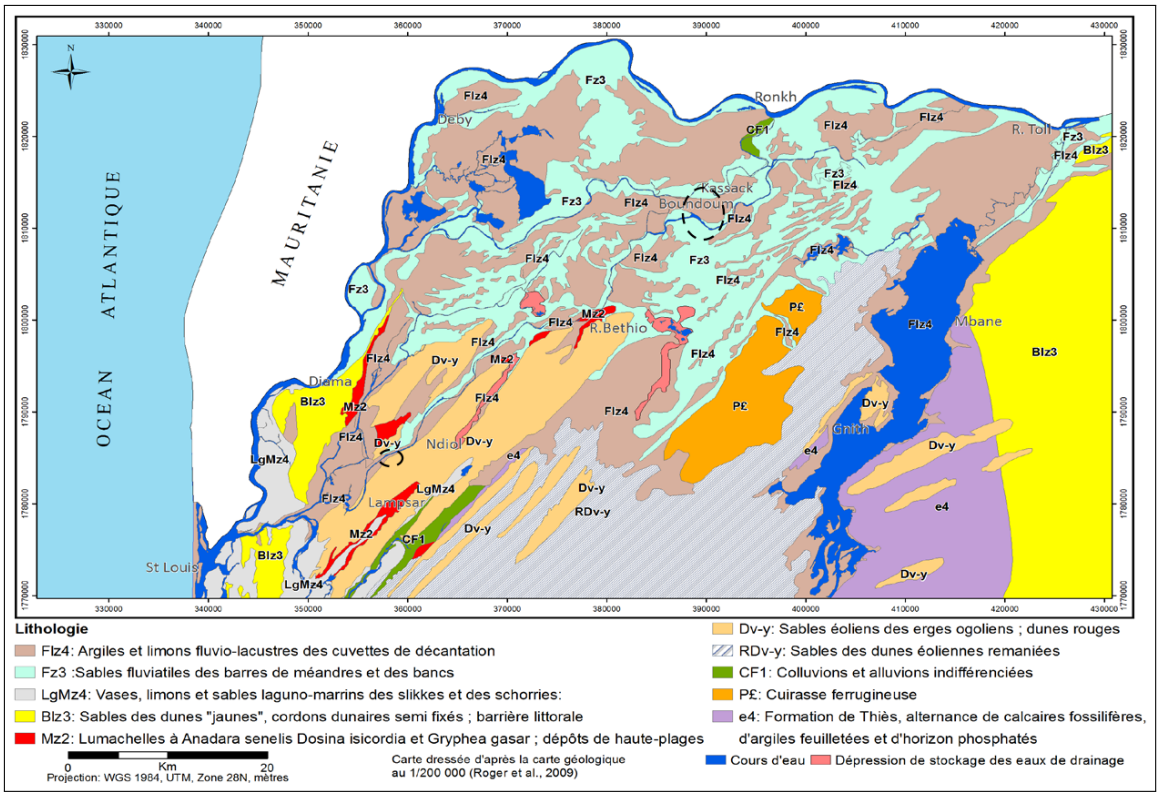

Figure 8: *Geological map of the Senegal River Delta, with study sites marked by dashed circles. From (Gning, 2015).*

the north-eastern site, near the village of Kassack, there is also significant presence of sediments "Fz3", fluvial sands making up point bars. On site, point bars are recognizable due to their higher elevation ($\pm$ 0.5 - 1 meter difference). Clay and silt layers are sometimes encountered below the surficial sands of these point bars. Finally, at the south-west site, near the Lampsar, a boundary with "Dv-y" red sand dunes is approached. It can be expected that these different morphological units will have differing salinity profiles.

A spatial difference in sediment is observed; in the N-NE, the soil has been most directly impacted by the River and it's evolving meanders, and is dominated by clay settling basins and alluvial sands making up point bars, whereas the S-SE contains ergs and dunar sands (yellow and red) and lagunar sedimentation, alongside settling basins and some alluvial sands.

4.1.1 Quaternary Transgressions

Three major transgressions have taken place during the Quaternary period. From (Gning, 2015), the timeline is as follows:

- A transgression during the Tafaritian, in the lower Quaternary, approximately 125000 years PB. The ocean penetrated over 100 km inland, and made a golf out of south-west Mauritania as well as the northern parts of the delta. Generally compact iron oxide deposits in the valley and delta in this era give testimony to a humid climate.
- An Inchirian transgression, during the middle Quaternary, approximately 40000 years

BP. This transgression was multi-phasic and consequently known under the Inchirian I and the Inchirian II. While the Inchirian I left more clay deposits, the Inchirian II left sandy-clay deposits, giving testimony of the difference in intensity of these two demi-transgressions. This period created once again a golf in Nouakchott, south-west Mauritania, although smaller than the golf which existed during the Tafaritian. Sediments from this period speak of shallow marine origins, falling in the range of sand and sandstone, clayish sands, and some presence of pure clays which speak of deeper marine environments.

- The Nouakchottian transgression, in the upper Quaternary, approximately 5500 BP. This transgression was smaller an magnitude than the Tafaritian or Inchirian, with sea levels roughly two meters higher than the current level.[1] The ocean infiltrated high into the River valley, creating an inlet up to the town of Bogué in Mauritania. The delta was entirely submerged during this time. The Nouakchottian is arguably the most influential transgression on the modern-day morphology of the delta. Upper Quaternary sediments in general contain some of the most important information of all delta sediments.
- Some authors discuss subactual transgressions, such as the Dunkerkian, approximately 4000 years ago.[5] This goes to say that fluctuations in sea level have continued to occur since the Nouakchottian, albeit in smaller magnitudes.

Each transgression was evidently separated by a marine regression. The most remarkable of these regressions was during the Ogolian, approximately 21000 years BP, between the Inchirian and Nouakchottian transgressions. The Ogolian regression, known worldwide as the "Würm Regression" was an extremely dry period during which the ocean retreated by approximately 100 meters. It was during this regression that the red dunes as well as the yellow dunes and sand bars (see fig. 8) were formed. Over 10 meters of medium and large-grained sands were deposited in the delta during this period. Due to the presence of these yellow sand bars, the Senegal River adopted an endorheic regime for some time.

Between regressions, transgressions often flooded out and reorganized much of the sediment deposited during previous dry periods. Between transgressions, the River played it's own role in cutting and reworking sediments deep into the delta. Large portions of the red and yellow dunes have been cut away by the ever-evolving meander paths of the River.

Since the Nouakchottian transgression, the current form of the valley and delta have evolved. As the sea level slowly regressed from the height of the last transgression to current levels, oceanic winds swept sands to the coast to form a barrier beach which separated part of the Nouakchottian golf, locking an important quantity of marine water into the continent as a lagoon. Much of this lagunar water has evaporated, leaving behind marine salt precipitates. The lagoon has since been filled with sediment deposited by the River, thus, most water left from this lagoon has concentrated into brines.[20] Some aspects of this evolution can be seen in figure 9. Currently, it is river dynamics which play the dominant hand in morphology and sediment dispersion. There are currently four to six meters of sub-actual and actual sediment on top of the Nouakchottian sediments.[5]

4.1.2 Soils and Landscape Morphology

The oscillations in sea level that have occured in recent geologic time, as well as river carving into lain out formations, have resulted in a characteristic geomorphology in the landscape,

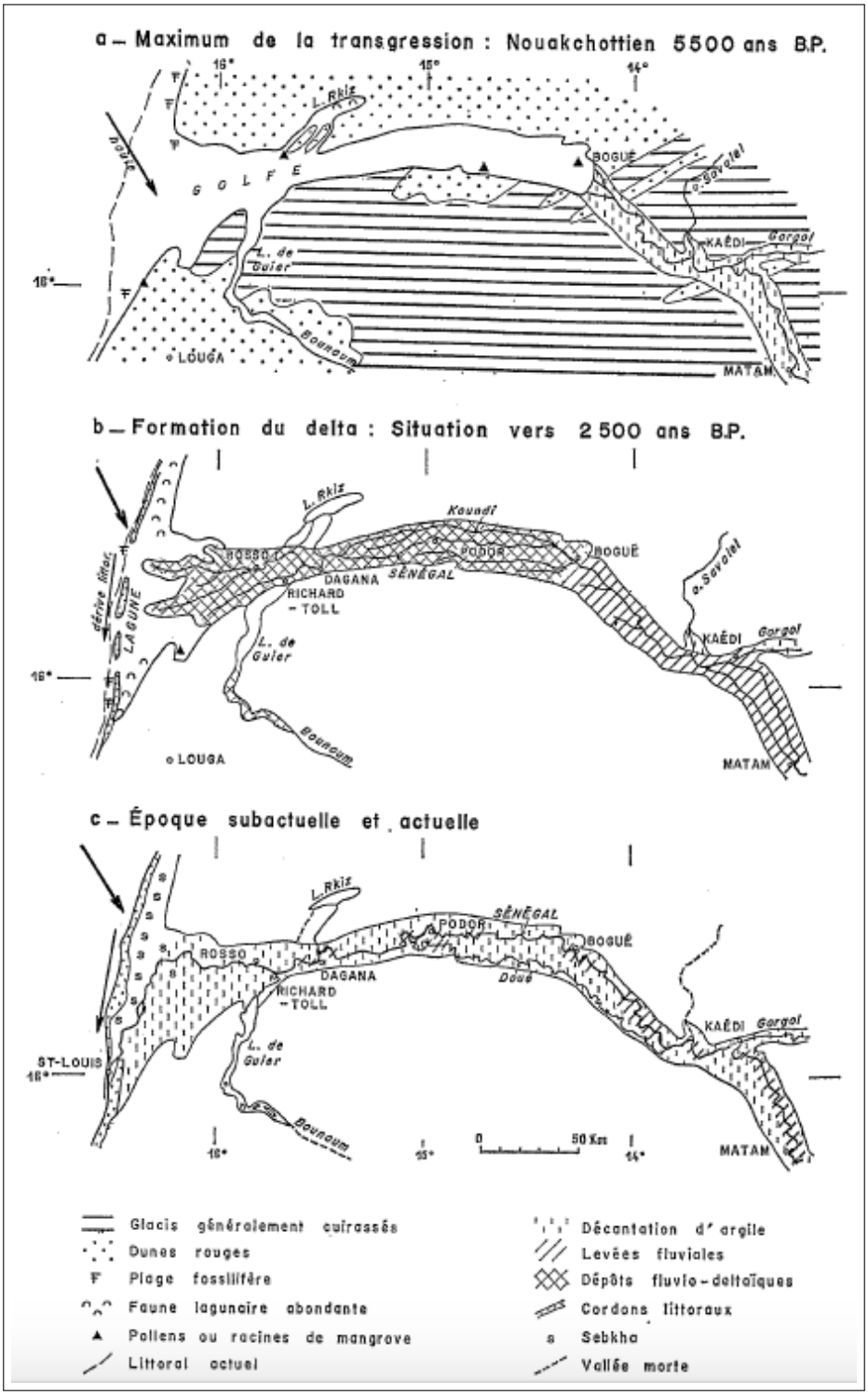

Figure 9: *Evolution of marine water presence and River path in the delta under subactual dynamics. Image from geological map notice of (Michel, 1973).*

made up of multiple units that can be tied to certain time periods and hydraulic activity as well as salinity characteristics. Tthese units may be sorted by their origins, topographical features and notably their sedimentary composition.

The morphological units found in this region are typical of a coastal environment and a fluvial environment. Some units are also common for arid regions. Units tied to river activity are those such as levees, point bars, settling basins, rupture deltas, and fluvial terasses, without mentioning the bed of the river and it's connected streams. Coastal landmarks include coastal sandspits (barrier beaches) and lagoons. Ergs and dunes are the major desertic landmarks. A concise schema of the deltaic landscape is taken from (Deckers et al, 1996) and offered in figure 10. All relevant landforms are noted, illustrating also the topographical differences between them.

The speed as well as the direction of the granular transport force - generally either wind or water - is what predominately controls landform content. The medium-to-large sand grains that comprise dunes, ergs, and sandspits are carried by relatively high winds, whereas clays and silts found in settling basins were deposited by slow moving waters at the bottom of a riverbed, or essentially stagnant waters at the bottom of ponds and lakes. Sands and silty sands found in point bars are deposited generally by moderately flowing river water.

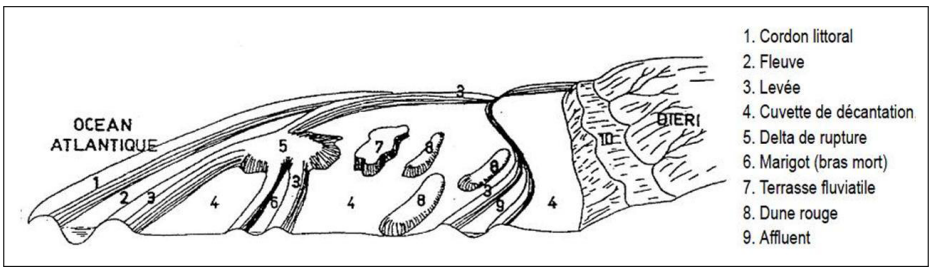

Figure 10: *Geomorphological units comprising the Senegal River delta, from (Deckers et al, 1996).*

The delta flood plain of the Senegal River includes a variety of geomorphological units - all areas which may be flooded by a river overflow; this includes sediment basins, riverbanks, and rupture deltas. The topography of the landscape is directly tied to these units. For example, sediment basins correspond to topographical depressions, whereas riverbanks correspond to elevated zones. In the event of a flood, the riverside levées can break down. This type of event can lead to berge formation.

The Dunar landscape of the delta contains two principal elements: marine terrasses and dunes. Marine terrasses are found between sand bars, and can extend over 4 km in length. Terrasses make up a transition zone between flood zones and non-flood zones. Dunes, on the other hand, come in several times: pre-littoral dunes, dune bars, and red dunes. Pre-littoral dunes are yellow dunes located in the upper quaternary sediments. These are covered by a shrublike and treelike clear steppe. Dune bars are the remains of large ergs of red dunes, have retained a large slope. Red dunes are of low relief also result from large middle Quaternary ergs, which have undergone a large amount of erosion.

A discussion on soils is an important element in fully understanding groundwater salinity mechanics. Nonetheless, such a discussion diverges somewhat on the current undertaking which focuses on groundwater and surface water interactions in a more direct manner. For now, further information on soil chemistry, the reader may consult the study on (Deckers et al, 1996), as well as (Gning, 2015).

5 Hydrology and Hydrogeology

The water cycle within the Senegal River delta represents one of a meeting place between fresh and saline surface waters, with the Atlantic Ocean having profound influence on the adjacent continental unit. The history of recent marine transgressions and regressions has left its mark not only on modern-day sediments, but also on water composition. Modern-day seawater invasion is still known to occur.

The Senegal River delta offers a relatively dense and complex hydraulic network, made up of the Senegal River, various tributaries and distributaries, holding ponds, groundwater, and eventually the Atlantic Ocean. Communication occurs between all of these elements punctually, if not continually. As it should be known to the reader, water body communication is facilitated by the water itself, as sediment and ion transport may move throughout the aqueous phase relatively easily. Sedimentary morphology also plays a large role in controlling which water elements communicate, to what extent, and where it occurs. There are multiple aquifer layers in this region, and the level of communication tends to decrease with aquifer layer depth. The Maastrichtian and Eocene aquifers in the delta are not as sensitive to external impact as the superficial aquifer system. Most surface water bodies leave significant impact on the composition of superficial groundwater and aquifer sediment.

Coastal transgressions have been a primary shape-makers of deltaic hydrogeology, although the river has also left an important mark, with ancient meanders and sediment transport effecting the modern-day water signature. The current course of flow is influenced by geomorphologic formations such as sand dunes, levees, and lagoons. Topographical depressions corresponding to a subsidence zone are able to serve as holding ponds. These depressions are found throughout the delta and are both natural and man-made.

It is in large part for these reasons that groundwater in the shallow delta is saline. Marine transgressions are ever-occuring, but historical events have left behind significant ionic deposits, which are now in contact and dissolving into any modern groundwaters which pass through the reservoir. The Senegal River is the only regular source of fresh water available to the groundwater. Communication between the River and the groundwater is a likely occurence, but the extent of such communication is indetermined.

5.1 Senegal River

The Senegal River runs over 1790 km in it's entirety.[10] The upper basin and headwaters are located in the Fouta Djalon highlands of Guinea, a region that is significantly more humid than the lower valley and delta. The entire river basin measures 289 000 km^2, of which nearly two-thirds are considered 'upper basin'.[30][10] Details on recharge and influential climactic factors, especially on rainfall patterns, in the Senegal River delta have been developed in section 1, 'Geography and Climate'. What should be taken away from this is that healthy rainfall patterns in the upper basin are essential for recharging the entire river every year.

The annual output of the Senegal River in and around the delta has been quoted by the local Senegalese organization, named *l'Organisation pour la Mise en Valeur du fleuve Sénégal*, or 'OMVS', at 20 billion $m^3/year$ on average, with such extreme variations as an average of 41 billion $m^3/year$ during surplus years, to 6 billion $cm^3/year$ during exceptionally

dry years. These values were calculated from data coming from Bakel, in the high valley. Studies by (Moctar 2010) has quoted an average annual output of 11 billion $m^3/year$ in the delta itself.

The availability of water from the River is a direct influence on the level of infiltration into groundwater along the entire length of the riverbed. The direction of flow between groundwater and surface river water is dependent on the height of the river, and under a natural regime, this can totally invert between the rainy season and the dry season. The flow rate and river head can also evolve significantly along the river's course due to the land topography and the width of the river bed. These characteristics of the main River will influence the availability of water and communication to the River's affluents and defluents.

The natural flow regime in the Senegal River is characterized by an alternance of river water levels which depend on the climactic rainy season and dry season. The river can go from 50 cm height in the height of the dry season to over 450 cm height in height of the wet season 'crue'.[10] Under this regime, water availability for agriculture and other use becomes a somewhat variable factor. To make for a more linearly constant availability of fresh water in the river, the two dams previously mentioned - the Manatali and the Diama - have been constructed such that an artificial flow regime is established in place of the natural regime. The Manatali dam is in the upper basin, in Mali, and the Diama dam is in the delta at Diama, Senegal.

Formation of holding ponds, carved out naturally by the River and the variability in it's seasonal flooding, has created a significant microrelief in the landscape.[20] This microrelief supports a relatively important quantity of fresh water in it's natural landscape depressions. A testimony to this fact is the potentiel of the depression that the Guirs Lake occupies.

Of more direct influence on fresh water availability in the delta would be the presence of secondary axes, which provide conduits deep into the delta landscape.

5.1.1 Secondary Axes

Secondary axes (tributaries and distributaries, holding ponds) are present along the entire river length. Their presence acts as a natural distribution system of an important fresh water resource, thus increasing the fertility of the neighboring land. The size of the River and the relative density of secondary axes (distributaries and tributaries) in the delta is such that it is possible to support the hydraulic needs of irrigated agriculture. It is the presence and effect these axes which are directly investigated in the subsurface.

Major tributaries and distributaries of the River in the delta include[10]:

- **Djeuss** is a natural water reserve which flows 35 kilometers, taking it's source from the Lampsar distributary and flowing towards the Gorom Downstream distributary. This flow takes place because of water-management construction.
- **Gorom Upstream** takes it's source directly from the Senegal River and runs for 25 kilometers. From personal observation, this distributary is significantly overrun by invasive plant species in some areas, which surely degrade the potential of flow.
- **Gorom Downstream** takes it's source from the Senegal River, further downstream where the riverbed is nearly parallel to the ocean. It runs for 31 kilometers from

the River to the village of Boundoum-Barrage where it joins the Gorom Upstream. Usual direction of flow is opposite of the direction of flow of the Gorom Upstream.

- **Kassack** takes it's source from the Gorom Upstream and flows for 20 kilometers until it joins with the Lampsar.
- **Lampsar** a tributary which takes it's source from the Gorom merging point and flows 71 kilometers into the Senegal River in the low delta. The Lampsar has one of the most important flow rates of all secondary axes in the delta. It is reinforced by a canal which was dug between the Gorom Downstream and the Lampsar, which increases alimentation.

The flux of water flow in these water formations is intimately tied to the flux of water coming from the Senegal River. Additionally, all of these axes are to some extent surrounded by irrigated parcels and used to aliment such parcels, which adds an anthropic element to surface water dynamics.

Station	H_0 [cm]	H_{crue} [cm]	$Q_0[\frac{m^3}{s}]$	$Q_{crue}[\frac{m^3}{s}]$
Ronq (Gorom)	150	175	8	13
Ross Bethio (Lampsar)	110	200	1.50	5

Table 2: *Average height and flux of some Senegal River secondary axes in the 1990's. Source: Bader and Cauchy with OMVS, 2013.*

Debit and height of river water measured at some stations in proximity to these primary axes is given in table 2. The Gorom Upstream and the Lampsar correspond to the locations of the study sites for this project.

This fresh water system's impact on the groundwater by recharge is an investigation point for this project. If such a communication exists, then the hydrodynamic and hydrochemical properties of the river will be an important factor for the impact of any interactions, especially when invading the groundwater. Despite this, parameters river water dynamics were not collected directly for this study.

5.2 Groundwater

There are three major aquifer systems: a shallow aquifer in the alluvial sediments and Quaternary sediments, the Tertiary (Eocene) aquifer, and the Maastrichtian aquifer. This system plays a very essential roler for resources in the large arid regions of Senegal. Currently, all of these aquifers are exploited for municipal or agricultural use.[21]

The Maastrichtian is the oldest aquifer in the delta and is present throughout the entire Senegalese basin. It is predominantely made of large-grained sandstone, although clay passages are known to exist. It's thickness is variable, increasing by an order of magnitude from the east side of the delta to the west and southwest. It reaches approximately 50 meters depth at Dagana (some 20 km east of Richard Toll), and between 150 to 200 meters depth to the west, and even up to 400 meters depth in the environs of Saint Louis.[28] It is presumed that this aquifer reaches close to 150 meters depth in the study zone in the delta. The Maastrichtian aquifer contains fresh water and is the most exploited aquifer for municipal distribution in Senegal.

The Tertiary aquifer includes Paleocene as well as Eocene layers, and is essentially made up of limestone and marl-limestone. While the paleocene is encountered around 50 meters, the Eocene is met around 25 meters depth. Saline water exists in parts of this aquifer within the delta.[28]

Near the surface, an aquifer system including alluvial sediments and Quaternary sediments is identified. Morphology, granulometry, and mild topographic changes separate the general Quaternary sediments (generally identified as yellow and red sand dunes) and the alluvial sediments (silty sands, silts, and clays of settling basins and of meander bars). This change leads to variations in communication between the two aquifers as well as differences in salinity. Throughout most of the delta, it is the alluvial aquifer where the focus lay.[10]

Within the alluvial aquifer system, two saturated reservoirs are identified. The upper reservoir is contained within the Nouakchottian sediments, and a lower reservoir is contained within the Incirian II. It is believed that these two reservoirs are separated by a layer of impermeable clays (aquitard) in certain locations, whereas in other locations, the two become a multi-layered single reservoir[7][10],[28]. In all cases, these two layers are in regular communication with one another. The thickness of the Quaternary aquifer is also quite variable, increasing from 5 meters to the NE at Richard Toll, down to 30 meters depth near Saint Louis.

Due to the partial permeability of the shallow aquifer from the surface, atmospheric conditions will affect shallow groundwater conditions. Notably, high atmospheric temperatures cause high groundwater temperatures. Where river water temperatures are in the environs of 20°C, data from the current study has measured shallow groundwater at 27°C and higher. High temperatures and high temperature differences is consequential for the rate of physico-chemical reactions between waters and with the aquifer matrix. The thermodynamics in this region play a role that is significantly more active than in such a temperate climate zone as Liège.

5.2.1 Hydrodynamics of the Alluvial Aquifer

The alluvial aquifer extends from the surface of the earth down to the Eocene, which has variable depth, from 15 to 30 meters. These two layers are in discordance. There are areas in the delta where the Eocene is not present, such that the alluvial and Quaternary extend to the Maastrichtian.

The hydrodynamic parameters of the alluvial aquifer found in literature vary from one study to another. This is due in part to the fact that the aquifer's granulometry is heterogeneous and anisotropic. While this aquifer is semi-captive, it may be fully captive to flow from N-S.

Some of these important hydrogeologic and hydrologic parameters can be found in (Bader et al, 2013), (Diaw et al, 2010), and (Gning, 2015), among others. An average can be calculated in order to formulate a general order of magnitude of such parameters. These averages are noted in table 3. When using these values, it must be kept in mind that they are useful for general estimating, but they do have spatial variation.

The range of hydraulic conductivities **K** is in agreement with 'standard' conductivities for unconsolidated clays, fine sands, silts, and only the occasional larger sands.[28] The presence of clay again signifies that the aquifer is only semi-permeable.

Parameter	Average Value	Variability
Groundwater Temperature	29°C	$\pm 3°C$
K (m/s)	$1.5\,x\,10^{-4}$	$\pm 10^{-2}$
T (m^2/s)	$6\,x\,10^{-4}$	$\pm 10^{-2}$
S	$1\,x\,10^{-4}$	$\pm 10^{-1}$
h	1 - 6 m	0.5 - 7 m

Table 3: *Average of values of hydraulic conductivity, transmissivity, and storage coefficient found for the alluvial aquifer.*

5.3 Groundwater Salinity

The level of intensity of salinization can lead to total devistation of cultivated lands. Due to the importance of land cultivation in the delta, efforts have been made to slow or stop these phenomena from occuring, as previously mentioned. The anti-sel aspect of the Diama dam has saved thousands of hectares from this fate. In addition, the River path of the low delta has been deemed an area that is essentially off-limits for marine waters which are looking to invade. In a natural flow regime, the annual magnitude of marine intrusion is dependent on pluviometric levels of at least the previous wet season. Since installation of the Diama dam, marine intrusiuns have been blocked along the riverbed of the low delta, which has indirectly slowed marine invasion into the groundwater. Nonetheless, especially as recent droughts have made additional space for seawater intrusion into the superficial aquifer, some level of marine invasion directly from ocean to groundwater may be occuring. The prolonged period of rainfall deficit which is currently underway may be re-compounding the issue.

In the studies of [14] and [23], a water salinity classification system between fresh, brackish, and saltwater is used, using Cl^- and conductivity values, with the following limits:

Water Type	**[Cl^-] (mg/L)**	**Conductivity (μS/cm)**
Fresh	<150	500
Brackish	150 - 10000	500 - 25000
Brine	>10000	>25000

Table 4: *Source: Kirsch 2009 and Nguyen et al. 2009*

Historical data from (Gning, 2015) and other studies have found the quaternary aquifer to be brackish, at best, and with some areas classified as shallow brines. Groundwater samples have been found with salinities falling between 4 and 50 ppt. For this reason, a classification system equipped specifically for saline waters is a better employment. A simple, more specific system which has been used in literature[12] can classify saline waters. Salinity is still represented by chlorine concentration.

In addition to the values in table **??** any salinized groundwater found in the delta could be classified as "polyhaline" when salinity is lower than the that of seawater, and "metahaline" when the measured salinity is higher than the salinity of the adjacent seawater.[25] To note, seawater on the coast of northern Senegal is reported to have a salinity value of approximately 35 ppt[29], or equivalently, roughly 50000 μS/cm.

Agricultural activity adds complexity to the system, as the semi-permeable shallow aquifer is open to infiltrating irrigation waters. Infiltrating waters can stimulate a rise in the

Water Type	[Cl^-] (mg/L)
Fresh	<500
Marginal	500 - 1000
Brackish	1000 - 2000
Saline	2000 - 10000
Highly saline	10000 - 35000
Brine	>35000

Table 5: *Source: Department of Water, Government of Western Australia*

already-shallow water levels, making for the presence of an *extremely* shallow aquifer (<1 meter, or <0.5 meter on riverside). Fresh irrigation waters tend to push the resident saline waters further down into the aquifer and dissolve the evaporites which exist in the rock matrix. When in the aqueous phase, salts can be driven to the surface via capillary rise, and deposit as precipitates when the groundwater evaporates. Recall that evapotranspiration measured in the delta falls between 2000 - 2500 mm/year.

Another issue with agriculture is the surface drainage system, which also stores water at the surface to evaporate and deposit precipitates. These waters may contain marine salts as well as ions in solution from agricultural activity itself (pesticides, herbicides, etc.).

If River water serves as a source of fresh water in the shallow aquifer, there is hope that some of the impacts of salinity in the soil may be mitigated. Freshwater intrusion into salinized groundwater is a well-recognized phenomenon and is discussed by many authors, for example (Reinhard, 2009).

5.3.1 Fresh and Saline Water Interfaces

The hydrodynamics of the delta portray sharp temporal contrasts, congruent with the availability of fresh water and fluctuations in surface water levels as well as groundwater levels. It is even possible for flow direction to invert between the dry and wet season due to considerable changes in water head. For these reasons it is expected that an interface between saline and fresh water, as well as the shape and extension of the intruding body (fresh water, in this case) will evolve each year to a certain extent, through a cycle corresponding to the rainy season and the dry season.

Conceptually, it is thought that during the dry season, river levels are low and groundwater levels are low due to lack of recharge. Surface water levels may fall below sea level, which, depending on groundwater head, may set or at least slow the direction of flow. Any possible groundwater recharge from the riverbed is diminished for an extended period of time. Marine invasions can also encroach on the riverbed under a natural regime.

During the wet season, important quantities of rainwater in the delta and especially from the upper basin flood into the river and the groundwater, stimulating a rise in the groundwater table and in river water levels and flow rates. Water levels can again rise above sea level, often to an extensive degree, and then reinforce a direction of flow from river to subsurface for an extended period of time.

(Gning, 2015) has organized hydrodynamical data from both dry and rainy seasons spanning over 10 years: from 1997 - 2011 and 2011 - 2014. Concise comparisons of river levels, water table, and pluviometry are included, allowing for dynamical correlations to

be detected. River levels are generally higher than groundwater levels in the rainy season. Throughout a given year, there are periods when surface and groundwater levels have reached levels that are roughly equivalent, and when groundwater levels depass river water levels. Even so, even during the dry season, groundwater head over surface River water is limited and is a minority event. The direction of flow is thus predominately from River into groundwater. The impact of the Diama dam is visible in the data, and it's net increase in control over seasonal water fluctiation is very evident. The increase in the water table due to irrigation is included. Other direction-of-flow factors include River and groundwater flow *rate* and local geology.

Seawater intrusions into continental regions have been studied rather extensively, to the point where analytical relations have been constructed to dimension marine and groundwater interfaces, modeled after a so-called 'salt wedge' effect. This rule *Ghyben-Herzberg relation* brings together an interface depth and interface form, dependent on relative densities member bodies of water. Fresh water intruding into the salty aquifer is another story. The form of this fresh water layer may be similar in form to what results from marine intrusion, but since the specific dynamics differ, the specifics of shape will also differ.

Some generalities of such a resulting form can be gathered by noting certain hydrodynamical characteristics. Again, water body density can be discussed. On the discussion of local terrain, site-specific flow paths can be drawn out. For example, as the Senegal River bed contains an important quantity of clay sediment, River water intrusion at the bottom of the River is probably of limited expanse.

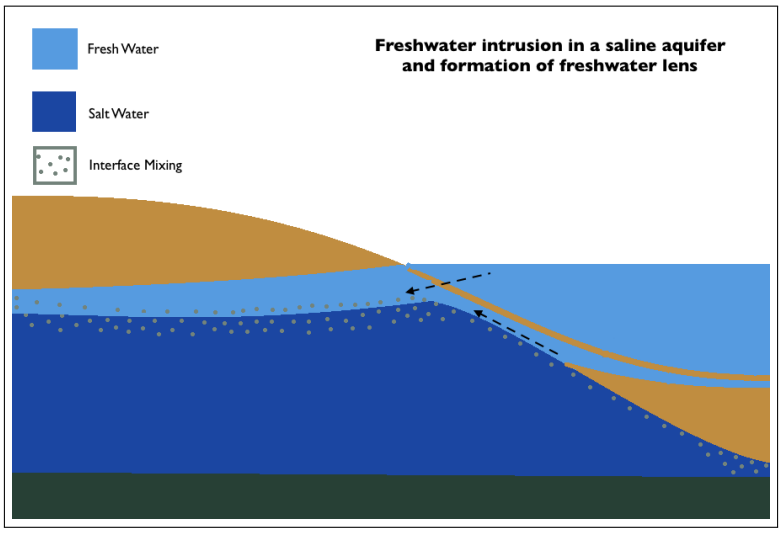

Figure 11: *Conceptual schema of hypothetical freshwater intrusion into salinized groundwater. The dark green slice represents an impermeable zone. This schema is based on the model of seawater intrusion into fresh groundwater. Not to scale.*

A generalized schema of river water intrusion is given in figure 11. Drawing out this simplistic model allows for formating a starting point for a model which will (hopefully) be more developed with time and as more data is collected. For example, fine sediments at the base of the riverbed means that fresh water is not leaking into groundwater at this point. Below the riverbed is likely already saturated in any case. Intrusion would then occur only at the sides of the riverbed, near the bank. Also, historical data suggests that an important interface zone of mixing would exist at the interface of the two bodies. To complete a model of the interfaces existing in the delta, thermodynamics and flow regimes

must also be integrated.

Part II

Experimental Approach

Multiple monitoring methods were used in the interest of characterizing groundwater salinization and River water intrusion in the Senegal river delta. Collection of data for this study was founded on field work. This included hydrochemical monitoring as well as geophysical profiling over multiple selected sites.

Field work was performed during the months of February and March 2016, in the middle of the dry season. This means that all data collected will reflect the conditions of this particular season. Hydraulic and hydrologic conditions in the rainy season may significantly differ (soil washing, increased water levels, change in direction of flow for surface and groundwater, ...). It is important to recognize these differences in order to properly analyse data and the dynamics that are represented. A more complete study should include data from both seasons, or rather, year-round data monitoring.

All field work was performed alongside two students from the University of Cheikh Anta Diop in Dakar - Cheikhna Dramé and Elhadji Moussa Sarr. Technician Jules Keita helped with peizometer installation and all field work that followed.

6 Description of Sites

Interactions between fresh surface water and saline groundwater are assumed to occur around the numerous tributaries and distributaries in the delta, as well as around the Senegal river itself. For this study, three sites were chosen, located in two areas - Kassack and Ndiaye, which integrated two distributaries into their networks. The locations of these areas are positioned in figure 8 found in section 4, along the Gorom Upstream and Kassack, and along the Lampsar. The choice of experimental monitoring sites for this study aimed to meet the needs for better understanding the complex GW-SW interactions. Based on previous findings[10][30], the expectation coming into this work is that groundwater adjacent to surface water will be considerably less saline than inland groundwater.

Piezometers at every site were installed along a linear axis which is perpandicular to the closest distributary. This configuration aims to capture a cross-section of the groundwater profile from riverside to inland. Each site differs in expanse, in proximity to surface water, and importantly in the surrounding physical environment. A simplified schema of this setup is given in figure 12.

There are mild differences in the distributaries considered for this project. The Lampsar, for example, is larger than the Gorom Upstream and the Kassack, and has a much more important flow rate. Within the Gorom Upstream, an important quantity of invasive plant species have overrun certain areas, which decreases the flow rate considerably. This plant invasion was observed on the riversides of both the Kassack 1 site and the Kassack 2 site. These characteristics are presumed to affect the magnitude of surface water penetration into the aquifer.[7]

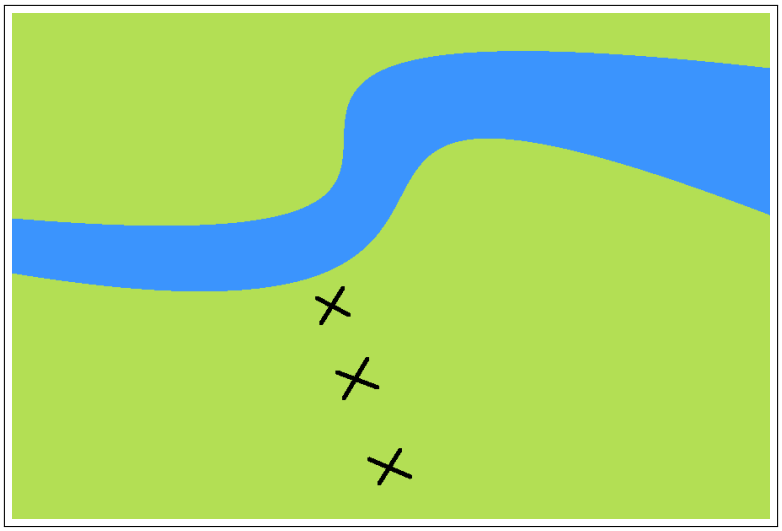

Figure 12: *Simplified schema of piezometer setup per site. Each* ***X*** *represents a piezometer up to the distributary stream, in blue. Each site differs in distance between piezometers and in land use.*

6.1 Kassack 1 and Kassack 2

Two sites - Kassack 1 and Kassack 2 - were chosen between the Gorom Upstream distributary and the Kassack distributary.

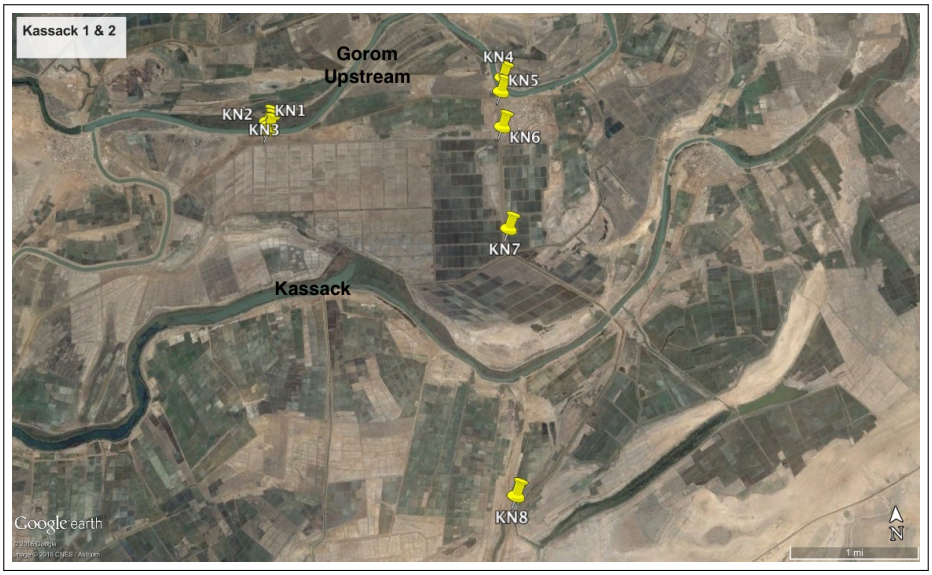

Figure 13: *Localization of piezometers installed at Kassack. Variable land use and distance from river distributary is visible. Satellite image via Google Earth.*

Figure 13 gives a satellite image of the area considered at both Kassack 1 to the west and the more extensive Kassack 2 to the east. Kassack 1 and Kassack 2 are separated by approximately 3 kilometers. Both are along the Gorom Upstream, but as shown in the satellite image, the Kassack 2 site also brings the Kassack distributary into account.

Kassack 1 is the smallest of all our study sites, with a total length of 150 meters from a

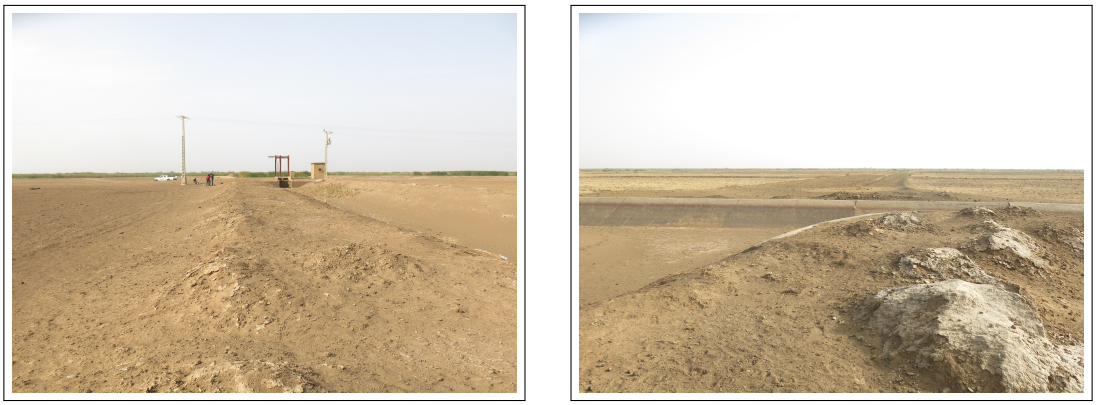

Figure 14: *The local terrain found at Kassack 1 shows dry, empty canals and a shut-off pump, with old, dry parcels in vicinity.*

first peizometer to a last piezometer, and a length of 200 meters for an ERT profile. There are dry irrigation canals and an out of use water pump on site. The dryness and imprint of ancient perimeters can be seen in the field images displayed in figure 14. It seemed that there was no significant land use going on around this site at the time of monitoring.

Kassack 2 extends over 5 kilometers and traverses land of mixed use, as can be seen in the satellite image (figure 13) of Kassack. An irrigation pump is located on the Gorom Upstream close to the riverside piezometer, active during the entire timeframe of study. A large primary canal at the site was filled by the pump, and was punctually included in field conductivity measurements. Three piezometers from the Kassack 2 configuration are also near secondary irrigation canals and active irrigated parcels, both of rice fields and onion fields (implementing different methods of irrigation).

Figure 15: *Salt precipitation observed at the surface near the KN4 piezometer, along the Gorom Upstream distributary.*

Salt precipitation was observed at the surface, notably near full primary irrigation canals and a water pump at Kassack. An example of surface salt precipitation can be seen in figure

15, which was observed within 20 meters of the Gorom Upstream riverside. Surface water overflow was observed near KN4 around the irrigation pumping station, and observation suggests that the evaporation of this surface overflow is the source of precipitation. With presence of such a shallow water table, this overflow greatly facilitates capillary rise to the surface, and thus vertical solute transport to the surface. High evaporation rates then lead to precipitates. Different levels of surficial salt precipitations were observed in many areas along the delta.

6.2 Ndiaye

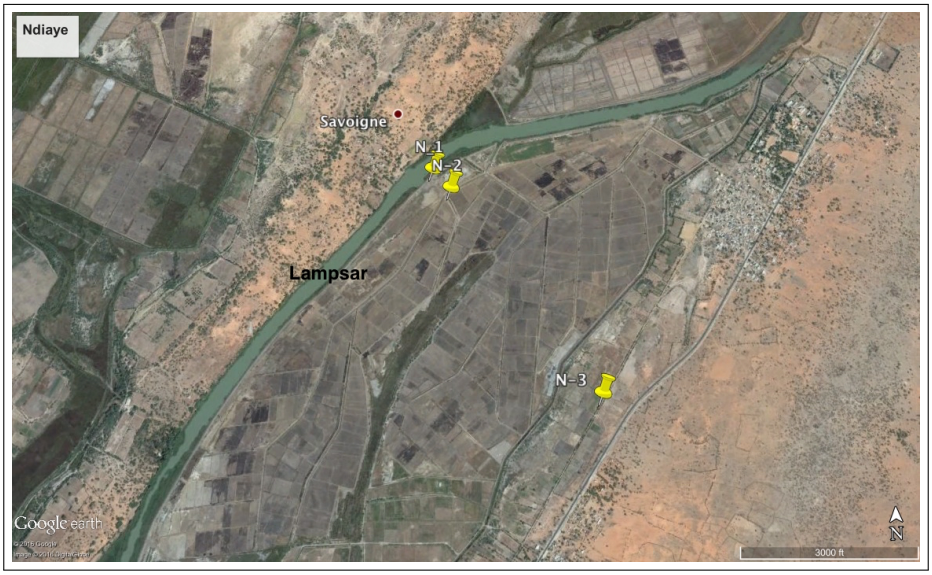

Figure 16: *Localization of piezometers installed at Ndiaye. Variable land use and distance from river distributary is visible. Satellite image via Google Earth.*

A third site is located at Ndiaye, in the lower delta, near the Lampsar distributary (figure 16). The Lampsar has a riverbed which is considerably wider than that of the Gorom Upstream.

Ndiaye is located within an alluvial settling basin, and is a site which has long been dominated by irrigated perimeters. Many sites which were observed were parcels of onion fields, receiving non-submersive watering once a week. The study site in particular extends over approximately 1.5 kilometers, and includes primary, secondary, and drainage canals. Fields all along the Ndiaye study zone were active for the entire duration of monitoring.

7 Piezometer Installation

A total of 11 new piezometers were installed over the span of 5 days at the end of February and beginning of March 2016. 3 piezometers were installed at Kassack 1, 5 piezometers were installed at Kasack 2, and 3 piezometers were installed at Ndiaye. **Nomenclature as follows: KN1 - KN3 and KN4 - KN8, and N1 - N3, respectively**.

Piezometers were drilled using a manual auger with an advancement tube. All piezometers were drilled to approximately 6 meters (between 5 - 6 m) depth, with screening be-

tween 1.5 - 5.5 meters depth, inclusive. PVC piping was used to secure the boreholes. Piezometers were localized using a standard GPS collection device. While x-coordinates and y-coordinates are available, elevation data is not precise, and in any event is not very important.

Figure 17: *Visual analysis of sediments made during the drilling process*

At Kassack 1, piezometers were installed at 50 meter intervals. K1 lies approximately 35 meters from the Gorom Upstream and is considered a riverside piezometer. KN3 is located approximately 180 meters inland.

The five piezometers installed at Kassack 2 were placed at increasing spatial intervals, from 100 meter to 3 kilometers between piezometers. Kassack 2 includes both the Gorom Upstream distributary and the Kassack distributary, in which the latter crosses between the last two piezometers in this series, located at over a kilometer distance from each piezometer. KN4 is located within 20 meters of the Gorom Upstream and is thus considered a riverside piezometer.

Finally, N1 lies within 15 meters of the Lampsar, and is labeled as a third riverside piezometer. N2 is at a crossroads of secondary irrigation canals (and thus irrigated parcels), and N3 is located inside a parcel which was in a preparation phase for cultivation. N3 was located within 30 meters of an active onion parcel.

Previous studies have classified up to three or four groups of piezometers from different areas in the delta in order to better organize the analysis.[10]. These have included classes of groundwater which are far inland, outside of irrigated zones, groundwater which is located along the river, and groundwater located in an irrigated parcel. In a very loose manner, the classifications in this study largely include what will be defined as riverside piezometers and inland piezometers. Irrigation-impacted piezometers will also be discussed.

The distances from each piezometer to a respective body of surface water are noted in table **??** for the Kassack sites and table **??** for the Ndiaye site. Distances were measured using Google Earth, with error of ± 10 meters. The regular meanders of these distributaries signifies that distances may be measured from several points along the distributary, and influence from distributary to groundwater occurs in a non-linear spatial distribution. As

Piezometer	$\mathbf{d}_{gorom}$ [m]	$\mathbf{d}_{kassack}$ [m]
KN1	35	2066
KN2	90	2010
KN3	150	1960
KN4	10	3300
KN5	200	3000
KN6	700	2600
KN7	2050	1600
KN8	5450	1600

Table 6: *Distance from Kassack 1 and 2 piezometers to proximal distributaries. Measured with Google Earth.*

Piezometer	$\mathbf{d}_{lampsar}$ [m]
N1	25
N2	160
N3	1550

Table 7: *Distance from Ndiaye piezometers to the Lampsar distributary. Measured with Google Earth.*

a rule of thumb, piezometers within 50 meters of riverside may be considered as riverside piezometers. Piezometers more than 50 meters of riverside may be considered as inland.

During the drilling process, general visual analyses of the sediments and evolution of saturation were recorded in order to confirm local conditions. Most importantly in these analyses, physical confirmation of the local presence or absence of an aquitard in the first six meters was made. In liaison with aquitard presence was confirmation of multiple distinct saturated zones (local aquifer separation). Two saturated zones were detected in four of our drillings, separated by a clay aquitard of apprixomiately 1.5 meters thickness. The remaining five drillings contained only one continual saturated zone in the top 6 meters. This aquitard discontinuity confirms that regular localized communication exists within the saturated layers of the quaternary. In many places, only one aquifer is considered.

Visual analysis also permitted the observation of local sedimentary or mineral conditions. First-hand observations were made for classifying areas shown the geological map in figure 8. As an example, ferric iron grains were observed semi-regularly. In addition, presence of certain mineral grains gave evidence of historical conditions, and information on geochemical reactions which could possibly be occuring. Historical studies have cited presence of gypsum, notably, and the soil dynamics that could be supported in connection.[16]

In all boreholes, both at the Kassack sites and at Ndiaye, the quaternary aquifer matrix in the saturated zone appears to converge with depth to near-homogeneity, over the entire study region. The aquifer evolves into grey silty-sandy layers, with some areas showing evidence of oxides. Otherwise, each borehole differs only in the ratio of sands to silts at depth.

Four existing piezometers were included in the current monitoring network: piezometers 119 and 120, which are several kilometers to the south of the Kassack distributary, and piezometers P3 and P4, located within irrigated parcels at Ndiaye, close to the N2 piezometer drilled during the current study. 120, P3, and P4 are screened into the same aquifer

as the piezometers installed during this project, while 119 is screened into the limestone aquifer of the Eocene.

8 Geophysics

Electrical geophysical methods were applied as a tool for characterizing the shallow aquifer. Two electrical methods, electrical resistivity tomography (ERT) and electromagnetism with an EM31, were utilized. With electrical geophysics, contrasting resistivity (or equally conductivity) of fresh and saline waters can be exploited to locate the horizon of each body. ERT measurements can provide a 2-dimensional vertical resistivity tomography into the subsurface, while EM 31 measurements can provide a 2D lateral slice.

Two of the three sites - one at Kassack 1, one at Ndiaye - were chosen for geophysical surveys, with both methods, ERT and EM31, being utilized at each site. Similar to the motivation for the installed piezometer configurations, ERT surveys were chosen in proximity and perpandicular to the Gorom Upstream and the Lampsar distributaries, with the hopes of identifying any groundwater-surfacewater exchanges or freshwater intrusion into the groundwater. With this configuration, a simplifying assumption is made that the resistivity profile is constant in the direction parallel to the riverside (perpandicular to the profile). The shoreline is in fact *not* even close to being linear, so this assumption may only be held to a very local scale.

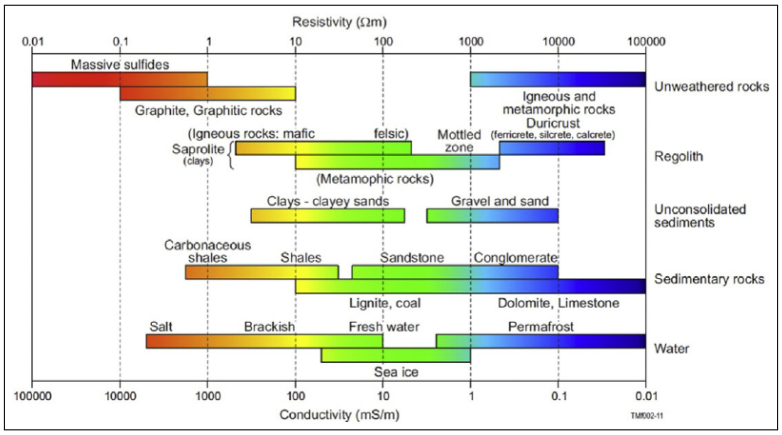

Figure 18: *Electrical properties of rocks, sediments, and water types. From (Gonzalez-Alvarez 2016).*

The results that arise from measurements of resistivity or conductivity in the subsurface are a product of the electrical properties of the subsurface's components, which in the delta will include loose sediment and water of varying salinities. Common resistivity and equivalent conductivity ranges of rocks and sediment types are given on a logarithmic scale in figure 18. Values of salt and fresh water are also reported. Keeping in mind that subsurface temperatures are higher than 25^{o}C, possibly up to 30^{o}C , the resistivity of clay is estimated between 10 and 50 Ω.m, of silts between 50 and 100 Ω.m, and of sands between 100 and 5000 Ω.m.

One ERT profile of 200 m^2 was carried out at each site. A 50 m^2 EM31 profile was had at Kassack, and a 20 m^2 EM31 profile was had at Ndiaye.

8.1 Electrical Resistivity Tomography

A wide range of theoretical background for ERT is availabile in literature. Additionally, several ERT studies revolving around seawater intrusion and water-type interfaces can be found in (Bahkaly et al, 2015), (Comte, J.C., 2009), (Nguyen et al, 2009), or (Ravindran et al, 2013), to name a few.

To resume, an ERT survey collects values of apparent resistivity during field measurements, and resistivity values for a model are then calculated using the prevalent smoothness-constrained least-squares method developed by (deGroot-Hedlin et Constable, 1990).

$$(\mathbf{J^T J} + \lambda \mathbf{F})\mathbf{\Delta q_k} = \mathbf{J^T g} - \lambda \mathbf{F q_k} \tag{2}$$

where $\mathbf{F} = \alpha_x \mathbf{C_x^T C_x} + \alpha_z \mathbf{C_z^T C_z}$;
$\mathbf{C_x}$ and $\mathbf{C_x}$ are horizontal and vertical roughness filters, respectively;
$\mathbf{J}$ is the jacobian matrix of partial derivatives of model parameters;
λ is the damping factor;
$\mathbf{q}$ is the model change vector;
$\mathbf{g}$ is the data misfit vector.

Assuming that data of quality has been collected from a properly performed survey, carrying out an inversion is rather straightforward, thanks to the help of a number of highly capable numerical software. Res2Dinv is used to invert the data that was collected for this study.

Schlumberger arrays were used for the profiles at Kassack and at Ndiaye. This array which was suggested by the lendor of material, Professor Mapathe Ndiaye, offers relatievely strong vertical and horizontal resolution, with a good signal strength, and a depth of investigation (DOI) generally exceeding 20 meters.[17] The general setup of current electrodes (C) and potential electrodes (P) in the Schlumberger array is given in figure 19. For our surveys, the P electrode separation, a was set to 15 meters. C electrodes were placed 95 meters from the corresponding P electrode, with $n = 6$ meters. The entire survey spanned 200 meters, with 5 meter spacing between electrodes. Reliable data down to 10 meters depth would be sufficient to capture the sought-after characteristics in the shallow aquifer, although the expected depth of investigation from this configuration to exceed 10 meters. Finally, while silicate materials make up the bulk of the solid phase, the presence of clays, evaporites, and small quantities of iron oxides may have a non-negligible impact on the common assumption that the rock matrix is an insulator.

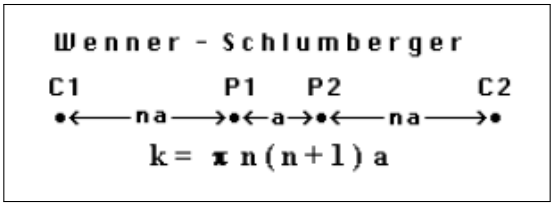

Figure 19: *Layout of current electrodes (C) and potential electrodes (P) for a Wenner-Schlumberger configured profile. Image after (Loke, 2001).*

8.1.1 Forward Model

A 2D synthetic resistivity model was constructed in order to better understand what is encountered in the terrain and to verify hypotheses about the ERT results which follow. To begin, a horizontal tabular resistivity model may be considered for the local geology. It is expected that the bulk resistivity (or conductivity) of the subsurface is dominated by the aqueous phase, with only small effects from the solid phase. And, save any fresh-water intrusion, it is assumed that the resistivity profile in the first 20 meters is largely homogeneous.

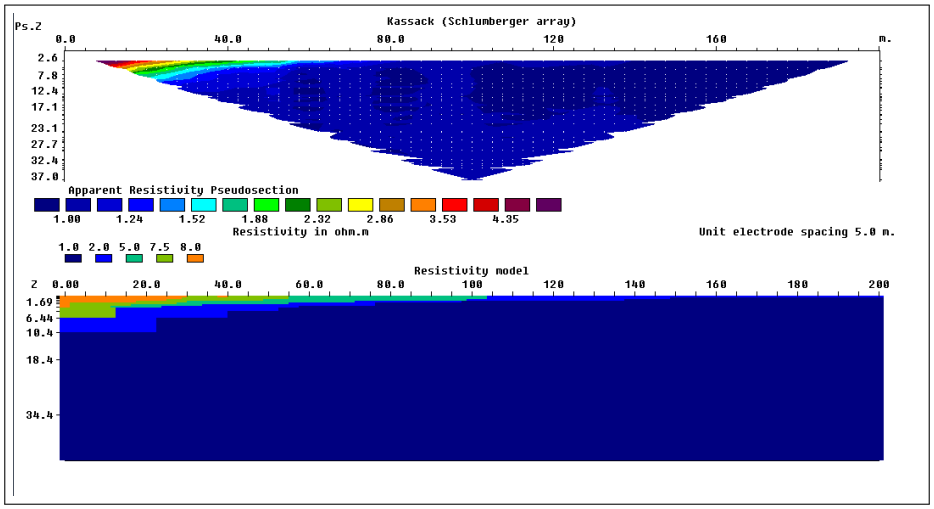

Figure 20: *Layout of cell resistivities constructed for a forward model.*

To evaluate the presence of a 'fresh' water lense, a high resistivity zone is added to the synthetic model, using historical and geochemical data as limiting factors on the resistivity values. The model resistivities in this case are set to approximately 10 $\Omega.m$ higher than what has been measured in hydrogeochemical data, a small account for the rock matrix. The array is set as a wenner-schlumberger of 200 meters length, and with 5 meter electrode spacing and equivalent model cell width. 2% Noise is added to the data.

The bottom image in figure 20 is the synthetic model. The homogeneous zone is set to 1.0 $\Omega.m$, assuming that this sandy zone is saturated with saline water. An 'intrusion' in the form of a steadily increasing resistivity tabs, from 2 to 8 $\Omega.m$. The intrusion was set to 10 meter depth at the riverside, approximately equivalent to the riverbed depth, and 5 meter depth farther inland. The intrusion leaves impacts extending 80 meters. The apparent resistivity pseudosection resulting from this cross-section is given in the top image of figure 20.

The forward model is then inverted, with results given in figure 21. An extended model was chosen in order to avoid undesirable boundary effects. The un-extended model is available in the Appendix. The fresh water intrusion is clearly visible, and the calculated resistivities in this model are not far off from the 'true' values defined in our synthetic model. The intruding lens is well dimensioned, as well.

Figure 22 offers the inversion of our synthetic model with a cell length of 2.5 meters instead of 5 meters. As the boundary between the resistive and the conductive zones is abrupt, a finer mesh can helpt to avoid unwanted numerical effects. In this case, the intruding lens

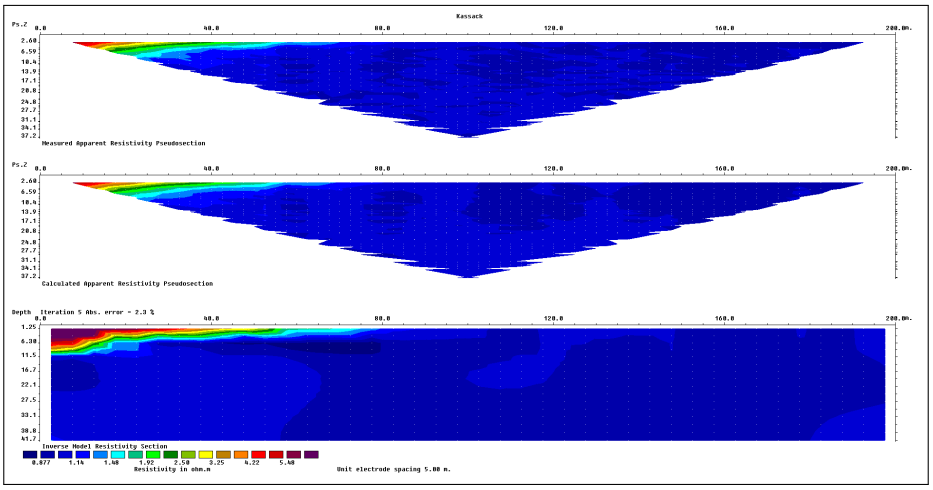

Figure 21: *Inversion of our constructed forward model, with extended blocks.*

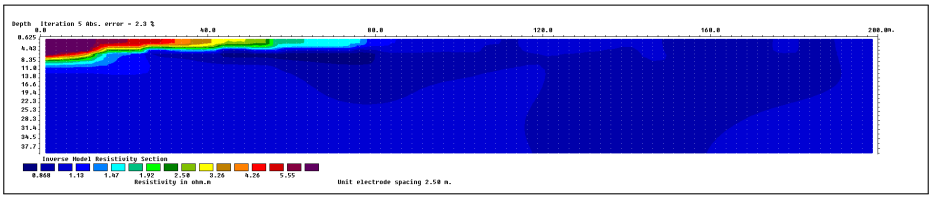

Figure 22: *Refined mesh inversion of our constructed forward model, with extended blocks.*

is still very visible, and it's step-like dimensions are better refined. A 2.5 meter cell width will be used in the analysis of our field data.

One thing to note in this model is that an exceptionally low-resistivity zone has formed below the intruding lens, on the inland side. This is clearly an artefact (as it was not defined in the original synthetic model) and is something to watch out for in the inversion of the real data. This zone gives the impression that some of the salt or saltwater in the original saline aquifer has been pushed out of the way and concentrated below the lens. This is likely not to be the case unless such an artefact was of a more deviatory value.

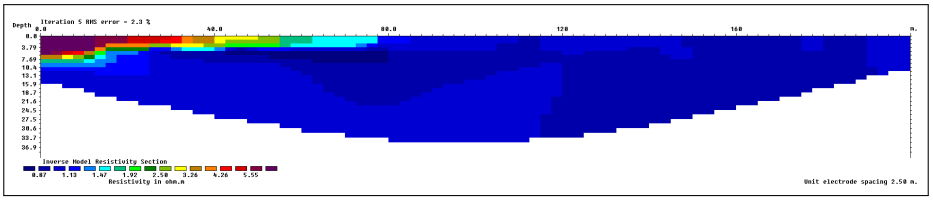

Figure 23: *Inverted model with removal of cells with sensitivity values lower than 0.02.*

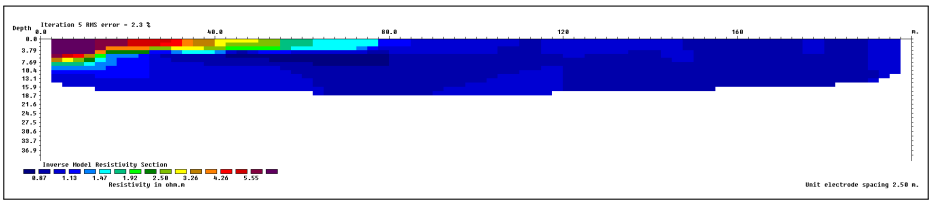

Figure 24: *Inverted model with removal of cells with resolution values lower than 0.01.*

Figures 23 and 50 represent the same inverted model as given in figure 22, with cells below a certain sensitivity or resolution parameter threshold, respectively, having been removed from the final result. While the sensitivity threshold is higher than the resolution parameter threshold in absolute value, the sensitivity-removed model still extends deeper than figure 50.

With image 50 as a foundational result, it is assumed that even the models (calculated from quality data) of the most limited resolution at depth will contain enough information to decode the necessary structures.

8.1.2 Quality of Data

To fully analyze the calculated results from ones data, the quality of the resulting model must always be investigated. In particular, as the sensitivity of model cells decreases exponentially with depth, it is necessary to evaluate these parameters for a complete analysis. While survey length and array type can be used to theoretically approximate resolution at depth, there are always site-specific parameters which will create a deviation between theory and reality. As an example, if there are high contrasts in resistivity values near the surface, the depth of investigation is often compromized.

There are several available methods for these types of evaluations. One of the most popular is likely the depth of investigation (DOI) index, as developed by (Oldenburg and Li, 1999). Another method is to calculate the model resolution parameter, $\mathbf{R}$, as defined by

$$\mathbf{R} = (\mathbf{J^T J} + \lambda \mathbf{F})^{-1} \mathbf{J^T J} \tag{3}$$

This parameter is related to the least-squares equation as well as to changes in the model. In essence, linear approximations are used to relate the 'true' resistivity of a cell with the apparent resistivity which was originally measured in the field.

The model resolution is often described as a 'filter' through which the measured apparent resistivity is fed, and from which the model resistivity arises. The resolution matrix contains resolution values in it's diagonal elements, and error or 'contamination' values in the off-diagonal values. While the resolution parameter is not as robust as the DOI index, it does have the advantage that it smooths out local peaks caused by sharp increases in resistivity or even simple noise.[17] This may prove advantageous if our data resembles the synthetic data of the previous section. When scaled correctly, the model resolution and the DOI index can give very similar results, and if anything, it is often the resolution which overestimates the depth at which results should be ignored.[17] The second benefit is that the resolution is a parameter which can be calculated for free from within the software used for analysis in this project, instead of using other programs which are expensive and difficult to obtain.

The model resolution will be applied to the results for quality analysis. Below a given resolution threshold, it will be concluded that the calculated model is unreliable and therefore these cells will be removed from the final model. A cutoff value of 0.05 is commonly used in literature,[17] howbeit the final cutoff value will depend on the parameters of the mesh used during inversion.

8.2 Electromagnetics: EM31

Electromagnetic methods are numerous and are well-suited for detecting highly-conductive bodies in the subsurface. These methods do not require direct contact with the ground, which greatyly simplifies their application. As with ERT, there is a innumerable range of information available on the theory behind EM geophysics, including studies dealing with saline groundwater and marine intrusions. The basics will only be briefly covered here.

EM geophysics makes use of a transmittor coil and a receiver coil, and reads the subsurface response of electromagnetic fields. A *Primary EM field* of a specified frequency is generated with alternating currents within a transmittor coil, and a *secondary EM field* is generated in the subsurface as a response to the primary field, with the same frequency as the primary field. Primary fields generate alternating currents (or eddy currents) within the conductive body, or subsurface, which directly produce the secondary field. The stronger the conductive body, the stronger the secondary fields.

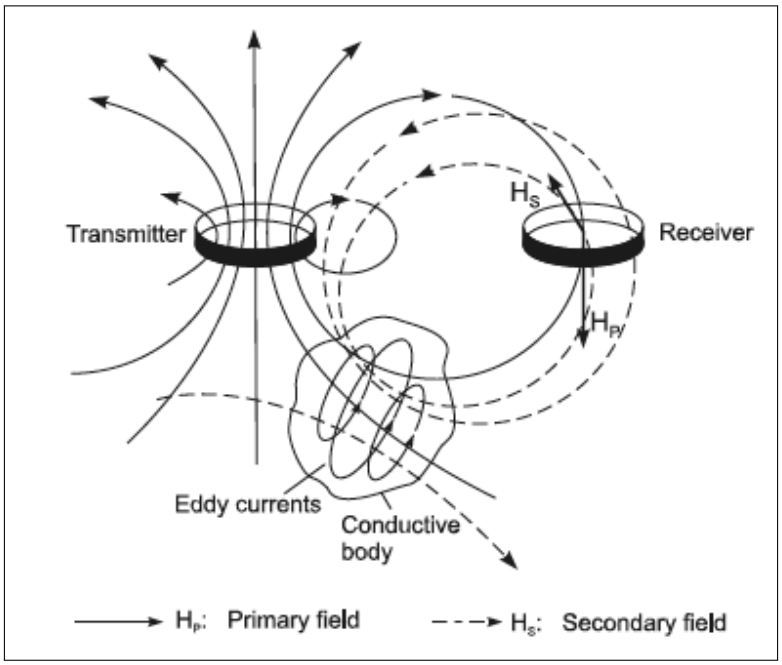

Figure 25: *Schema depicting the function of EM geophysical methods, from (Lange et Seidel, 2007)*[15].

In figure 51, the dynamics of produced and induced EM fields is displayed. The primary field is read from the receiver coil, including it's trajectory below the surface, and including the secondary field. The difference in primary and secondary fields (phase, amplitude) characterize a conductive body. A saline aquifer produces a highly conductive body which should be easy to differentiate. To note, important parameters for an EM survey setu include frequency, conductivity, and coil spacing.

The EM31 used in this project is a time-domain EM (TDEM), meaning that a primary field is emitted in pulses instead of continual emission. This means that there are periods when the primary field is 'inactive' and thus the secondary EM field can be better detected with less noise. The dispersion and decay of the primary field may be used to dimension a conductive body.

8.2.1 Quality of Data

An important characterizing factor of an EM survey would be the depth of penetration, otherwise known as the *skin depth*. The depth is a factor of the EM field frequency and the conductivity of the subsurface. Lower frequencies and low conductivities will increase the skin depth.[15] It is expected that the entire subsurface of profiles in the delta will be highly conductive, thus the depth of penetration will be limited. As with ERT, this application does not necessarily require information at great depths, so this may not be a problem. It is hoped only that any existing salinity evolution be detected.

The depth of investigation, or skin depth, d is defined as follows:

$$d = \frac{503.8}{\sqrt{\sigma f}} \tag{4}$$

where d is depth of investigation; 503.8 is a common ratio; σ is the subsurface conductivity; f is the applied frequency.

Equation 4 is a theoretical relation. An effective depth of penetration z_e is more often applied:

$$z_e = \frac{100}{\sqrt{\sigma f}} \tag{5}$$

Along the surveys carried out here, it is assumed that the entire subsurface will be highly conductive. Some variation in conductivity may exist, but estimations with historical data lead to the assumption that the effective depth will fall somewhere between 5 and 10 meters. Lastly, a coil spacing of 3.6 meters was used for surveys at Kassack and at Ndiaye, and a frequency of 9 kHz was applied.

9 Hydrochemistry

In this project, chemical characteristics of groundwater are used to identify a water signature and to quantify the level of salinity at different points. With a proper chemical analysis, saline waters (sea water) can be discerned from fresh waters, and a salinity flux can be traced to depict a spatial evolution. An attempt to discern the precise origins of the present salinity (modern intrusions, fossil waters, dissolution of ancient marine salt precipitates) will also be made. Quantifying the magnitude of salinity is rather straightforward, but flow properties and the determination of origins requires a more in-depth analysis.

In the end, identifying the sources of fresh water in the alluvial aquifer and their subsequent propagation will be the most interesting information. The working hypothesis is that fresh surface water intrusion comes from irrigation practices, from seasonal groundwater recharge, and likely also directly from river water.[1],[7],[21]

Geochemical data collection included multiple tasks:

1. Regular measurements of temperature, pH, and conductivity from every piezometer in our monitoring network, using a CyberScan series 600 multiprobe, along with groundwater levelling. Surface water (distributaries, primary irrigation canals, secondary irrigation canals) properties were also sporadically measured.

2. CTD divers installed in piezometer KN1, 20 meters from the Gorom Upstream riverside, and piezometer KN8, 2.3 kilometers inland, to allow for continuous chemical monitoring in two different environments.

3. Water samples collected from piezometers for testing in the ULg geochemistry labs.

In total, multiprobe data collection spans from March 9 to March 27 - three weeks. In theory, it is assumed that the water measured is coming from the top of the groundwater column, though it should be kept in mind that piezometer installation and groundwater mixing in a more open space (inside the piezometer) might have an important impact on the vertical salinity flux at all points. Water in the piezometer column may have self-redistributed according to density, so that the most concentrated saline waters fall to the bottom of the column, and the freshest waters remain at the top. After some weeks, an important amount of mixing between any different water bodies could occur in the column.

CTD divers were installed on March 9. A baro diver was installed in KN1 along with one of the CTDs, and the pressure data collected from this baro was considered relevant for the CTD diver in KN8. The devices were configured to take measurements every 10 minutes for the duration of installation, also three weeks. The diver installed in KN1 was set at a depth of 4.21 meters, and the diver installed in KN8 was at a depth of 2.25 meters. Both of these are considerably greater depths than the measurement level with the multiprobe.

For the last field outing on March 27, water samples were collected from all of our installed piezometers, as well as from P3, P4, 119, and 120. Piezometers were not pumped before collection. Samples were filled to ensure a minimum of contact with atmosphere, but underwent extreme change in temperature and pressure when transported from the sub-sahara to northern Europe. These samples were measured on April 16 at the University of Liège, nearly three weeks after collection. Only one sample was collected from each piezometer due to a limited number of available sample jars. Some simple analyses do exist in order to gauge the reliability of th (ionic balance, systematic change in pH compared to measurement by other methods, conductivity changes, ...).

Part III

Results

10 Hydrogeophysics

Results from both ERT profiles seem to be of good quality and are very useful. EM31 results, however, marked many conductivity values which were out of range for the frequency that was applied.

10.1 ERT

ERT results are analyzed by constructing 2D tomographies for each dataset. Topography was ignored for these models, as the terrain relief is predominantly flat (less than 1 meter over the length of both ERT profiles).

Some pre-analysis organization was carried out by Pr. Ndiaye before delivery of data files. For example, erratic datapoints were removed by him. No additional points were removed for construction and analysis presented below.

10.1.1 Kassack

The ERT data from Kassack was inverted with a refined mesh, using a model cell width of 2.5 meters. A 'fine' mesh was chosen in order to optimize the treatment of relatively large resistivity variations near the surface. The tradeoff is a superficial numerical 'rippling' effect might be observed in some areas.

Kassack profile inversion results are given as an extended model in figure 26, with resistivity values corresponding to this model given in figure 27 (due to the low readability in the beginning image). The resulting model is of good quality and represents well what was hoping to be found. The number of iterations chosen were 5, from which a satisfactory and relatively stable RMS error was obtained (see figure 26). Between 4 and 6 iterations, the RMS error deviated by 0.35%. An extended model was chosen to limit numerical boundary effects. The non-extended model can be referenced in Appendix 2.

In this tomography, the position labeled at -105.0 meters is located along the riverside, whereas the position labeled at 95.0 meters is inland. Each tick mark counts 2.5 meters. Piezometer KN1 is located between electrodes at -85 and -80 meters, KN2 is located next to the electrode at -25 meters. Finally, KN3 is located at +30 meters.

With knowledge on the local geology and other subsurface conditions, and with information gathered from the synthetic model which was previously constructed, it is nearly certain that the high-resistivity lens at the top left of this tomography results from an intrusion of river water from the Gorom Upstream. Indication from the synthetic model also suggests that the low-resistivity zone just below the inland side of this lens may be an artificial ripple, although this cannot be said with certainty. Nevertheless, this freshwater recharge is limited in depth and in impact. These readings alone suggest that intrusion in the region does not surpass 7 meters depth before a sharp boundary is encountered and the model

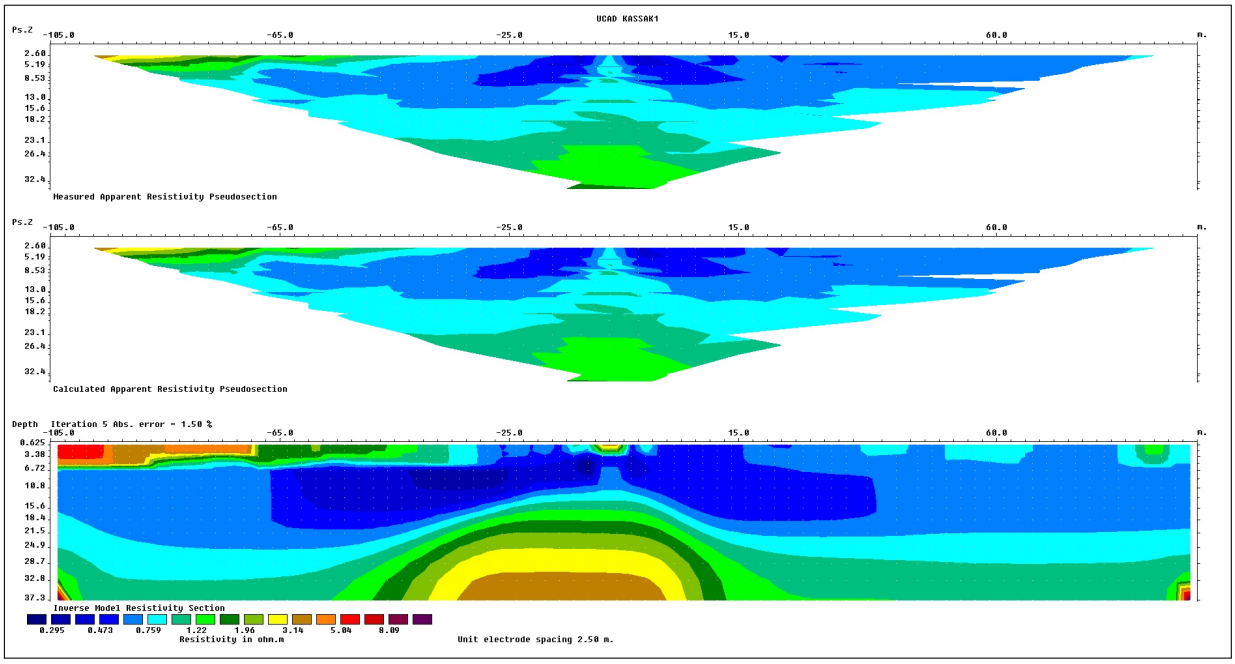

Figure 26: *Least squares finite difference inversion of ERT profile at Kassack 1 using an extended model. A distinctive increase in resistivity is observed to the left (corresponding to the riverside end of the profile) of the inverted model.*

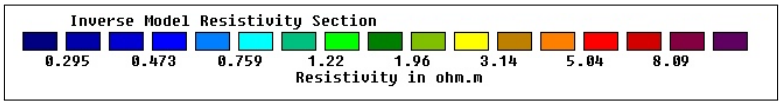

Figure 27: *Resistivity values corresponding to the resistivities calculated in figure 26.*

becomes highly saline. In addition, the word 'fresh' in this context is extremely relative. Water at 5 Ω.m is still not suitable for human consuption or agriculture.

Keep in mind that these measurements were taken near the height of the dry season. If even a small signature of fresh water is present in the alluvial aquifer during the months of February and March, the mark and impact during the rainy season - and for as long as river levels remain high during the months that follow - must be more significant than what has been measured here. Simple data on water heads suggests that flow rates from the River to the groundwater would be more intensive during the rainy season. It is hypothesized that this fresh water strip would not only be larger in dimensioin - reach farther inland, and penetrate to further depths - but the magnitude of resistivity would be considerably greater within the lens. As a thought, the small resistive body near the right extreme of this profile could be an indicator of how far fresh water is able to penetrate during the rainy season. Or it could be a numerical artefact.

The small resistive body detected in the upper middle portion of the tomography could be the result of one of several sources. It could be water which invaded from the river several months before, which has not been able to evacuate due to physical geological barriers. It could also potentially be the result of a point of contact between the Eocene and the alluvial aquifer. Less interestingly, it is possible that this is a detection of some subsurface installment, although this is not expected. It could also be simply a numerical artefact, as it is located directly between our two potential electrodes in the middle of the profile. In any case, it is difficult to define with certainty the source of this resistive point.

A highly resistive (again, relative) body is also possibly detected at depth. This may be detection of a deeper, freshwater aquifer, likely the Eocene. However, the depth of this body puts it's reliability in question. Reliability of data at depth will be discussed in the following section. The high resistivity points shown at the bottom right and left corners of the final model are numerical artefacts. It is certain that these areas are outside the zone of detection of this survey.

Resistivity in this section does not attain even 10 Ω.m. Knowing that the water table is located at approximately 1 meter depth, it is assumed that the aqueous phase dominates the resistivity readings. Thus the confirmation (or suggestion) of a blunt truth: the groundwater in the shallow Senegal river delta is highly saline. In addition to this argument, noting that the resistivity of sea water is in the environs of 0.35 Ω.m, this model suggests that this area is less saline than sea water. This may be due to the rock matrix which almost certainly elevates the resistivity measurements, and hydrochemical measurements signify that some of the water along the Kassack profile has resistivities significantly lower than that of sea water. The highest resistivity measured in the shallow zone is approximately 5 Ω.m, or 0.2 S/m conductivity, and the lowest resistivity is at approximately 0.3 Ω.m, or 3 S/m conductivity.

10.1.2 Kassack Profile - Quality of Data

To evaluate the quality of the resistivity results, specifically to what depth the resulting model is relevant, the resolution parameter is used. This parameter is calculated with Res2Dinv.

Figures 30 and 31 show the Kassack model as blocks, with removal of all cells below a resolution threshold of 0.01 followed by cutoff from a threshold of 0.02. A commonly used

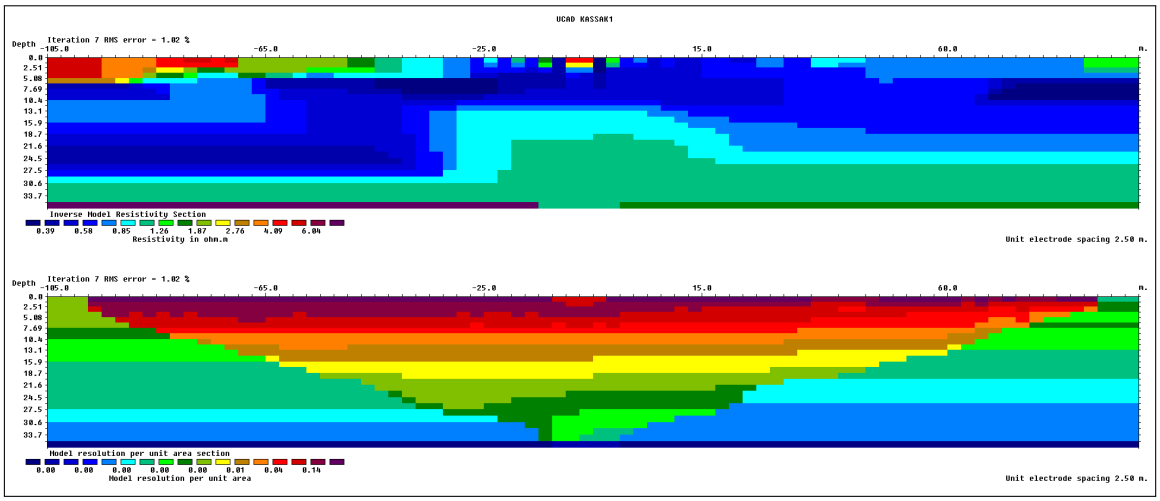

Figure 28: *Model resolution value (lower image) for individual cells of Kassack inversion.*

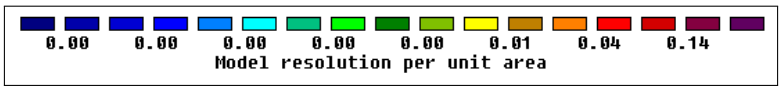

Figure 29: *Resolution values corresponding with image 28.*

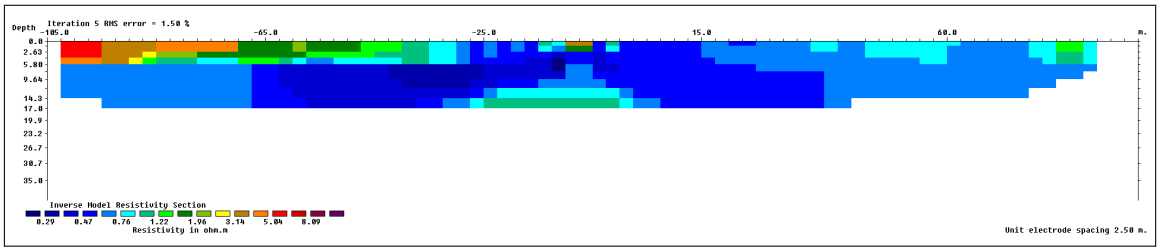

Figure 30: *Inverted Kassack model with removal of cells with a resolution value lower than 0.01. Resistivity values are defined as in figure 27.*

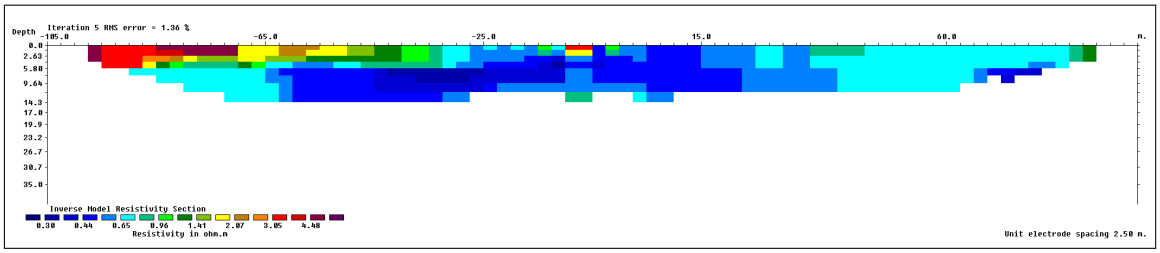

Figure 31: *Inverted Kassack model with removal of cells with a resolution value lower than 0.02. Resistivity values are defined as in figure 27.*

cutoff value is 0.05[17], though with a refined mesh, this cutoff value should also be refined. The cutoff of 0.02 would be the more conservative choice.

In figure 31, the intruding resistive lens on the riverside is visible so that it's existence is certified. The existence of the resistive body in the center of the tomography at depth is less certain. A resolution cutoff of 0.01 confirms it's existence, although the cutoff of 0.02 brings in a healthy level of doubt. As this depth of the subsurface is not necessarily of direct interest for this project, this is not an issue. If ever a wider, more extensive resistive lens exists, the interest of depth would increase accordingly.

The cut model suggests that there exists a factor which has somewhat compromised the depth of resolution. Where some terrains might offer 30 meters or more of resolution, with the resolution parameter apparently only 15 to 17 meters are offered. This may be due to the low resistivity values overall, and the contrasting values located at the surface. It should also be noted that the resolution cutoff may be overestimating the depth to which data may no longer be trusted in comparison to the DOI index.

10.1.3 Ndiaye

As with the Kassack data, the Ndiaye dataset was inverted with a refined mesh in order to optimize treatment with large resistivity variations.

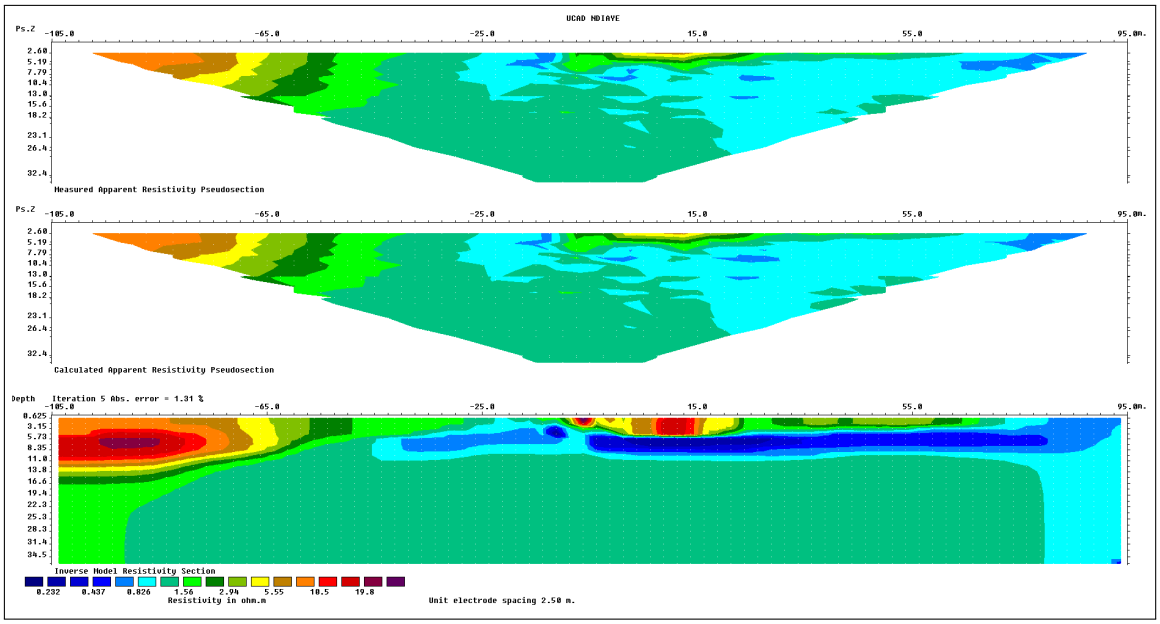

Figure 32: *Least squares finite difference inversion of ERT profile at Ndiaye. Similar to Kassack, a zone of increased resistivity is observed to the left on the riverside.*

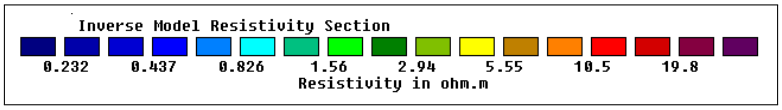

Figure 33: *Resistivity values corresponding with figure 32.*

Figure 32 is the inverted, extended model from data gathered at Ndiaye, with the Lampsar riverside close to meter -105. The non-extended model is availabile in the Appendix. The

RMS deviated by 0.42% between iterations 4 and 6.

Similar to the Kassack profile, there is a large resistive body on the river side of this profile. It is assumed that this body represents river water intrusion from the Lampsar. Assuming this case, it appears that the intrusion at this site has both larger dimensions and a larger magnitude than was observed at Kassack. If the hydrodynamics of the Lampsar distributary versus the Gorom Upstream is accounted for, this is not surprising. The Lampsar has a larger riverbed and a faster flow rate, and the Gorom Upstream is additionally weighed down by invasive plants, especially at the riverside in the water. It is feasable that water penetrates at much greater rates from the Lampsar to inland.

A second high resistivity body is observed at the 15 meter mark. This coincides with an area where the profile intersected the terminus of an irrigation canal, and not far from an irrigated onion field. The high resistivity is assumed to be a result of penetrating irrigation waters.

The very low resistivity body below the presumed irrigation field is of concern. It is unlikely that this would be a numerical artefact, due to it's extension and contrast in value, although an artefact should not be completely disregarded. If in fact this is a true contrast in resistivity, it leads one to believe that it is a result of irrigation. Irrigation waters may be pushing salts and saline waters further into the subsurface, or it is possible that that some of the ions are coming directly from the irrigation waters. It has been seen that complex ionic exchanges are evolving around irrigated rice fields in the delta.[5]

The background resistivity of this profile is generally slightly higher than the background resistivity at Kassack, suggesting that the water is slightly fresher in this zone. This is likely due to a stronger output from the Lamspar.

It should be noted that, due to the density of irrigated fields in the vicinity of the profile carried out at Ndiaye, the theory that the subsurface resistivity profile is constant in a direction perpandicular to the profile is weak, and some of the bodies to the right side of the 0 meter mark may have influence from variable resistivity profiles around these zones.

10.1.4 Ndiaye Profile - Quality of Data

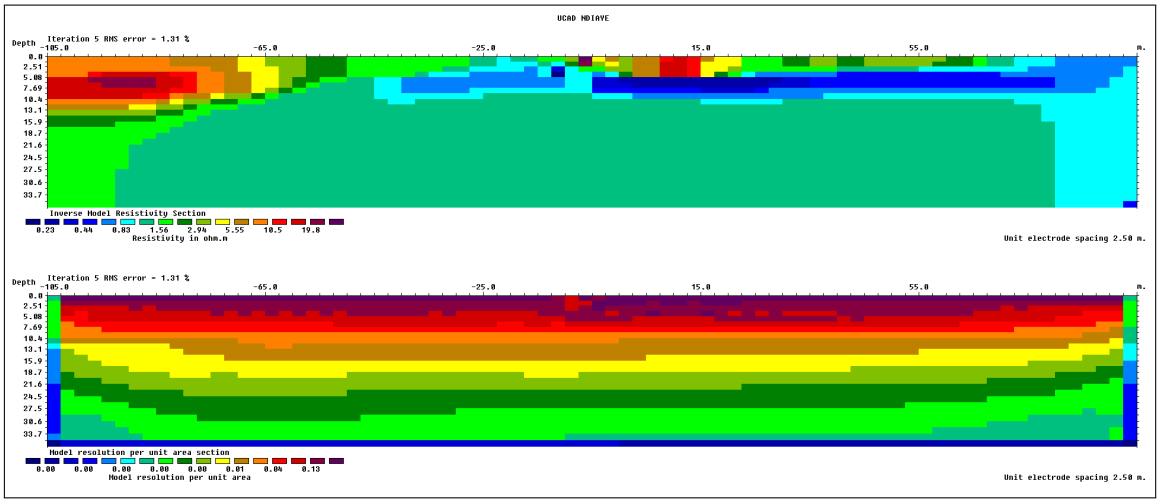

Figure 34: *Model resolution calculation for cells making up entirety of Ndiaye model.*

The resolution parameter has been used once again to evaluate the quality of results at depth for the Ndiaye profile. Resolution is displayed over the entire model in figure 34.

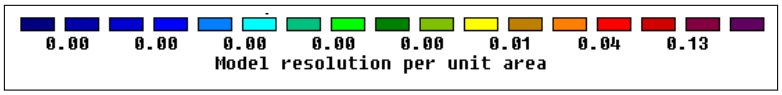

Figure 35: *Resolution values corresponding with image 34.*

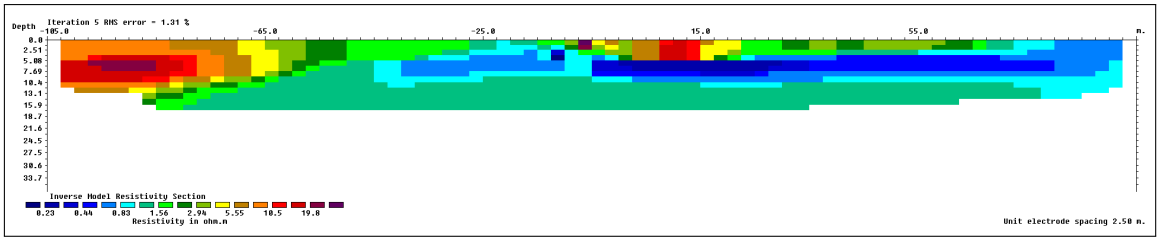

Figure 36: *Inverted Ndiaye model with removal of cells with a resolution value lower than 0.01. Resistivity as in figure 33.*

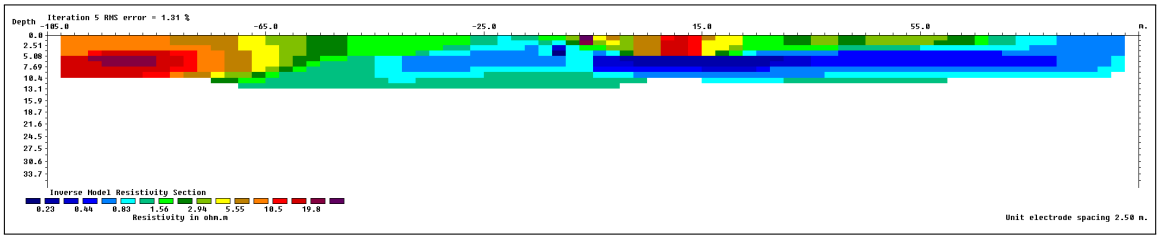

Figure 37: *Inverted Ndiaye model with removal of cells with a resolution value lower than 0.02. Resistivity as in figure 33.*

Figures 36 and 37 show the inverted Ndiaye model as blocks, with removal of all cells below a resolution threshold of 0.01 followed by 0.02. As with Kassack, the cutoff of 0.02 is a conservative choice.

The intruding resistive lens which represents river water intrusion is preserved, for the most part. In the case of both cutoff values, depth is substantially compromised, probably due to the extensive resistivity variations occuring at the surface. In figure 37, it would be quite difficult to understand what each different zone represents without geographical information as well as information on land use. In the end, it is presumed that data quality is acceptable at least up to 10 meters, and possibly up to 20 meters. Again, use of the actual DOI index may give evidence of qualitative data farther down that 20 meters.

10.2 EM 31

The data gathered with the EM 31 is of questionable quality. Nearly the entirety of both profiles, at Kassack and Ndiaye, returned a stagnant conductivity value of 20.5 mS/cm. Inland areas are not expected to vary in a significant way from one point to another, especially at a 'fixed' depth. However, to detect zero evolution in conductivity is difficult to believe. The most useful information that has been gathered from these profiles is that - indeed - the Quaternary aquifer is salinized.

Geographical plots of the two EM31 surveys are available in the Appendix. It is shown that the walking survey at Kassack displays no evolution, and is therefore not very useful. On the other hand, at Ndiaye, there is a given amount of evolution in the conductivity values which were detected. Notably, a limited decrease in conductivity is measured at riverside, and an even more limited decrease is also detected in vicinity of cultivated lands.

In order to calculate the effective depth of these measurements, recall equation *5*. With a frequency $f = 9$ kHz, at Ndiaye the effective depth is at 7.4 meters in areas of high conductivity, and 16.5 meters at the areas of lowest conductivity.

11 Hydrogeochemistry

Hydrochemical analysis begins with the data gathered from our field multiprobe. Laboratory chemical analysis, discussed afterwards, verifies the ionic characteristics of the groundwater.

Conductivity, along with pH and temperature of tested waters, measured in the field with the multiprobe, renders a preliminary grasp into the state of the groundwater in the delta. The data obtained from field measurements allowed us to quantify the level of salinity over each site.

PIEZO	Temperature (C)	pH	Conductivity (µS/cm)	CTD (µS/cm)
KN1	27.1	6.6	8128	45439
KN2	27.3	6.3	37332	
KN3	28	6.4	66273	
KN4	26.6	6.8	6223	
KN5	27.6	6.4	36019	
KN6	26.8	6.4	32592	
KN7	28.7	6.4	51045	
KN8	29.4	6.5	30080	36120
N1	30.7	6.6	3258	
N2	29.3	6.5	34155	
N3	30.5	6.4	34773	
P3	29.1	6.1	70560	
P4	28.7	6.4	4540	
120	28.6	6.4	2365	

Figure 38: *Results of multiprobe field measurements in groundwater. Values collected during the monitoring period have been averaged, as they remained stable during the time of study.*

A first scan of the multiprobe results - averaged over 5 weeks of rather stagnant data - in figure 38, and a trend in groundwater conductivity magnitudes is immediately evident. Every groundwater point measured is salinized. Nonetheless, the electrical conductivity measured at each riverside piezometer is at least an order of magnitude less than even it's closest inland neighboring piezometer. The weakest conductivity is measured at N1 along the Lampsar, with a value of 3258 $\frac{\mu S}{cm}$. To note as well are the remarkably high conductivity values at KN3, KN7, and P3, all of which are higher than 50000 $\frac{\mu S}{cm}$.

Another point from this table is the magnitude of groundwater temperature. Temperatures are much higher than what is commonly found in northern climates with less sun. Groundwater temperature should bring into question the thermodynamics of ionic reactions in the subsurface. However, it is difficult to identify invasive river water in the aquifer with the assumption that surface water would be cooler than groundwater. While KN1 and KN4 have relatively low temperatures, N1 groundwater is quite warm.

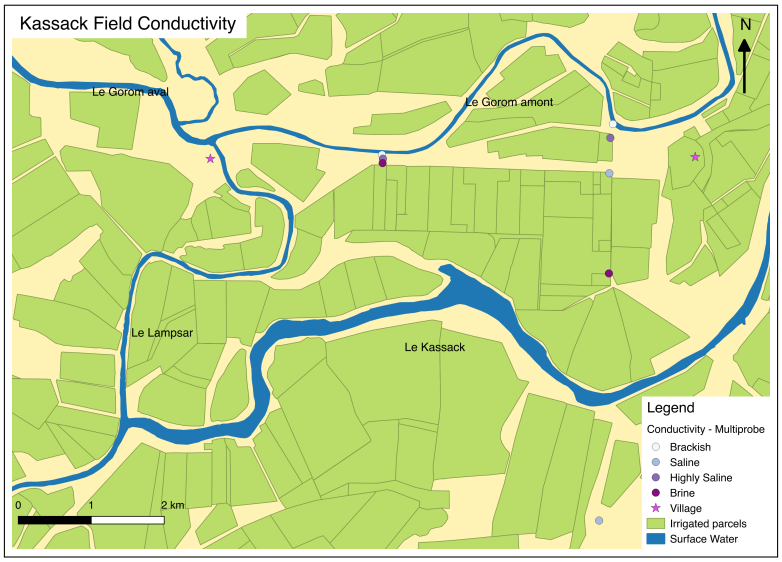

Figure 39: *Averaged measurement of groundwater conductivity multiprobe data. Conductivity remained rather stable at each point for the duration of monitoring. Conductivity classification is based on table 5 of this report.*

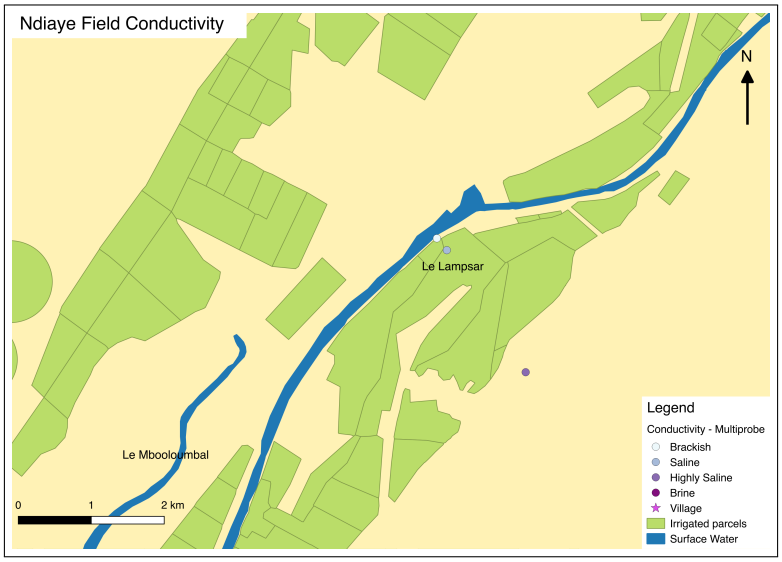

Figure 40: *Averaged measurement of groundwater conductivity multiprobe data. Conductivity remained rather stable at each point for the duration of monitoring. Conductivity classification is based on table 5.*

Figures 39 and 40 offer spatial representation of the average field conductivity measured over the span of our six-week study. These simple graphics, which are classified using the system in table *5* (subsection: Groundwater Salinization), clarify a trend of increasing salinity from riverside to the inland points. The riverside piezometers at Kassack 1, Kassack 2, and Lampsar measure brackish waters, which is the lowest salinity class encountered in the delta. Brackish was detected exclusively at riverside piezometers and piezometers located in irrigated parcels. All inland piezometers were categorized as 'saline' at minimum. Brines were detected at multiple points.

Recalling figure 8, note that the majority of the piezometers are located in settling basins with a fine granulometry that limits the surface porosity. Piezometers located on the riverside may be in a sandier environment, but this zone is almost certainly affected by the annual river 'crue' and thus rinsed semi-regularly. Only one piezometer is located in or near the red sand dunes, which are generally brines.

What should take one's attention is that the rate of salinity evolution is not equivalent from site to site. It is found at Kassack 1 that the groundwater seems to evolve from brackish to brine in a space of 200 meters. At Kassack 2, over 200 meters it is found that water evolves from brackish to highly saline, and a slight decrease from highly saline to saline waters further inland. Only KN7 is measured to be brine, while KN8 is saline. KN8 is across the Kassack distributary and also located on a point bar. The complex salinity pattern at Kassack 2 is also very likely to be influenced by irrigation practices, most notably by the large primary canal and running pump on site. There are no irrigation practices in proximity to the Kassack 1 site.

The salinity increase at Lampsar is lighter than either profile at Kassack. This is likely due both to the important flow rate of the Lampsar distributary, and to high density of irrigated parcels. N3 is located at a border with red sand dunes, which are generally more saline than settling basins because they are isolated from the annual river 'crue' or recharge. Salinity is likely diluted at N3 in the shallow subsurface because of irrigation water recharge.

11.0.1 Water Column

Regular monitoring via multiprobe collected samples at the height of the water table (the same may be said for samples collected for laboratory measurement). These data are of extreme necessity for the purposes of this study, but do not give any significant information on a water column of the shallow aquifer. What is the salinity profile of the alluvial aquifer at 5 meters depth, 10 meters depth, or even 20 meters depth? The only data from this study that is available on the hydrochemistry of the alluvial aquifer at depth is from the CTD divers, principally at KN1.

The two divers placed at Kassack were installed at differing depths (see subsection *Hydrochemistry* in section on Experimental Approach) below the water table, somewhat haphazardly. This meant that on the average, the KN1 diver is immersed more than 1 meter below the water table, whereas the KN8 diver is immersed less than 1 meter below the water table. Figure 38 reports the average conductivity measured at KN1 and KN8 with the CTD diver. Notably in KN1, the conductivity measured via the CTD diver is much higher than that measured with the multiprobe.

It has been noted previously by (Michel, 1973) that across the delta, the water salinity

found in the alluvial and other shallow aquifers tends to increase quickly with depth, giving a more sharply defined interface zone, although the phenomenon is not homogeneous. Comparison of CTD diver data with hydrochemical multiprobe data gave evidence for this type of salinity increase:

- KN1, a riverside piezometer, has measured a relatively low conductivity 38 with multiprobe data. The CTD diver at depth in this piezometer gives measurements in the neighborhood of 44000 $\frac{\mu S}{cm}$, nearly five times higher than measured by the multiprobe (approx. 8000 $\frac{\mu S}{cm}$).
- KN8, an inland piezometer, is measured to have a high conductivity and is saline. The CTD diver in this piezometer still gave measurements of a mildly higher conductivity at a slight depth, measuring 30000 $\frac{\mu S}{cm}$.

This data leads us to believe that vertical groundwater salinity evolution is more dynamic along the riverside than it is farther inland. It also suggests that the interface is encountered much more shallow than suggested from ERT data. However, water body mixing is in a piezometer is not at the same equilibrium as would be found in a sandy aquifer, as a body of fresh water which is considerably less dense than saline water could easily concentrate at the top of the water column found in the piezometer. The reliability of these data should be put into question.

11.1 Ionic Characterization

Piezo	Site	pH	Cations total	Anions Total	ION Balance
KN1	Kassack 1	7.50	83.10	82.08	1.0
KN2	Kassack 1	5.87	428.73	416.06	12.7
KN3	Kassack 1	7.19	785.02	763.83	21.2
KN4	Kassack 2	7.50	83.85	81.01	2.8
KN5	Kassack 2	6.98	388.28	372.94	15.3
KN6	Kassack 2	7.14	178.55	173.63	4.9
KN7	Kassack 2	7.59	601.07	575.59	25.5
KN8	Kassack 2	6.91	353.79	336.98	16.8
119	existing	6.93	364.68	348.29	16.4
120	existing	7.04	832.05	812.87	19.2
P4	existing - Ndiaye	7.50	54.94	52.22	2.7
P3	existing - Ndiaye	7.25	15.09	14.55	0.5
N1	Ndiaye	7.95	22.16	22.18	0.0
N2	Ndiaye	7.33	389.54	376.56	13.0
N3	Ndiaye	7.08	398.13	379.80	18.3

Figure 41: *Total cations and anions measured in groundwater samples and ionic balance calculated from these values.*

Ionic measurements water samples were carried out at the University of Liège Geology Department. Semi-complete results are available in image 67 in the Appendix (ions with negligeable concentration were left out of this table). A summary of the total ionic balance is given in figure 41. pH measured in laboratory is reported alongside the ion balance; laboratory-measured pH is in good agreement with the pH measured in the field. Temperature of measurement in the laboratory was approximately 23°C, while field temperatures were closer to 27 and 28°C, which could impact the quantity of ions in solution. Conductivity measured in the lab was nonetheless in good agreement with field measurements, despite the difference in temperature of water at the time of measurement.

From these results, a clear and logical correlation is noted between ionic concentrations and electric conductivity (which is why conductivity is used to quantify salt content in the first place). On the other hand, pH does not seem to be correlated with any specific ionic

concentrationts. Temperature is likely to play a role, although the temperature reported in laboratory results is not applicable to actual field conditions.

The majority of groundwater samples are oversaturated in cations. The samples which measure an ionic balance under 5.0 correspond to riverside samples (KN1, KN4, and N1) or samples in close proximity/within irrigated fields (KN6, P4, and P3). These samples were poor in all measured ions when compared to more inland samples.

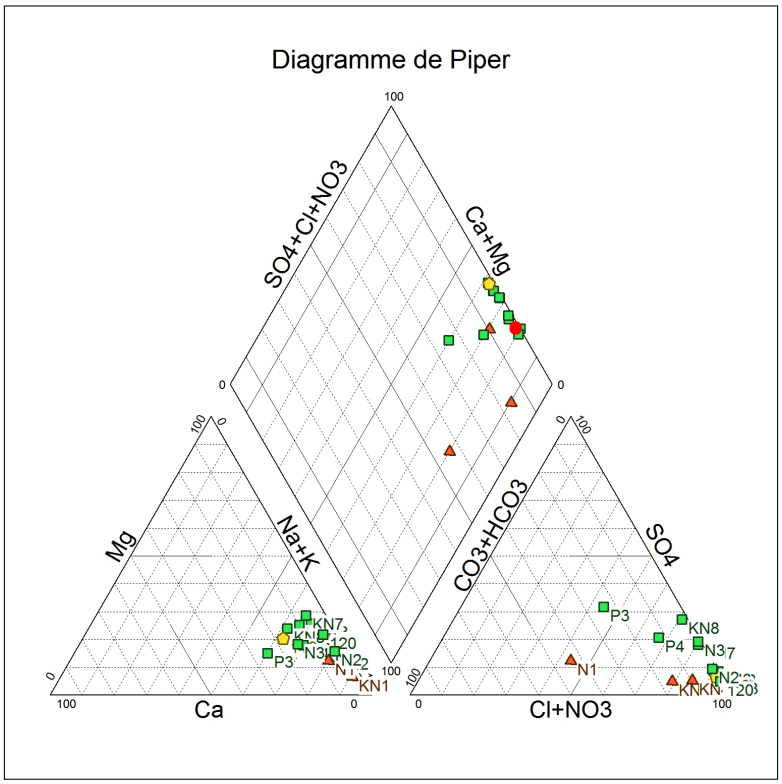

Figure 42: *Piper diagram of groundwater samples collected for this study, including seawater facies for comparison. The* ***red circle*** *denotes seawater* ***Green squares*** *are inland piezometers,* ***orange triangles*** *are riverside piezometers (<20m from surface water), and the yellow pentagon is from piezometer 119 which captures an aquifer below the quaternary.*

Figure 42 is a Piper diagram constructed from the results of the water sampling campaign using the University of Avignon program *Diagrammes*. For all points included at the Kassack and Ndiaye sites, a classification of **riverside piezometers** (>40m from surface water), i**nland piezometers** (<40m from river water). A third class includes piezometer 119, which is implanted into a deeper aquifer than all remaining piezometers, which are capted within the shallow aquifer.

All of these sites are found to have water of a dominant sodium-and-potassium-chloric nature, and a strong Na-Cl facies. Some points show a tendancy towards facies of Ca/Na-HCO_3 and Ca/Na-Cl.

Points which 'deviate' from a strong signature of NaCl are KN1, KN4, N1, P3, and P4; in other words, all riverside and irrigation piezometers. P3 and P4 are slightly more 'acidic' due to their location inside irrigated parcels. In general, a glance at the measured concentrations of ions brings attention to Mg^+, K^+, HCO_3^-, and SO_4^{2-} in addition to Na^+ and Cl^-. Higher HCO_3 concentrations signify that rain water - or other fresh water

sources - recharge is probably affecting that given zone in a notable way.[7] Piezometer N1, for example, has a relatively fresh signature. N1 is in close proximity to irrigated fields of mixed cultures, and is also implanted within 10 meters of the Lampsar distributary, which is one of the largest distributaries in the delta, with an important surface flow rate in comparison to such other distributaries as the Gorom Upstream or the Kassack. These important features of the Lampsar are the probable reason for the relative freshness found in N1.

A more subtle detail from the Piper diagram is that all riverside piezometers are poor in Ca^{+}+Mg^{+} concentrations compared to Na^{+} concentrations. It has been proposed that since Ca^{+}+Mg^{+} is only present in the groundwater of the delta, the diminution of their concentration is another testimony to softening, and therefore river water (or irrigation water) intrusion at the riverside.[?][10] Relative Ca^{+} and Mg^{+} concentrations signify a cation exchange, which requires that a certain residence time of saline waters in the aquifer in order for these exchanges to occur. Calcium and magnesium presence in the sediment is relatively weak, but is significant in that it means that sodium that adsorbs into the rock matrix can lead to a release of calcium or magnesium into solution in exchange.

P4 and P3 are relatively rich in Ca^{+} and Mg^{+} probably as a result of ions carried from irrigation waters. These two piezometers are very ionized, although their ionization is more diverse than in piezometers outside of irrigated areas.

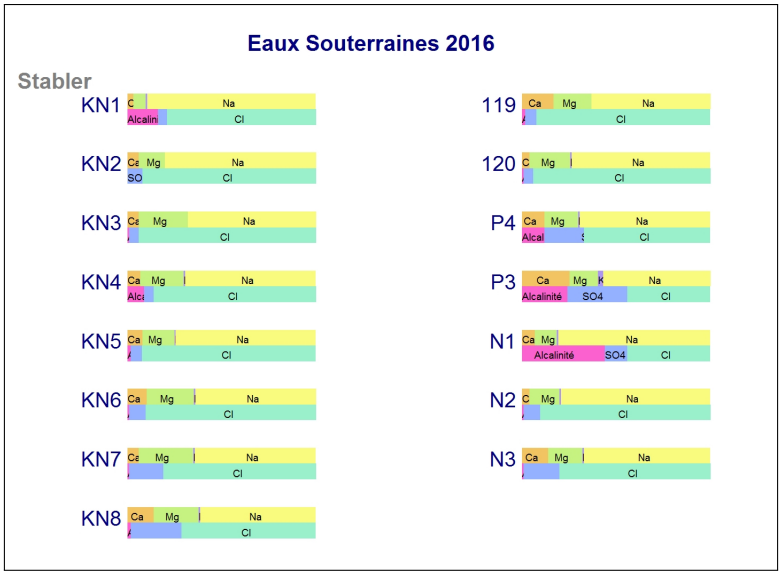

Figure 43: *Stabler diagram of groundwater samples highlights the deviation of facies measured in KN1, KN4, N3, and N4. All of these points represent an increased level of alcalinity.*

The Stabler diagram in figure 43 offers more evidence on the dominant facies measured in groundwater, representing visual proof of water types which are being classed by location. There is an increase in alkalinity (HCO_3-) in all piezometers which are classified as riverside as well as those located in an irrigated parcel. On the contrary, alkalinity is highly suppressed in all other piezometers. In addition, presence of a SO_4^{2-} facies seems to show itself in the P4 and P3 piezometers, as well as in N1 and KN8. This acidity is likely to correspond to location in agricultural parcels as well as low zones, where gypsum dissolution may be occuring.

Other reactions involve magnesium, which is present in all piezometers, and sulfate. Magnesium may also be of marine origin as it is commonly found in ocean waters, and the same is possible for sulfate.[10] The fact that these minor ions are significantly present regardless of the localisation of the piezometer suggests this fact.

11.1.1 Ion Correlation

Ionic binary ratios offer a wealth of information, and ratios for a group of measurements help to visualize which species are correlated and which are not. Binary relations also help to determine the apparent origins of the measured salinity. The most relevant relations for application to shallow groundwater in the Senegal River delta would be Na/Cl binary diagrams. Na/Cl ratios of marine waters and of waters containing pure halite dissolution have been established. From these relations, follow-up reactions such as brine formations can be defined.

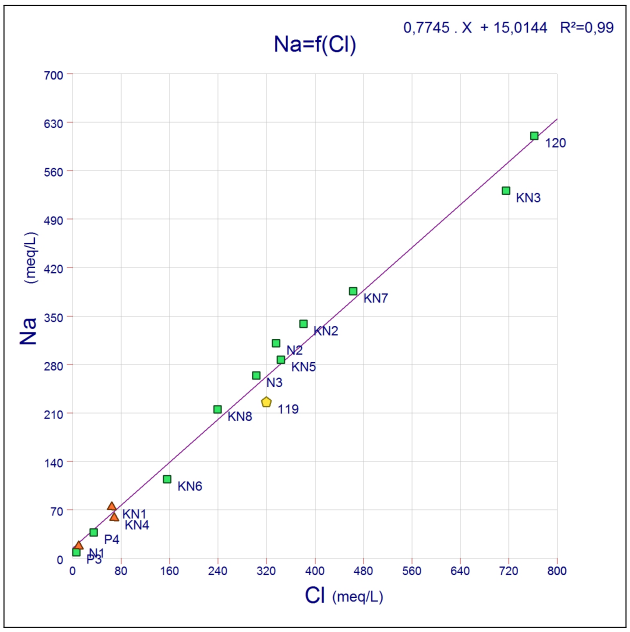

Figure 44: *Na/Cl binary diagram from groundwater sampling campaign in the delta. Equivalent to piper diagram,* ***Green squares*** *are inland piezometers,* ***orange triangles*** *are riverside piezometers (<20m from surface water), and the yellow pentagon is from piezometer 119 which captures the Eocene aquifer.*

Figure 44 is an Na/Cl binary diagram constructed from the sampling campaign carried out on the deltaic groundwaters. With an $R^2 = 0.99$, it is certain that these two ions are strongly correlated in the groundwater. There is very little deviation from a net linear relation between points. Nevertheless, the deviations that do exist from a perfect linear relation is significative in the information they hold.

Taking things a step further, note from (Gning, 2015) that marine waters exhibit an Na/Cl ratio of 0.86, and a ratio of 1 signifies that salinity is a result of halite dissolution, as the reaction is ideally in perfect ionic balance. Otherwise, an Na/Cl ratio between these two values will represent a mixing of the two phenomena. A ratio greater than 1 may indicate cation exchanges between saline groundwater and the aquifer matrix, as seen by an enrichment of Na^+ in solution, or more rarely, a dissolution of silicate minerals. A

ratio less than 0.86 indicates evaporation of marine waters and evolution into brines. It has previously been found that many groundwater measurements in the delta display an Na/Cl ratio less than 0.86.

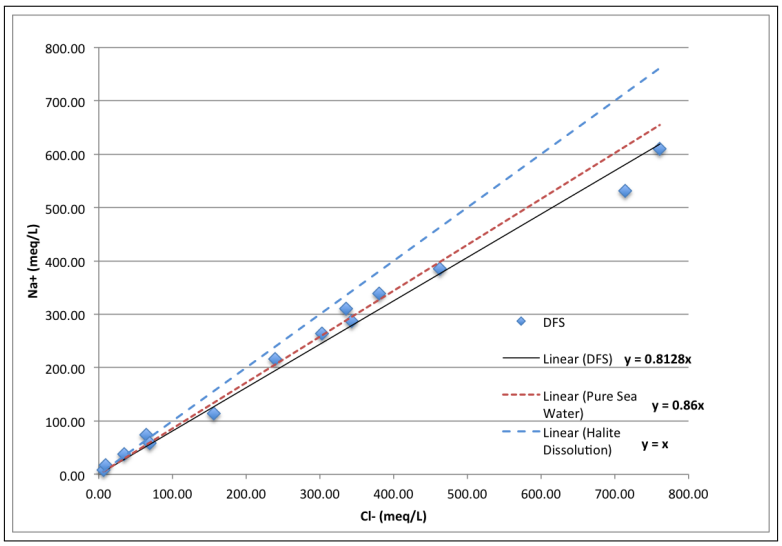

Figure 45: *Na/Cl binary diagram with definition of bouning ratios which define origins of NaCl.*

Figure 45 represents the same set of data as in figure 44, with a linear regression defined at the origin, fit to the data, as well as the linear trends of Na/Cl = 0.86 and Na/Cl = 1 added for analysis.

The trend for the group of data points sampled in these images falls below the 0.86 mark, which would confirm, once again, that brine formation is regularly occuring in the groundwater. However, only half of the individual samples fall below the mark of 0.86. There is also an interesting number of samples which appear to be more-or-less in line with marine waters. Notably, all riverside piezometers are found with a Na/Cl ratio greater than 1 except for KN4, which has a ratio of 0.86 exactly. P4 and P3 also fall into this camp. Further than this, some other piezometers which have Na/Cl ratios greater than 0.86 are very far inland - KN7, KN8, and N2 especially. Two possibilities: one being that halite dissolution is complementing marine salinity, which is an envisageable occurence at inland points, another being that all of these points are located in settling basins, with higher clay content, and therefore likely with higher ion exchange rates.

This simple analysis brings in to evidence the near certitude that a large portion of saline groundwater in the delta is of direct marine origin. The trends on display in this analysis also suggest a spatial element in salinity origins. Riverside locations are likely to contain less marine water and more salinity due to evaporite dissolution.

Another figure to analyze is the trend of the Cl/Na ratio vs Cl^-, in figure 46. Clearly, while Cl^- concentrations increase to extreme values, Na^+ concentrations do not reach the same extremities. Riverside and irrigation piezometers are located on a sharp linear slope when concentrations are low, however the central cluster around Cl^- = 400 meq/L are all inland piezometers, increasing in chlorium and stagnating in sodium concentrations. It seems that the linear correlation between Na^+ and Cl^- is thus limited to a certain after a certain point. As a side note, the cluster of points around 400 meq/L of chlorium all have an Na/Cl ratio very near to 0.86.

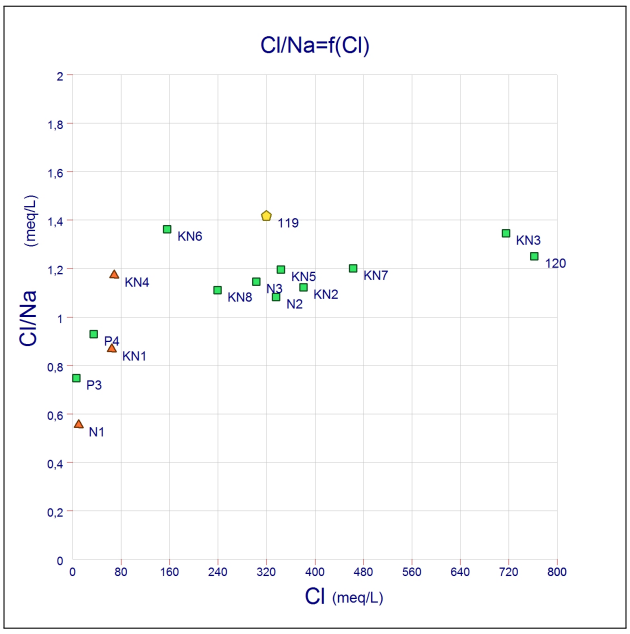

Figure 46: *Cl/Na vs Cl binary diagram from groundwater sampling campaign March 2016.*

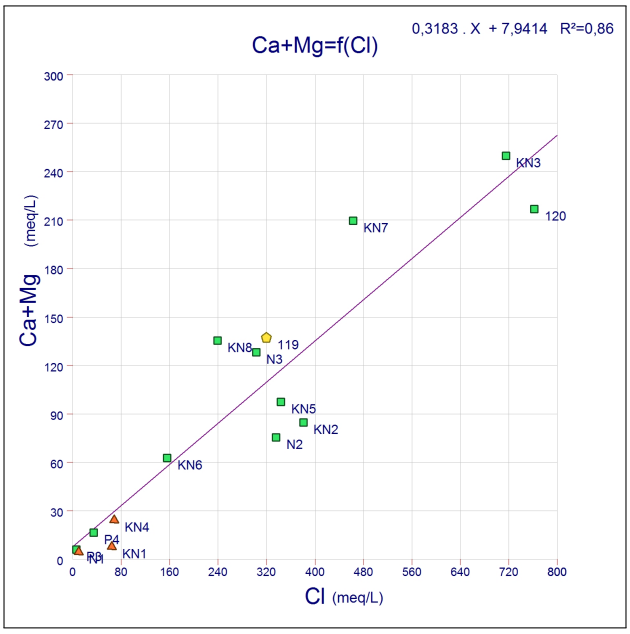

Figure 47: *Binary diagram of Ca+Mg vs Cl from March 2016 groundwater sampling campaign.*

Figure 47 gives evidence of the increase in calcium and magnesium concentrations with chlorine concentrations. Correlation is quite strong, and all samples which are more enriched in Ca+Mg with respect to the linear regression are from piezometers which are far inland.

12 Discussion

Analysis of geochemical and geophysical data collected during the course of this study has brought together strong evidence of river water recharge into the shallow aquifer from the Senegal River delta, and to have dimensioned the sub-surface hydraulic intrusion. The magnitude of intrusion seems to be a function at least of the relative difference in head and of the debit of the surfacewater that is in closest proximity. In other words, even the most simple hydrodynamic parameters play an important role in the phenomenon. Other factors - geologic, climactic, chemical - have their part. Comparing the data of this study with historical context and data that has been collected over at least the past century has aided in constructing such additional factors controlling water dynamics.

The contexts brought together in this report proved to be of extreme value and necessity for properly interpreting data and new results. Geology and hydrogeology are evidently primordial factors in beginning one's study on physical and chemical aquifer hydrodynamics. The geography of the zone, which lead to the climate of the region, which lead to rainfall levels (or lack thereof) and evaporation, made it clear that the mechanism of salinization is mult-faceted. As an agricultural environment, understanding of the land use (both modern and historically), and the hydraulic regime-change that came as a result, tied up the image of the delta.

Two sites were chosen to carry out the desired experiments. The choice of two sites permitted the study and comparison of two contrasting hydraulic environments. Standard groundwater monitoring was made possible by the installation of new piezometers as well as use of old piezometers, where two ancient piezometers brought irrigated parcels directly into the study. However similar, different characteristics were nonetheless quantified from these differing sites. To be sure, there remains a large quantity of soil types and River flow dyanmics which have been untouched. Each distributary, each soil type, each specif localisation, will have it's own specific dynamic.

With the data collected up to now, it would appear that the conceptual schema which was constructed at the end of the hydrogeological conceptual study is not far from reality. General forms of freshwater lenses existing in the subsurface around the river have been decrypted, most notably with ERT surveying. The difference between the conceptual model and the current data suggests that the size and especially the thickness of these lenses is extremely limited.

The seasonal contrast in rainfall and humidity, typical of a semi-arid sahelian climate regime, plays an important role in the hydraulic and hydrochemical regime. While direct rainfall and infiltration may not leave such a direct mark on the terrain of the delta, the higher pluviometric levels found in other areas of the river, and cumulation of moving waters at the surface and in the subsurface, have a marked effect on surfacewater-groudwater hydrodynamics in the delta. Evapotranspiration is an additional driver of such aspects as capillary rise that rob water from the subsurface and drive salt precipitation at the surface. On the topic of humidity and lens formation, it is possible that the size freshwater lenses become more important not only during the rainy season, but also in periods of relative humidity, as was experienced during most of the 20th century.

There were several contextual subjects which were *not* approached as part of this study, which, in hindsight is regrettable. This would most notably be the supplement of a thorough study of soils. There are many previous studies which have expanded on the topic of

soils in the Senegal River delta. It seems evident after-the-fact that a complete understanding of soil dynamics would be necessary in order to properly analyze the hydrochemical data which was collected. Hydrochemical data created evidence for the occurence of certain chemical reactions between water and soils, but there are certainly more potential reactions which have gone unnoticed. This type of data would also be of extreme use for anticipating which types of reactions with soils are likely to occur, and where. Hydrogeology, in it's essence, is also often pedologic. In addition, chemical thermodynamics was not discussed to any extensive level. This topic has also been discussed in previous studies, however, the important changes in chemical reactions due to the temperature of groundwater remains an unknown factor to the present study.

In a more general sense, there are still questions remaining on the subject of surface and groundwater interections in the delta, and there is still work to be done to improve the current approach. Most importantly, an inter-seasonal study absolutely must be carried out in order to capture changes in the fresh water lens when water is more abundant. ERT surveys seem to be highly efficient for physical dimensioning, and it is suggested that electrical geophysics continue to be used for these purposes. Sampling campaigns are evidently a necessity. River-groundwater dynamics should be collected alongside such a study, such as velocity profiles, tracer tests, pump tests, flow nets, slug tests, among other surfance and groundwater quantifying methods. These measures have been carried out in the delta for multiple historical studies, however, due to often strong inter-annual variability in river dynamics and water availability, continuing such measurements will ensure data availability as well as data characteristics over evolutionary time periods. Improvements to the current approach could additionally include monitoring of electrical and ionic variables at multiple depths in the aquifer, in order to quantify vertical evolution in hydrochemistry of the Quaternary aquifer. Geophysics can capture vertical evolution for the purpose of physical dimensioning, but cannot capture some important chemical characteristics which are so very central in such a study. With historical and futur data, it iwould be interesting in the long term to arrive at a point where it is possible to define the multiple hydraulic*modes* which occur under different climactic conditions.

Shallow geophysical well logs could be an interesting method for imaging the salinity profile in the water column from one location to another. Electrical resistivity methods have the capability of identifying not only the salinity of an aquifer, but also the location and size of confining beds, and thus the local aquifer thickness. The presence of water freshening, the level of salinity by layer, as well as the local flow regime could be determined with electrical water logs. Despite these facts, this method does demand a certain quantity of material which are relatively expensive, and could thus be blocked by financial constraints. In the interest of a serious advance on saline aquifer analysis in an important region of the delta, geophysical well logs should certainly be collected.

The extreme salinity that is present in these terrains is troublesome, especially when facing the hard fact that the agricultural activity needs to continue in order to attain food self-sufficiency as well as to support a growing population. But solutions to this quagmire do exist, it just takes finding the right balance, and always reaching for progress. Irrigation in itself has opened thousands of hectares up for activity, parcels which would otherwise be dead lands. Finding the most sustainable solution for these issues is the end game.

In essence, as long as the Senegal river delta remains an important area for agriculture, the dynamics of salinity in the quaternary aquifer should continue to be monitored.

Appendix 1: Supplemental Context

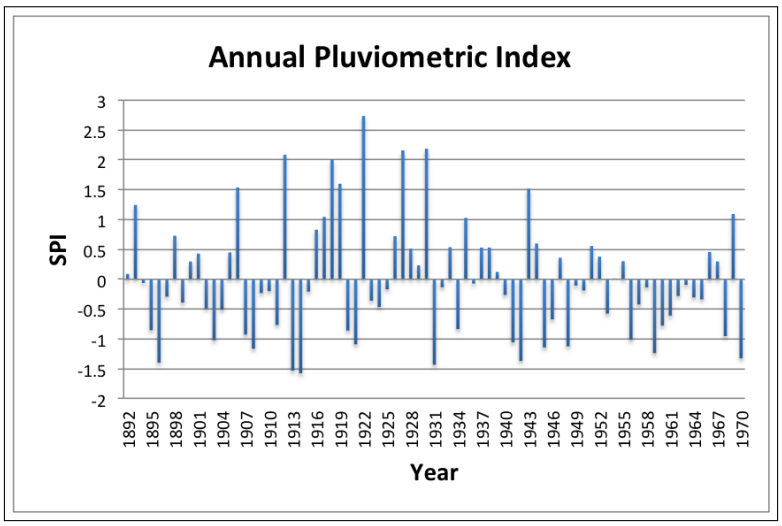

Figure 48: *Standard pluviometric index (SPI) ,as developed in Part I, section 1.1, for the time period between 1900 - 1970. This is from a recent humid regime, when regular exceptional dry seasons were well balanced by regularly occuring exceptionally rainy seasons.*

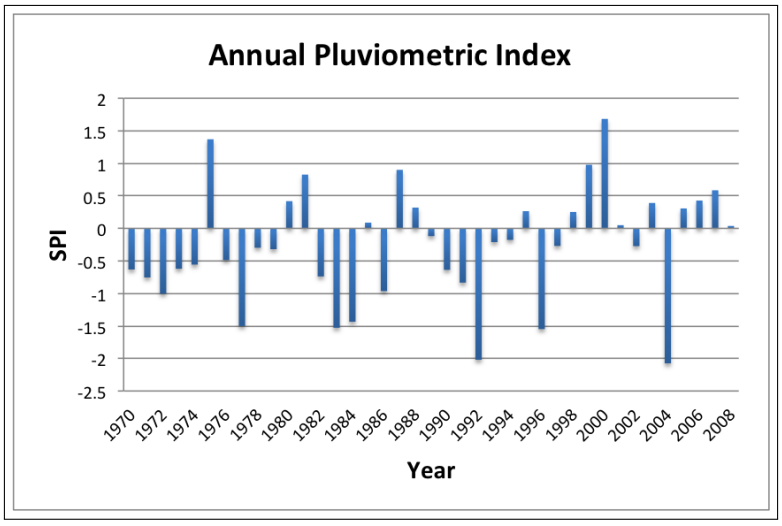

Figure 49: *Standard pluviometric index (SPI) ,as developed in Part I, section 1.1, for the time period between 1970 - 2008. A dry climate regime took hold around 1970 and has not yet recovered. Extremely dry seasons occur every 5 years and are increasing in magnitude. Extremely rainy seasons occur approximately every 7 years.*

Appendix 2: Supplemental Geophysics

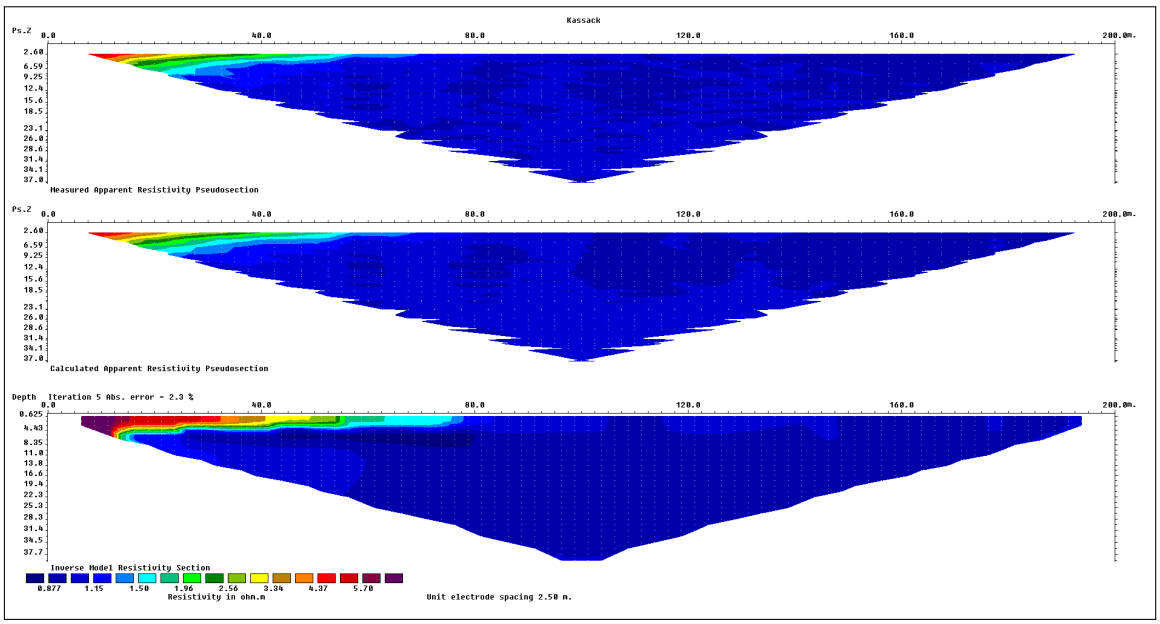

Figure 50: *Non-extended inverted model, calculated from constructed forward model presented in Experimental Approach section.*

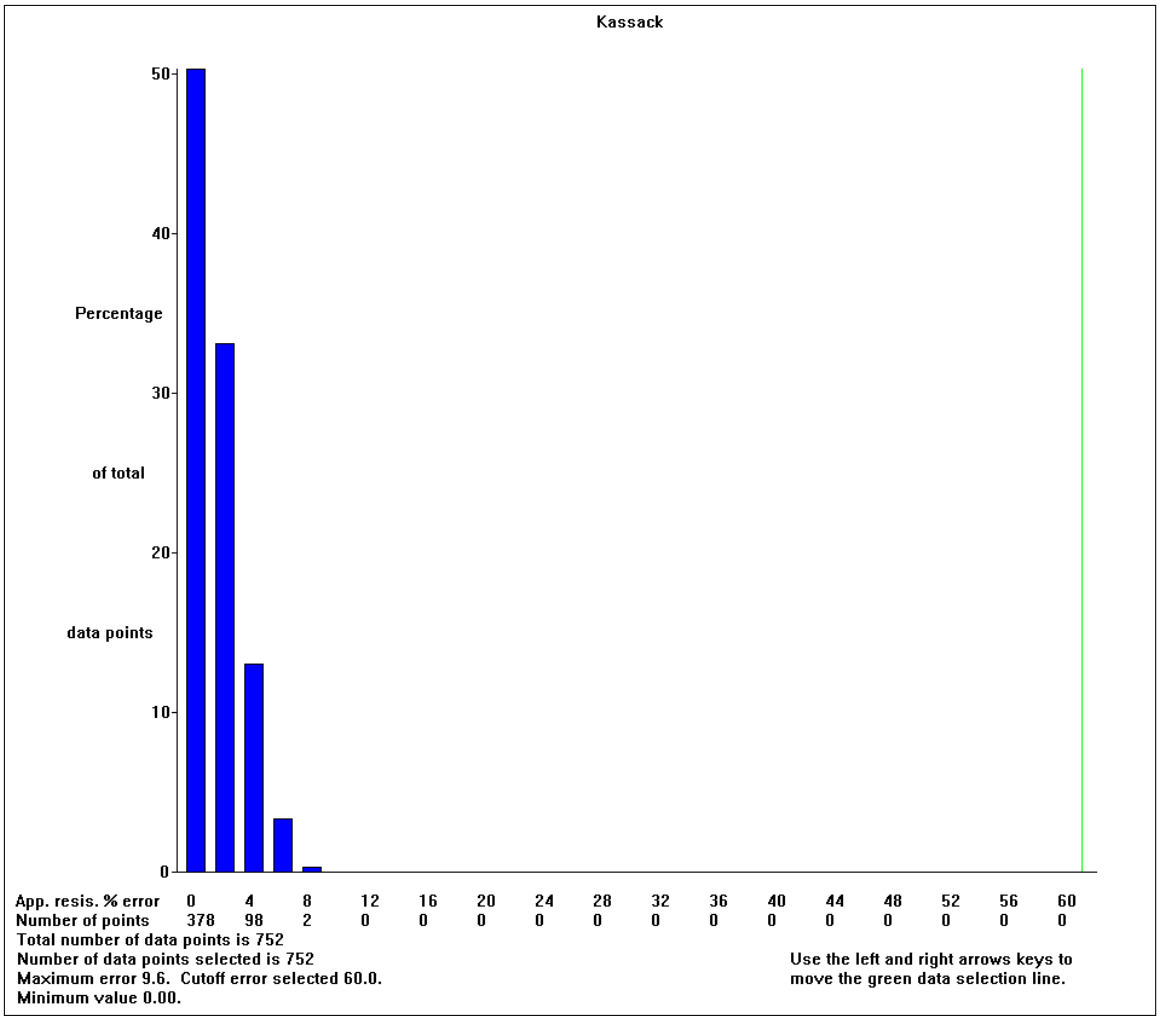

Figure 51: *RMS distribution of inverted model calculated from constructed forward model presented in Experimental Approach section.*

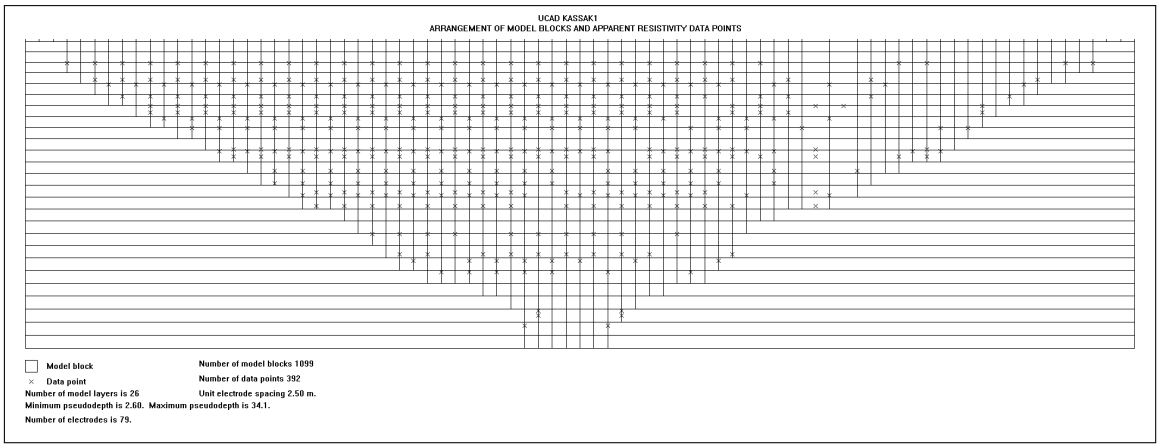

Figure 52: *Model block layout for Kassack interpretations. Extermination of certain data points leads to wider model blocks noted on the left side of this dataset.*

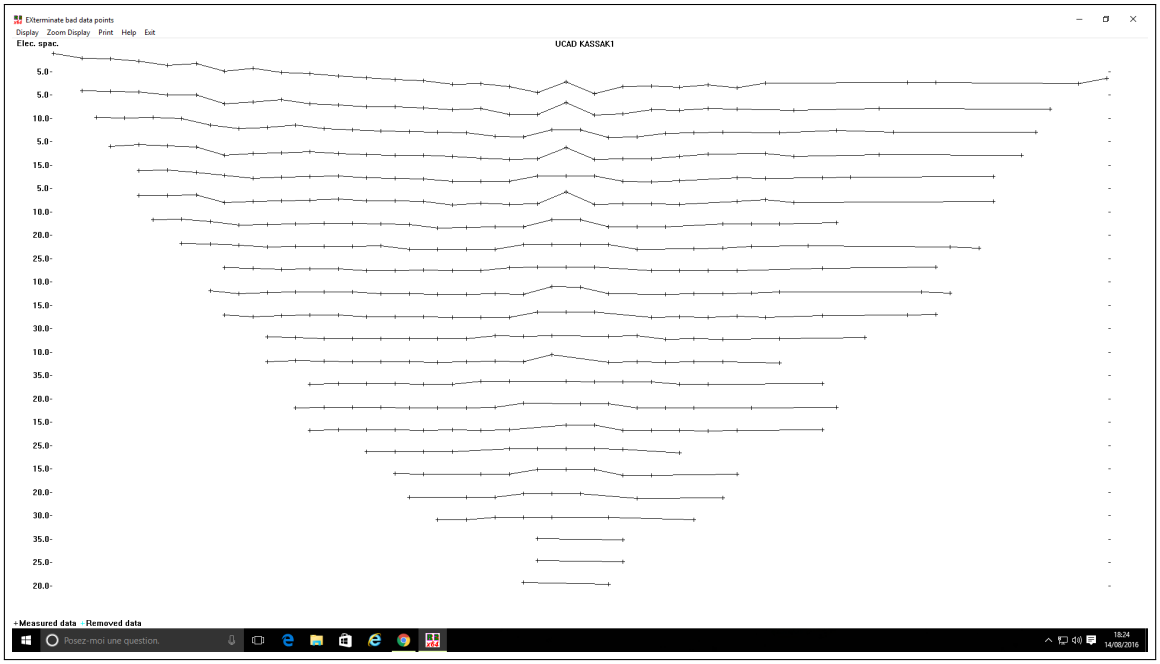

Figure 53: *Kassack layout of datapoints used for inverse calcuations.*

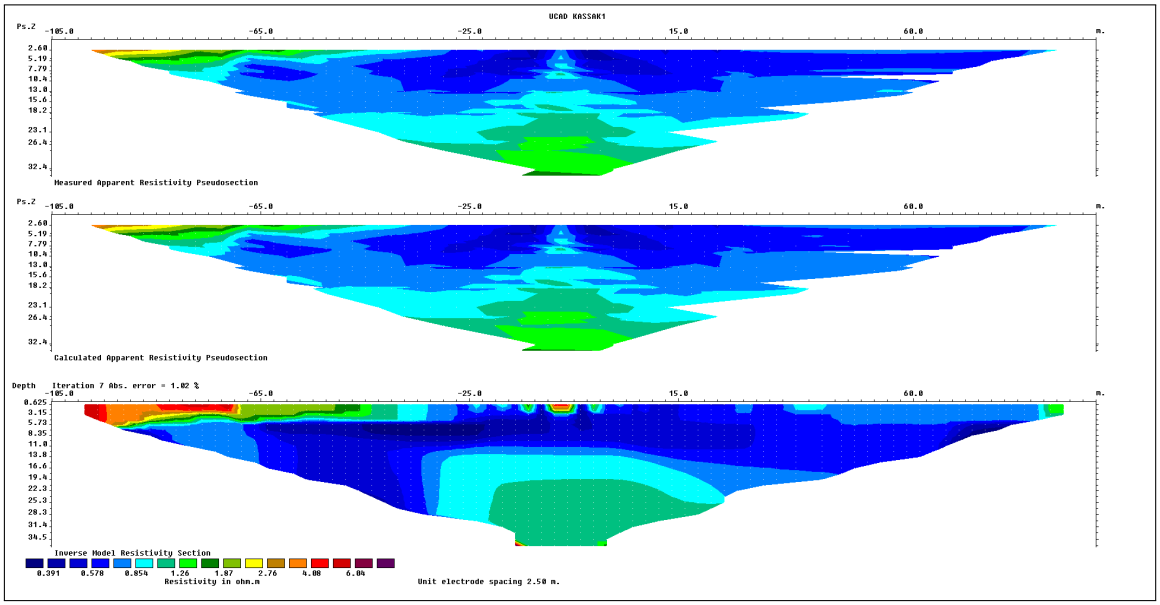

Figure 54: *Least squares finite difference resistivity inversion at Kassack, no model extension.*

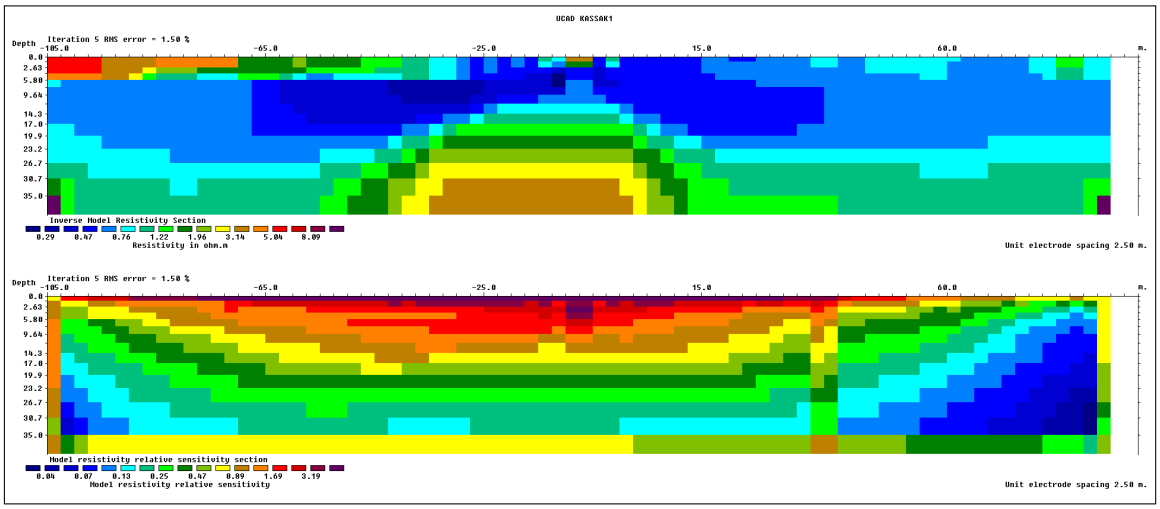

Figure 55: *Sensitivity values for individual cells used in Kassack inversion.*

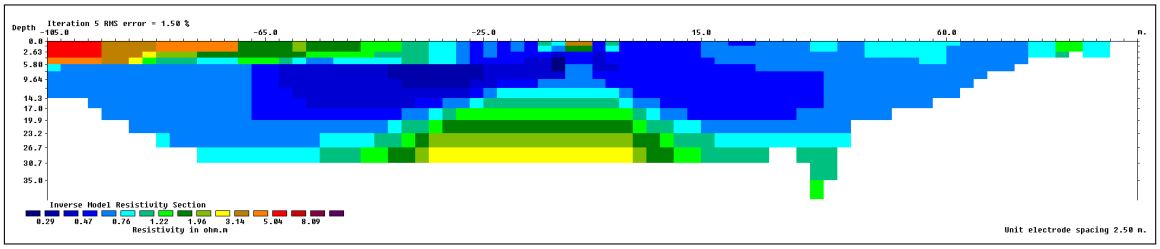

Figure 56: *Inverted Kassack model with removal of cells with a sensitivity value less than 0.2.*

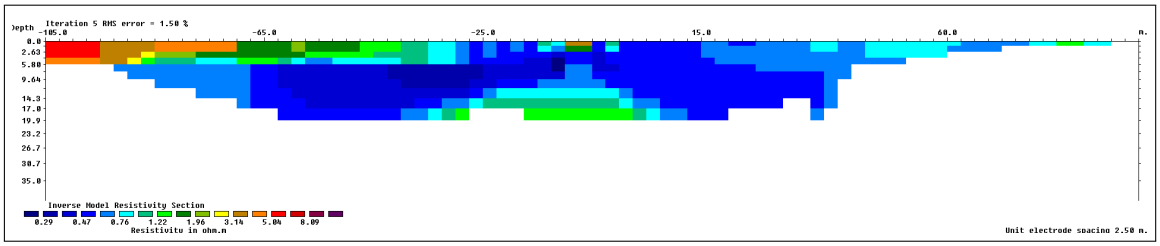

Figure 57: *Inverted Kassack model with removal of cells with a sensitivity value less than 0.5.*

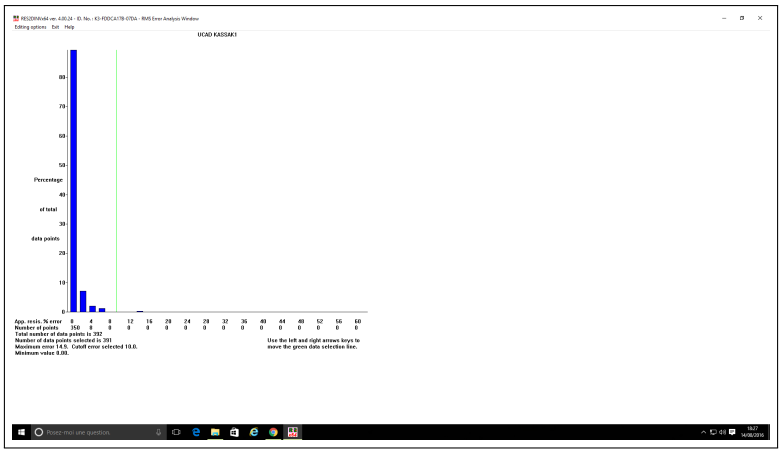

Figure 58: *RMS plot - Kassack.*

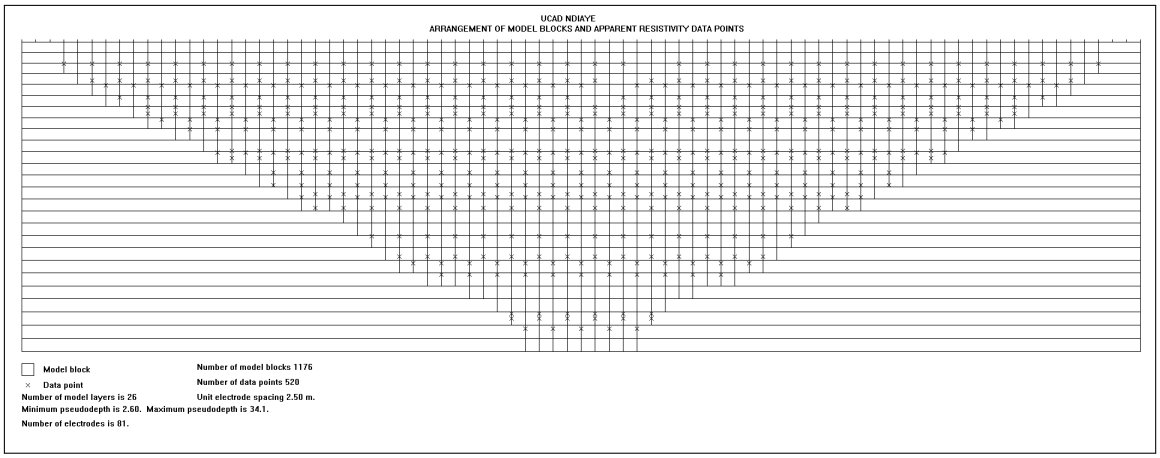

Figure 59: *Ndiaye mesh used for inversion calculations.*

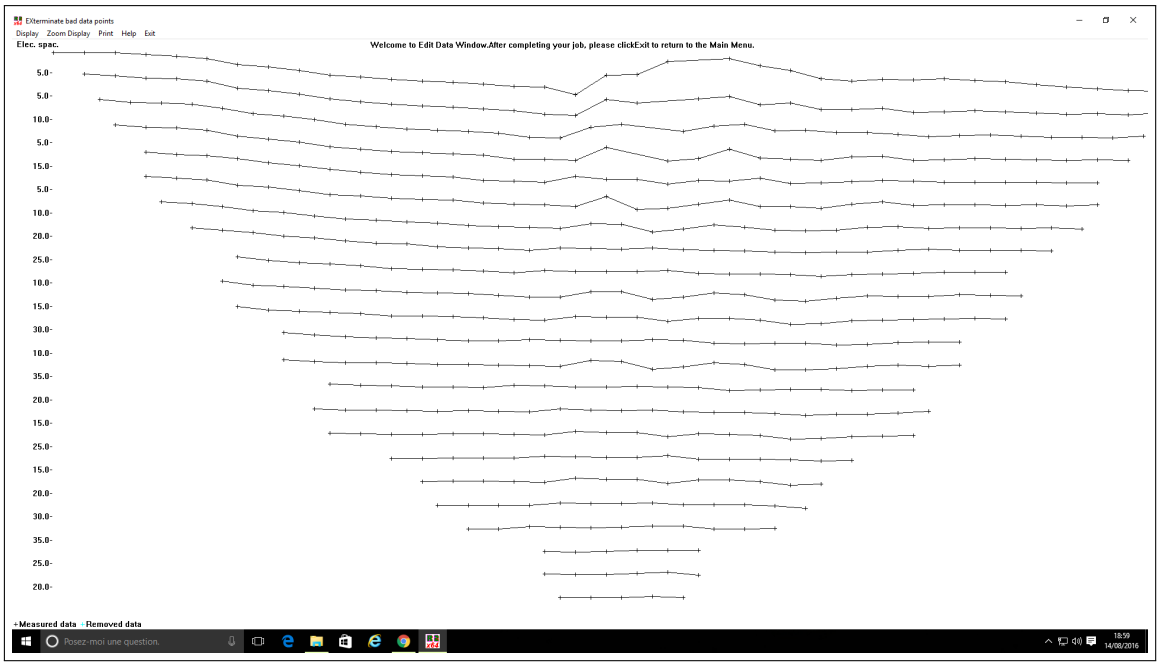

Figure 60: *Ndiaye data point locations used for inversion calcuations.*

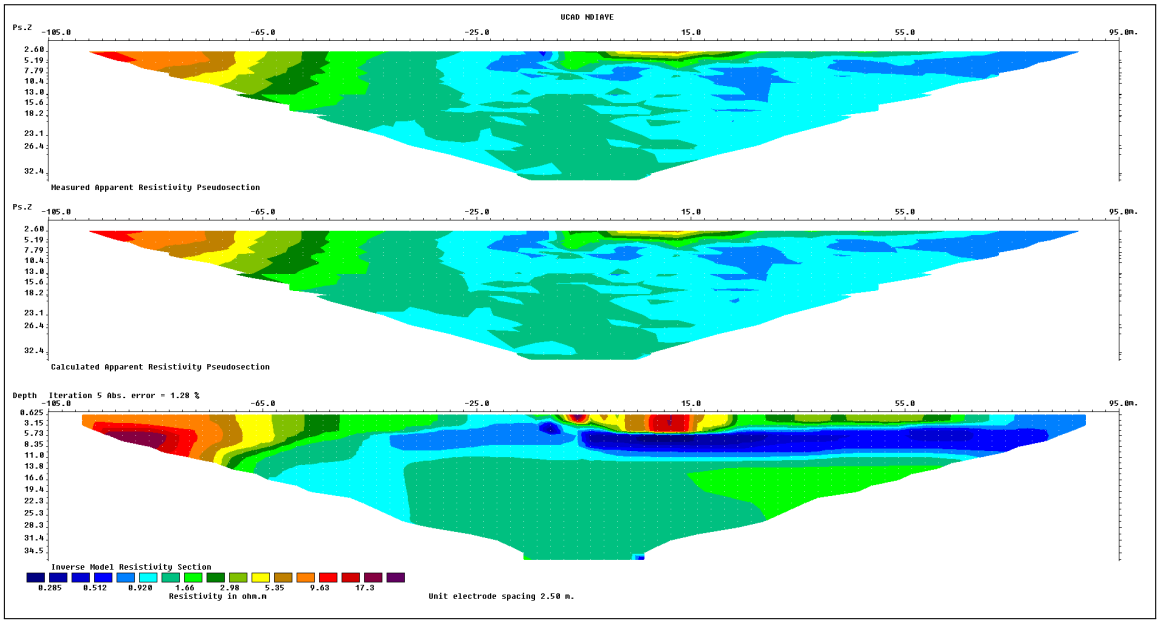

Figure 61: *Least squares finite difference inversion at Ndiaye, no model extension.*

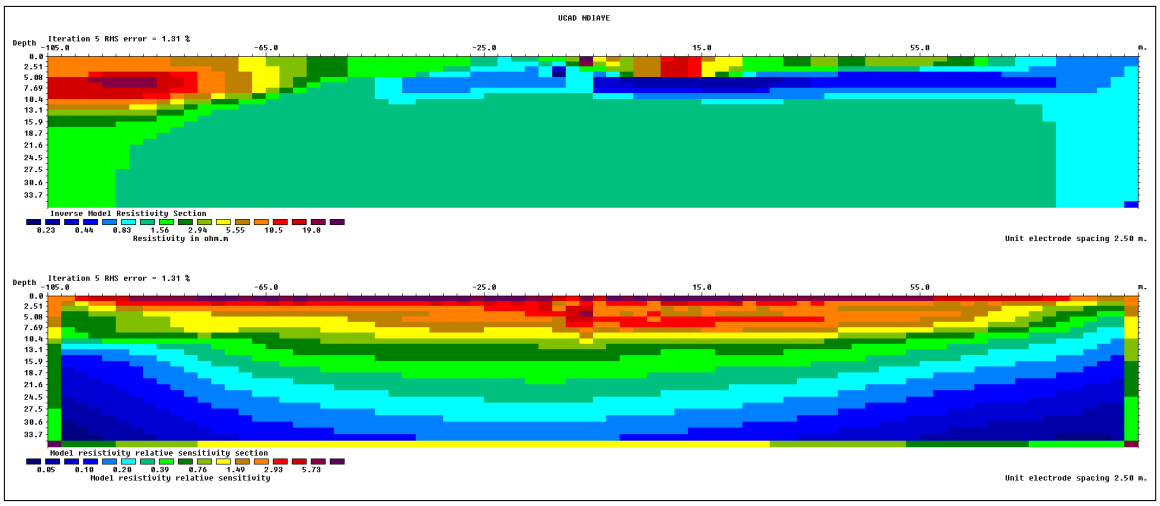

Figure 62: *Ndiaye model sensitivity values.*

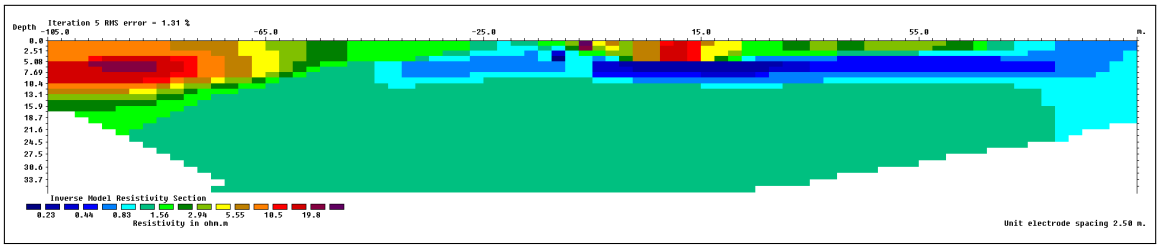

Figure 63: *Ndiaye model sensitivity values beneath the threshold of 0.1 removed.*

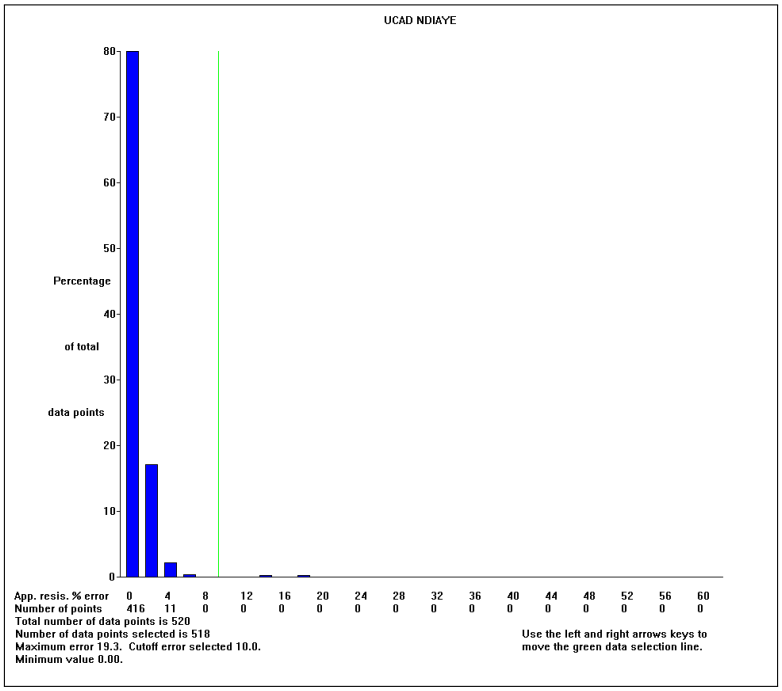

Figure 64: *Ndiaye RMS.*

Figure 65: *Geographical representation of the EM profile at Kassack (split into two data sets). The entire dataset measured a conductivity of 20.5 mS/cm.*

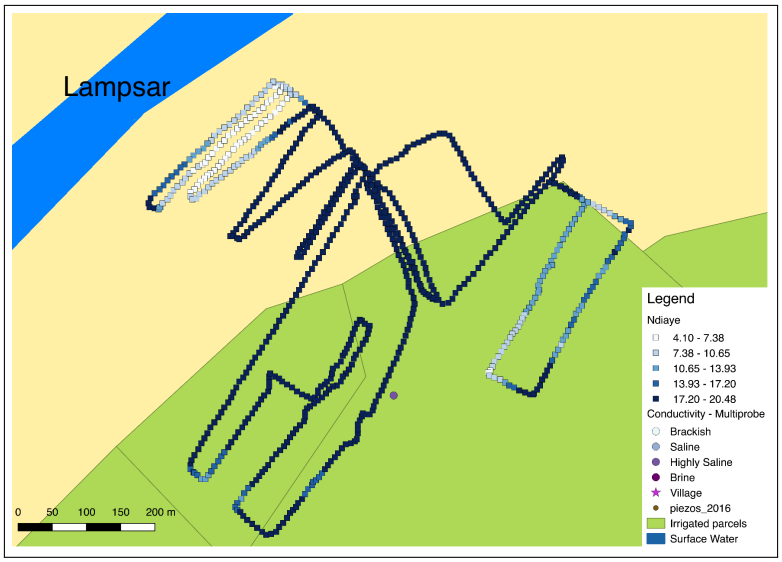

Figure 66: *Geographical representation of the EM profile at Ndiaye (split into two data sets). Conductivity variation is visible.*

Appendix 3: Supplemental Geochemistry

Piezo	Site	pH	Na+ (meq/L)	Ca2+ (meq/L)	Mg2+ (meq/L)	Fe3+ soluble (meq/L)	K+ (meq/L)	Mn2+ soluble (meq/L)	Sr2+ (meq/L)
KN1	Kassack 1	7.50	74.68	2.34	5.50	0.01	0.50	0.04	0.03
KN2	Kassack 1	5.87	338.87	24.08	60.76	0.01	2.11	2.74	0.15
KN3	Kassack 1	7.19	530.98	48.19	201.69	0.02	3.71	0.12	0.32
KN4	Kassack 2	7.50	58.67	5.61	18.94	0.00	0.56	0.04	0.03
KN5	Kassack 2	6.98	287.13	32.01	65.60	0.01	2.81	0.59	0.14
KN6	Kassack 2	7.14	114.28	17.83	44.76	0.01	1.50	0.10	0.06
KN7	Kassack 2	7.59	385.46	37.58	172.19	0.02	4.42	1.16	0.25
KN8	Kassack 2	6.91	215.49	51.03	84.25	0.01	2.53	0.32	0.16
119	existing	6.93	225.68	63.40	73.84	0.01	1.49	0.01	0.25
120	existing	7.04	609.83	36.82	179.77	0.03	5.22	0.09	0.29
P4	existing - Ndiaye	7.50	37.52	6.79	9.84	0.00	0.75	0.00	0.03
P3	existing - Ndiaye	7.25	8.56	3.75	2.27	0.01	0.48	0.00	0.01
N1	Ndiaye	7.95	17.32	1.59	2.73	0.01	0.22	0.01	0.01
N2	Ndiaye	7.33	310.08	13.66	61.74	0.01	3.80	0.13	0.13
N3	Ndiaye	7.08	264.16	55.13	72.93	0.01	5.45	0.14	0.17

Piezo	Site	Cl- (meq/L)	Br- (meq/L)	SO4 2- (meq/L)	CO3 2- (meq/L)	HCO3- (meq/L)	CO2- free (mg/L)	SiO2 (mg/L)
KN1	Kassack 1	64.68	0.13	4.01	0.05	13.09	17.67	13.65
KN2	Kassack 1	380.16	0.59	34.92	0.00	0.28	16.20	49.00
KN3	Kassack 1	714.09	1.11	41.97	0.01	6.47	17.83	23.17
KN4	Kassack 2	68.79	0.11	4.32	0.03	7.65	10.33	56.74
KN5	Kassack 2	343.18	0.51	22.96	0.01	6.13	27.41	46.50
KN6	Kassack 2	155.59	0.19	14.90	0.00	2.60	8.03	20.72
KN7	Kassack 2	462.49	0.62	104.64	0.03	7.69	8.43	31.88
KN8	Kassack 2	239.08	0.46	91.34	0.01	6.05	31.79	41.21
119	existing	319.48	0.61	22.52	0.01	5.43	27.25	52.03
120	existing	761.00	1.21	39.22	0.01	10.79	41.99	20.71
P4	existing - Ndiaye	34.89	0.06	10.78	0.02	6.42	8.66	14.84
P3	existing - Ndiaye	6.40	0.01	4.59	0.01	3.49	8.38	24.59
N1	Ndiaye	9.62	0.01	2.68	0.10	9.54	4.57	27.93
N2	Ndiaye	335.34	0.55	35.41	0.01	5.07	10.12	20.06
N3	Ndiaye	302.49	0.56	72.34	0.01	3.75	13.33	38.21

Figure 67: *Ionic analysis of water samples from all piezometers used in this study. No surface water included.*

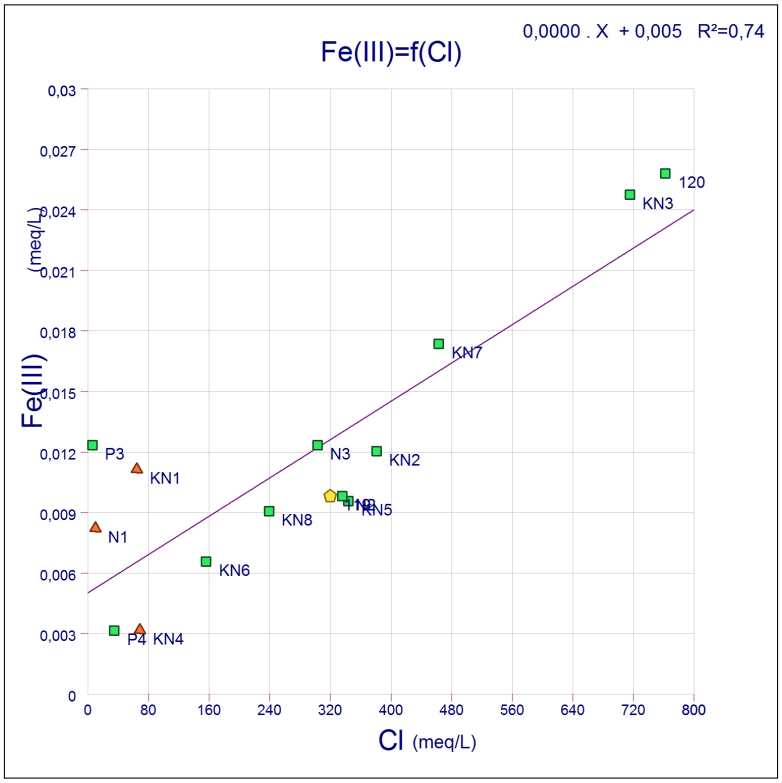

Figure 68: *Schematic representation of diver setup between piezometers KN1 and KN8. Multiprobe results are assumed to come directly from the top of the water table, or within 20cm.*

Appendix 4: Drilling Logs

The following logs offer general descriptions of the soil layers encountered while excavating boreholes for 8 different piezometers in 3 principal zones in the Senegal River delta. Boreholes were created using a manual auger with advancement tubes, and each are between 5 and 6 meters deep. Analysis was made mostly via vision and touch (and a little tasting as well). For these reasons, these logs rest only as rough descriptions. Even so, soil type and aquitard presence were determined on a site-specific level from these observations.

Site 1: Kassack North

KN1

- Black compact clayish layer encountered near 0.5 m and continues over the next 3 meters. Small amounts of brown silt and red sands intermittent in clay.
- Brown silt/sand layer met under water table
- Bottom section of saturated zone consists of grey silty-sand

KN1 appears to be located on sandy point bar soils of limited depth (0.5 meters)

KN2

- Small pebbly layer encountered near 0.4 meters, with a thickness of around 0.25 meters (see figure 69)
- Black clay persistent up to 1.5 meters
- Past 1.5 meters, layer becomes red and white silty/sandy
- When aquifer is reached at 1.75 meters, layer is brun-clair clayish, seemingly not very silty (but probably contains some silt)
- Near 3 - 3.5 meters, layer becomes grey silty-sandy

KN2 appears to be located within a sedimentary settling basin.

Figure 69: *Pebble layer in shallow part of KN2*

Figure 70: *Brown silty clay in shallow part of KN2*

Figure 71: *Black clay with intermittent red sand in shallow part of KN2*

KN3

- Now familiar topsoil to black clay
- Near 0.7 meters, black clay contains intermittent red silty clay. As depth increases, the red layers dominate the black clay, and black clay is replaced with grey silty-clay near 1 m. Salt is tasted in the grains.
- Transition to clear brown clayish silt around 1.4 meters. Aquifer is found in this layer.
- Near the bottom of the first detected nap (3m), black clay is once again encountered. Brown and red silts are marbled into clay.
- Clear brown silt increases over clay with depth (clayish silt). Dry sand lentils are encountered within this silt.
- Prominent red silt/sand becomes present in the clayish silt
- Red silt becomes large-grained sand within a gray silty matrix. Salt is tasted.
- At 4 meters, sand lentils disappear and saturated grey clayish silt is met. This is now recognized as our main shallow aquifer and is continuous to the bottom of the borehole.

KN3 is located within a sedimentary settling basin.

Figure 72: *Entire log of samples from KN3. Not to scale.*

2: Kassack South

KN4

Evaporated surface water areas show precipitated salt on the ground near KN4.

- Black clay with sand lentils found around 0.7 m depth
- Black/dark grey clay/silt with intermittent red persistent for 2 meters
- Water table is detected within grey clayish-silts. Large red sand lentils (cuirasse?) present in this layer
- Grey silt becomes more and more sandy below 3 m depth
- Below 4 meters depth, aquifer layer is almost entirely large grained grey sand
- Below 5 meters, grey clay-silt quantities re-increase

KN4 is located on a sandy point bar of limited depth.

KN5

- Around 0.5 meters, soil becomes clayish with presence of red sand lentils
- Solid black clay encountered around 1 m
- At water table, black clay transitions to light grey silt with large red sand lentils (cuirasse?)
- Grey clay becomes siltier and sandier with depth. Red sand lentils become more prominent in layers.
- Grey silt becomes more homogeneous with depth (red sand disappears). Fine grained aquifer.

KN5 is located on a sandy point bar of limited depth.

KN6

- Thin superficial white and red sandy layer (less than 0.5 m depth).
- Compact black clay just below this layer.
- Intermittent red sand comes into presence in black clay.
- Over 1 meter, clayish red & grey silt of varying grain size. Black clay marbled throughout this.
- Sandiness increases with increasing saturation. Brown, white, and red sand is present.
- W/in aquifer we find fine grained brown sand and large grain red sand (cuirasse?). Aquifer is in a silty/sandy layer.
- Near 2 m, unsaturated, compact black clay pebbles are found within the saturated brown silt/red sand.

- Grey silt/sand appears near 4 m.

KN6 is located in a sedimentary settling basin.

KN7

KN7 is found on the opposing side of an irrigation canal from KN5 and KN6. Salt is present in the first few cm of soil upon scratching the surface. On ground near piezo.

- Black clay to brown silt/clay at surface.
- Red sand intermittent near 0.4 m
- Red and grey sand dominate near 0.5 m, black clay intermittent.
- Dominant red sand has black bits of clay, grey sand intermittent
- Black sand present near 1 meter. Increasing water content.
- Aquifer: red, black, and light brown sands of various grain size. Some layers are dominant red sand, some are grey, etc. Color is tied to grain size. "Cuirasse" is present in dark red sands. Red and white are larger grained, grey is silty-clay, and black is mostly clay.
- Bottom of aqui is grey silty sand with diminishing water content.

KN7 is located in a sedimentary settling basin.

KN8

Piezometer is dug out on a slight hill of sands. There is a drainage canal close by. At time of excavation, all canals are bone dry, so h is expected to be low.

- First layer is clayish with grey silt and red sand present. This layer extends to around 1 m and is completely dry.
- Clayish layer contains large salt crystals (maybe a little quartz? Taste is salty) around 1.5 or 2 meters.
- Below 2 m depth, clay turns silty and grey. Intermittent red sands (cuirasse?).
- Water is in a compact grey sandy-silt layer.

KN8 is located on a thick sandy point bar, with raised elevation leading to low h.

Site 3: Ndiaye

N1

- Black clay layer present under surface sediments.
- Mix of grey and brown silts, presence of black grains (black salt?) and large red sands (cuirasse) Near 1 meter

- In saturated zone (below 1.37 meters), mix of sands and silts. Hard sand/clay pebbles are present within layers. Sand is mostly RED.
- Soil is mostly homogeneous between 2 and 6 meters. Grey silts, brown sand/silts, etc.

N1 is likely located in a sedimentary settling basin.

N2

Next to onion fields which are never flooded like rice fields, but are irriguated a few times a week. Small canals are 1/2 full on day of excavation, and a large field is flooded across from onion fields.

- Black clay with brown and red intermittent sands are shallow layers. Cuirasse is present and possibly salt is precipitated.
- Brown silt-clay and red + white sands dominate around 1 meter.
- Salt is possibly present w/in red sands (cuivre + NaCl?). There is no salt at the surface, but is present in the subsurface. Precipitations follow laminar patterns.
- Saturation found in grey silty layer
- With depth (around 2-3 meters to 6), silts become large-grained grey sands.

N2 is located in a sedimentary settling basin.

N3

- Red and orange white sands encountered near surface (<1 meter).
- Sand is increasingly white and large grained with depth. Intermittent black clay in small amounts, Orange sand and RED sand is present as well.
- White sand transitions to light grey with depth, and then from light grey to grey.
- Enter into grey sandy aquifer. Relatively large grain size.
- Near 4 meters, Sand is intermittent grey/clear and still saturated. Brown sand intermittent.
- Close to 5 meters, aquifer becomes almost exclusively brown sand.

N3 is evidently located in the red sand dune zone!

References

[1] Audibert, M., 1970. *Etude hydro-agricole du bassin du fleuve Sénégal. Delta du Fleuve Sénégal: Etude Hydrogéologique*. Généralités et rapport de synthèse, Organisation des Nations Unies pour l'alimentation et l'agriculture (FAO). Accessed January 2016.

[2] Bader, J.C. and Cauchy, S., 2013. *Actualisation de la monographie hydrologique du fleuve Sénégal*. OMVS Haut Commissariat Rapport Final. Groupe Hydraulique et Régulation, et Service Hydraulique et Ouvrages. Accessed February 2016.

[3] Bear, J., et al, 1999. *Seawater Intrusion in Coastal Aquifers - Concepts, Methods, and Practices*. Theory and Applications of Transport in Porous Media. Kluwer Academic Publishers. Accessed June 2016.

[4] Comte, Jean-Christophe, 2009. *Apport de la tomographie électrique à la modélisation des écoulements densitaires dans les aquifères côtiers - Application à trois contextes climatiques constrastés (Canada, Nouvelle-Calédonie, Sénégal)*. Hydrology. Université d'Avignon, 2008. Accessed May 2016.

[5] Deckers, J. et al., 1996. *Évolution de l'acidité dans les sols du delta du fleuve Sénégal sous influence anthropogène*. Étude et Gestion des Sols, vol. 3, no. 3 (p. 151 - 163). Accessed November 2015.

[6] deGroot-Hedlin, C. et Constable, S., 1990. *Occam's inversion to generate smooth, two-dimensional models from magnetotelluric data*. Geophysics, vol. 55, no. 12 (p. 1613 - 1624). Society of Exploration Geophysicists. Accessed May 2016.

[7] Diaw, M. et al, 2010. *Isotopic and Geochemical Characteristics of Groundwater in the Senegal River Delta Aquifer: Implication of Recharge and Flow Regime*. Environmental Earth Science (p. 1011-1020). Accessed November 2015.

[8] "Ghyben-Herzberg Principle". *The Dictionary of Physical Geography* Third Ed. Thomas, David and Goudie, Andrew. Blackwell Publishing, 2000. Accessed May 2016.

[9] Gilli, É et al, 2008. *Hydrogéologie*. 2ème édition, Dunod, Paris. Accessed February 2016.

[10] Gning, A., 2015. *Etude et Modélisation Hydrogéologique des Interactions Eaux de Surface-Eaux Souterraines dans un Contexte d'Agriculture Irriguée dans le Delta du Fleuve Sénégal*. Doctoral Thesis. University of Cheikh Anta Diop de Dakar Geology department, and University of Liège, GEO^3 sector. Accessed June 2015.

[11] Gonzalez-Alvaraz, I., et al, 2016. *A geological assessment of airborne electromagnetics for mineral exploration through deeply weathered profiles in the southeast Yilgarn Cratonic margin, Western Australia*. Ore Geology Reviews 73-3, p. 522-539. Accessed April 2016.

[12] Government of Western Australia, Department of Water. *Understanding Salinity*. `http://www.water.wa.gov.au/water-topics/water-quality/managing-water-quality/understanding-salinity`. Accessed May 2016.

[13] Gourlez de la Motte, Louis, 2012. *Salinisation Progressive des Eaux et Sols Liée aux Conditions Hydrogéologiques et aux Pratiques d'Irrigation dans une Riziculture du Delta du Fleuve Sénégal*. Master Thesis. University of Liège - Gembloux.

[14] Kirsch, R., 2009. *Groundwater quality - saltwater intrusions.* Groundwater Geophysics, a tool for Hydrogeology, second edition, (p. 475 - 488). Accessed November 2015.

[15] Lange, G. et Seidel, K., 2007. *Electromagnetic Methods.* Environmental Geology: Handbook of Field Methods and Case Studies, (p. 239 - 281). Springer Publishing. Accessed March 2016.

[16] Le Brusq, Jean-Yves, 1980. *Étude Pédologique des Cuvettes de la Vallée du Lampsar (Région du Fleuve Sénégal).* Office de la Recherche Scientifique et Technique Outre-Mer (ORSTOM). Dakar, Senegal. Accessed February 2016.

[17] Loke, M.H., 2001. *Tutorial : 2-D and 3-D electrical imaging surveys.* Geotomo Software, Malaysia. Accessed April 2016.

[18] McKee, T. B. et al, 1995. *Drought Monitoring with Multiple Time Scales.* 9th AMS Conference on Applied Climatology, 15-20 January 1995. Dallas, Texas. Accessed June 2016.

[19] Mean, A., 2011. *Caractérisation hydrogéologique du Delta du Fleuve Sénégal.* Master Thesis, University of Liège, Faculty of Sciences, Department of Geology. Accessed November 2015.

[20] Michel, P., 1973. *Les Bassins ed Fleuves Senegal et Gambie. Etude Geomorphologique.* Office de la Recherche Scientifique et Technique Outre-Mer. Accessed January 2016.

[21] Ministere de L'agriculture, de L'hydraulique Rurale et de la Sécurité Alimentaire, Direction de la Gestion et de la Planification des Ressources en Eau, 2006. *Contribution du Point Focal Thematique Eaux Souterraines du Sénégal aux Travaux de L'atelier Eaux Souterraines Prevu à Saint Louis du 3 au 9 Decembre 2006.* Republic du Senegal, Division hydrogéologie.

[22] Mohammadi, Z. et al, 2012. *Delineation of groundwater salinization in a coastal aquifer, Bousheher, South of Iran.* Environ Earth Sci. Accessed April 2016.

[23] Nguyen, F. et al, 2009. *Characterization of seawater intrisuion ising 2D electrical imaging.* European Associated of Geoscientists and Engineers, Near Surface Geophysics. Pages 3 - 15. Accessed January 2016.

[24] 1967. *Notice Explicative de la Carte Géologique au 1/200 000: "Saint-Louis".* Presentee par le Bureau de Recherches Geologiques et Minieres, Dakar. Accessed February 2016.

[25] Por, F.D., 1972. *Hydrobiological notes on the high-salinity waters of the sinai peninsula.* Marine Biology 14. Pages 111 - 119. Accessed May 2016.

[26] Ravindran, A. et al, 2013. *Delineation of Saltwater and Freshwater Interphase in Beach Groundwater Study Using 2D ERI Technique in the Northern Sector of the Gulf of Mannar Coast, Tamilnadu.* Water Journal, vol. 5. Pages 1 - 11. Accessed June 2016.

[27] RES2DINV ver. 3.59 User Manual, 2010. *Rapid 2-D Resistivity & IP inversion using the least-squares method.* Geotomo Software, Malaysia. Accessed April 2016.

[28] Roger, J. et al, 2009. *Notice explicative des cartes géologiques à 1/200 000 du Bassin sédimentaire sénégalais.* Republic du Senegal, Ministère des Mines, de l'Industrie et des PME, Dakar. Accessed March 2016.

[29] Sea Surface Salinity Remote Sensing at CATDS Ocean Salinity Expert Center, *Salinity Distribution at the Ocean Surface*. http://www.salinityremotesensing.ifremer.fr/sea-surface-salinity/salinity-distribution-at-the-ocean-surface. Accessed May 2016.

[30] Summary of a Workshop, 2013. *Scientific Data for Decision Making Toward Sustainable Development: Senegal River Basin Case Study*. National Academies Press online. http://www.nap.edu/catalog/10546.html Accessed February 2016.

[31] Taïbi, A.N., et al, 2009. *Le bas delta du fleuve Sénégal face aux risques de dégradation et conflits d'usage dans un contexte de restauration des écosystèmes et des activités. Approche par les outils d'analyse spatiale.* Université d'Angers. Accessed January 2016.

[32] Telford, W. M., et al, 1990. "Electrical Properties of Rocks and Minerals. *Applied Geophysics*. Second Edition. Cambridge University Press. Pages 283 - 292. Accessed April 2016.